

---

---

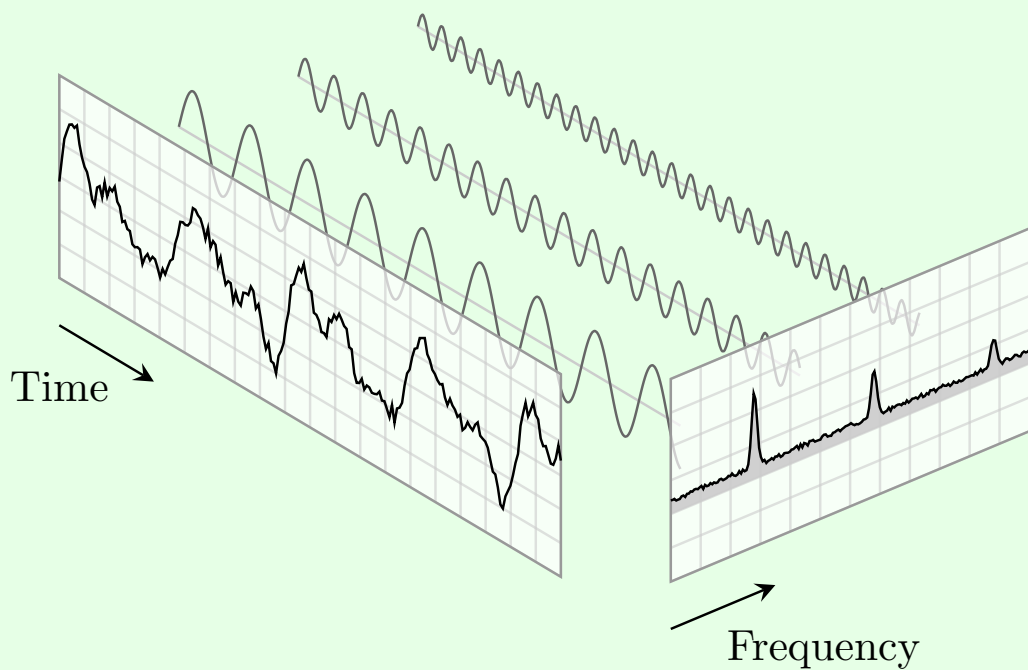
**LECTURE NOTES  
OF  
DIGITAL SIGNAL PROCESSING**

---

---

COLLECTION OF THE LECTURES NOTES OF PROFESSOR FEDERICA BATTISTI.

EDITED BY  
ARDINO ROCCO  
ACADEMIC YEAR 2020-2021





## Abstract

In this document I have tried to reorder the notes of the Digital Signal Processing course held by Professor Federica Battisti at DEI of the University of Padua during the first semester of the 2020-21 academic year of the master's degree in Physics of Data.

The notes are fully integrated with the material provided by the professor in the Moodle platform. In addition, I will integrate them, as best as possible, with the books recommended by the professor.

There may be formatting errors, wrong marks, missing exponents and even missing parts, since I'm still working on them. If you find errors or if you have any suggestions, let me know (you can send an e-mail at [rocco.ardino@studenti.unipd.it](mailto:rocco.ardino@studenti.unipd.it), labeled with **DSP::TYPO/SUGGESTION**) and I will correct/integrate them, so that this document can be a good study support. However, these notes are not to be intended as a substitute of the lectures held by the professor or of lecture notes made by other people.

Padova, Thursday 24<sup>th</sup> December, 2020  
Rocco Ardino



# Contents

|          |   |           |
|----------|---|-----------|
| <b>1</b> | <b>Introduction</b>   | <b>1</b>  |
| 1.1      | What is a signal? . . . . .                                       | 1         |
| 1.2      | Is sampling of a continuous signal always possible? . . . . .     | 3         |
| 1.3      | Discrete time and amplitude . . . . .                             | 3         |
| 1.4      | Advantages and disadvantages of digital signals . . . . .         | 5         |
| <b>2</b> | <b>Discrete-Time signals</b>                                      | <b>7</b>  |
| 2.1      | Time-Domain representation and basic definitions . . . . .        | 7         |
| 2.1.1    | Categorization of discrete-time signals . . . . .                 | 8         |
| 2.1.2    | Norm of a discrete-time signal . . . . .                          | 9         |
| 2.2      | Operations on sequences . . . . .                                 | 10        |
| 2.2.1    | Basic operations . . . . .  | 10        |
| 2.2.2    | Ensamble averaging . . . . .                                      | 11        |
| 2.2.3    | Samping rate alteration . . . . .                                 | 12        |
| 2.3      | Classification of sequences . . . . .                             | 13        |
| 2.4      | Basic signals . . . . .   | 16        |
| 2.4.1    | Unit sample sequence . . . . .                                    | 17        |
| 2.4.2    | Unit step sequence . . . . .                                      | 17        |
| 2.4.3    | Real sinusoidal sequence . . . . .                                | 17        |
| 2.4.4    | Exponential sequence . . . . .                                    | 17        |
| <b>3</b> | <b>Discrete-Time systems</b>                                      | <b>21</b> |
| 3.1      | Examples of discrete-time systems . . . . .                       | 21        |
| 3.1.1    | Accumulator system . . . . .                                      | 21        |
| 3.1.2    | $M$ -point moving average system . . . . .                        | 22        |
| 3.1.3    | Exponentially weighted running average system . . . . .           | 23        |
| 3.1.4    | Linear interpolation system . . . . .                             | 23        |
| 3.1.5    | Median system . . . . .   | 24        |
| 3.2      | Classification of discrete-time systems . . . . .                 | 25        |
| 3.2.1    | Linear systems . . . . .  | 25        |
| 3.2.2    | Shift-Invariant systems . . . . .                                 | 27        |
| 3.2.3    | Causal systems . . . . .  | 28        |
| 3.2.4    | Stable systems . . . . .  | 29        |
| 3.2.5    | Passive and lossless systems . . . . .                            | 29        |
| 3.3      | Impulse and step response . . . . .                               | 30        |
| 3.4      | Shift-Invariant systems . . . . .                                 | 30        |
| 3.5      | Time domain characterizatio of LTI discrete-time system . . . . . | 30        |
| 3.6      | Convolution sum . . . . .   | 30        |
| 3.7      | Stablility and causality conditions . . . . .                     | 30        |
| 3.8      | Correlation and autocorrelation . . . . .                         | 30        |
| <b>4</b> | <b>Fourier Analysis</b>   | <b>31</b> |

|          |   |           |
|----------|---|-----------|
| 4.1      | Continuous-time Fourier transform . . . . .               | 31        |
| 4.1.1    | Energy density spectrum . . . . .                         | 32        |
| 4.1.2    | Band-limited continuous-time signals . . . . .            | 32        |
| 4.1.3    | Discrete-time fourier transform . . . . .                 | 33        |
| 4.1.4    | DTFT properties . . . . .                                 | 38        |
| 4.1.5    | Energy density spectrum . . . . .                         | 40        |
| 4.1.6    | Band-limited discrete-time signals . . . . .              | 41        |
| 4.2      | Linear convolution using DTFT . . . . .                   | 42        |
| 4.3      | The frequency response . . . . .                          | 44        |
| 4.4      | The concept of filtering . . . . .                        | 48        |
| 4.5      | Discrete Fourier Transform . . . . .                      | 50        |
| 4.5.1    | Matrix relations . . . . .                                | 53        |
| 4.5.2    | DTFT from DFT by interpolation . . . . .                  | 54        |
| 4.5.3    | Sampling the DTFT . . . . .                               | 55        |
| 4.5.4    | DFT properties . . . . .                                  | 56        |
| 4.5.5    | Circular shift of a sequence . . . . .                    | 56        |
| 4.5.6    | Circular convolution . . . . .                            | 57        |
| 4.5.7    | DFT of real sequences . . . . .                           | 58        |
| 4.6      | Linear convolution using the DFT . . . . .                | 60        |
| <b>5</b> | <b>The Z transform</b> . . . . .                          | <b>65</b> |
| 5.1      | The definition . . . . .                                  | 65        |
| 5.2      | Rational z-transforms . . . . .                           | 67        |
| 5.3      | Inverse z-transform . . . . .                             | 71        |
| 5.4      | Z-transform properties . . . . .                          | 73        |
| 5.5      | Stability condition . . . . .                             | 75        |
| <b>6</b> | <b>Filter design</b> . . . . .                            | <b>79</b> |
| 6.1      | Phase and group delay . . . . .                           | 79        |
| 6.1.1    | Phase delay . . . . .                                     | 79        |
| 6.1.2    | Group delay . . . . .                                     | 79        |
| 6.2      | Type of transfer functions . . . . .                      | 80        |
| 6.2.1    | Ideal filters . . . . .                                   | 80        |
| 6.2.2    | Bounded Real transfer functions . . . . .                 | 81        |
| 6.2.3    | Allpass transfer function . . . . .                       | 83        |
| 6.2.4    | Phase characteristics . . . . .                           | 86        |
| 6.2.5    | Frequency response from transfer function . . . . .       | 88        |
| 6.2.6    | Geometric interpretation of frequency response . . . . .  | 89        |
| 6.3      | Simple digital filters . . . . .                          | 90        |
| 6.3.1    | Lowpass FIR digital filters . . . . .                     | 90        |
| 6.3.2    | Highpass FIR digital filters . . . . .                    | 92        |
| 6.3.3    | Lowpass IIR digital filters . . . . .                     | 93        |
| 6.3.4    | Highpass IIR digital filters . . . . .                    | 94        |
| 6.3.5    | Bandpass IIR digital filters . . . . .                    | 95        |
| 6.3.6    | Bandstop IIR digital filters . . . . .                    | 96        |
| 6.3.7    | Higher-Order IIR digital filters . . . . .                | 97        |
| 6.4      | Linear-phase FIR transfer functions . . . . .             | 98        |
| 6.4.1    | Symmetric impulse response with odd length . . . . .      | 100       |
| 6.4.2    | Symmetric impulse response with even length . . . . .     | 102       |
| 6.4.3    | Antisymmetric impulse response with odd length . . . . .  | 103       |
| 6.4.4    | Antisymmetric impulse response with even length . . . . . | 104       |
| 6.4.5    | General form of frequency response . . . . .              | 104       |
| 6.4.6    | Zero locations . . . . .                                  | 106       |

|              |     |
|--------------|-----|
| Bibliography | 109 |
|--------------|-----|



# Chapter 1

## Introduction

In this course we will enter into the world of Digital Signal Processing, trying to understand the theoretical fundations of this field with several examples. In particular, we will follow this outline of arguments:

- What is Digital Signal Processing?
- Discrete-time signals.
- Signals and Hilbert spaces.
- Fourier analysis.
- Discrete-time filters.
- The z-transform.
- Filter design, in particular A/D and D/A conversions and the design of a digital communication system.

Concerning the study material, along with the teaching professor's notes and slides, several textbooks are suggested to integrate the study material:

- [1] *Signal Processing for Communication*, P. Prandoni and M. Vetterli.
- [2] *Digital Signal Processing*, A. V. Oppenheim and R. W. Schafer.
- [3] *Digital Signal Processing: A Computer-Based Approach*, S. K. Mitra.

### 1.1 What is a signal?

Let us start with a definition of what we are going to deal with for most of our time. A signal is the description of the evolution of a physical phenomenon. For example, we can have:

- **continuous-time signals**, such as voltage, current, temperature and speed, whose spectrum is sketched in Figure 1.1;
- **discrete-time signals**, such as minimum/maximum temperature, lap intervals in races, sampled continuous signals, with an example spectrum showed in Figure 1.2.

Signals may have to be transformed in order to:

**Lecture 1.**  
Tuesday 29<sup>th</sup>  
September, 2020.

Signal definition  
and types of signals

Operations on  
signals

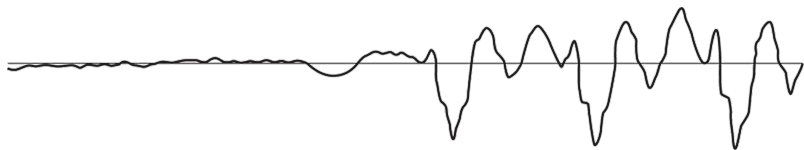


**Figure 1.1:** Example of continuous-time signal spectrum.

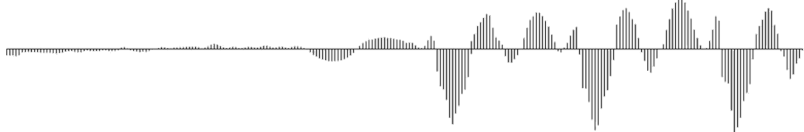


**Figure 1.2:** Example of discrete-time signal spectrum, obtained from sampling of the signal in Figure 1.1.

- be analyzed: this is necessary to **understand** the informations carried by the signal itself. For example, we can amplify or filter out embedded information, detect patterns, prepare the signal to survive a transmission channel and much more;
- be synthesized: this is necessary to **create** a signal to contain a specific information. Some common examples in this case are the cellphones, tv, radio and synthetic music.

Therefore, to do these operations we need specific methods to measure, characterize, model and simulate transmission channels, but also mathematical tools that split common channels and transformations into easily manipulated building blocks.

#### From analog to digital signals

Now, we enter more into the detail of digital signals. When we are dealing with analog signals, we can record them but we can hardly find a function that can describe them. In order to have an idea of the difficulty of this task, let us look at the signal in Figure 1.3: how can we describe this function? This is where the digital part comes into practice.

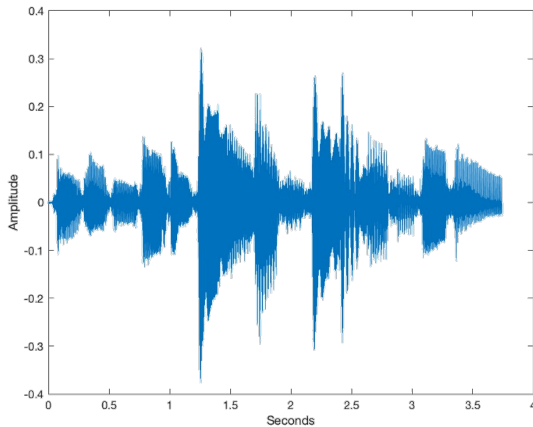


**Figure 1.3:** Example of analog signal.

#### Mathematical definition of digital signals

A continuous-time (analog) signal is defined along a continuum of time and is thus represented by a continuous independent variable. Discrete-time signals are defined at discrete times, and thus, the independent variable has discrete values. Therefore, the ladders are represented as sequences of numbers  $x$ , in which the  $n^{\text{th}}$  number in the sequence is denoted  $x[n]$ , and it is formally written as:

$$x = \{x[n]\}, \quad -\infty < n < \infty \quad (1.1)$$

where  $n$  is an integer. An example is showed in Figure 1.4.

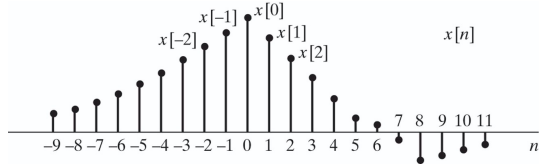


**Figure 1.4:** Example of graphic representation of a discrete-time signal.

Digital signal  
sampled from  
periodic signals

Such sequences can arise from periodic sampling of an analog signal  $x_a(t)$ . In this case the numeric value of the  $n^{\text{th}}$  number in the sequence is equal to the value of the analog signal, namely  $x_a(t)$ , at time  $nT$ :

$$x[n] = x_a(nT), \quad -\infty < n < \infty \quad (1.2)$$

where  $T$  is the sampling period.

## 1.2 Is sampling of a continuous signal always possible?

At this point we ask ourselves a question: when we represent an analog signal as a digital one, are we loosing information? The question has been answered by C. Shannon and H. Nyquist: under specific conditions, the analog and the digital representations of a signal are equivalent. Here we come to the sampling theorem. An analog signal can be represented as a linear combination of cardinal sine (denoted by sinc and plotted in Figure 1.5) functions shifted ad scaled by the values of the discrete time sequence. Mathematically, this translates into:

$$x(t) = \sum_{n=-\infty}^{\infty} x[n] \operatorname{sinc}\left(\frac{t - nT_S}{T_S}\right) \quad (1.3)$$

Sampling theorem

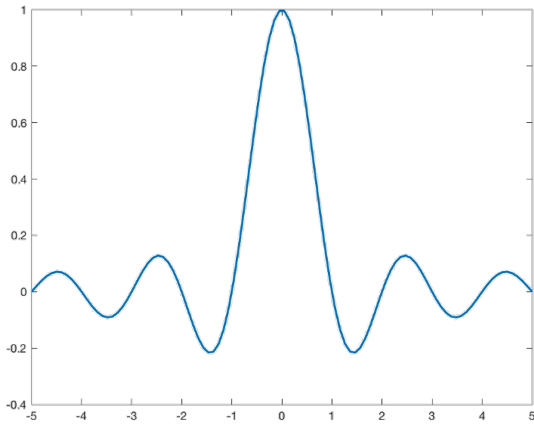


**Figure 1.5:** Cardinal sine sinc function.

Utility of Fourier  
transform

It is important to determine the value of  $T_S$  so that the sampling theorem holds. The Fourier transform helps us understanding how fast the signal moves and consequently guides us to the selection of  $T_S$ .

## 1.3 Discrete time and amplitude

Till now we discussed the discretization of time. What if we discretize also the amplitude of the signal? In this case each sample can take predetermined values

in a countable set. Moreover, as consequence, we can always map the level of the sample onto an integer. An example of a sampled sin function is showed in Figure 1.6.

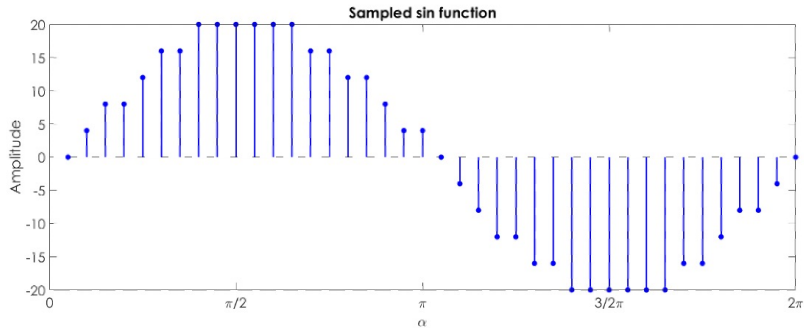


**Figure 1.6:** Sampled sin function.

It is of paramount importance to discretize both time and amplitude. By this way, we can ease tasks like storage, processing and transmission. In particular, let us describe the ladder.

#### Signal transmission

Transmission is one of the fields that most benefits from discrete signal representation. We give an idea of this fact through an example. Let us consider the channel scheme in Figure 1.7 and a sinusoidal analog signal, which is attenuated and acquires a noise component, as represented in Figure 1.9

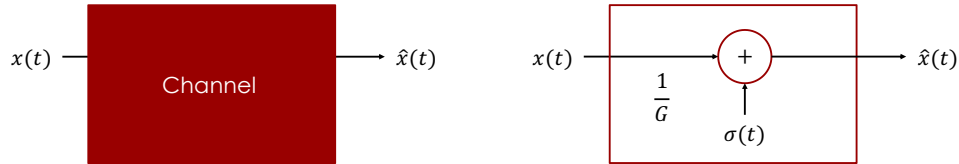


**Figure 1.7:** Scheme of an example of transmission channel.

We can counteract this problem by trying to undo the errors introduced by the signal (only the gain):

$$\hat{x}_1(t) = G \left[ \frac{x(t)}{G} + \sigma(t) \right] = x(t) + G\sigma(t) \quad (1.4)$$

By this way, we also amplify the noise. Sometimes this is unavoidable, but what we can do is to amplify the signal as near to the place where it is acquired as possible, so that the noise is amplified before it increases in the transmission to the place where it is analyzed. In particular, noise amplification becomes more relevant if we put in cascade several transmission blocks, as represented in Figure 1.8. In this case, the output of the transmission chain reads:

$$\hat{x}_N(t) = x(t) + NG\sigma(t) \quad (1.5)$$

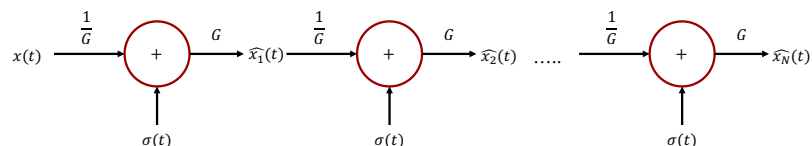


**Figure 1.8:** Scheme of an example of a cascade of transmission blocks.

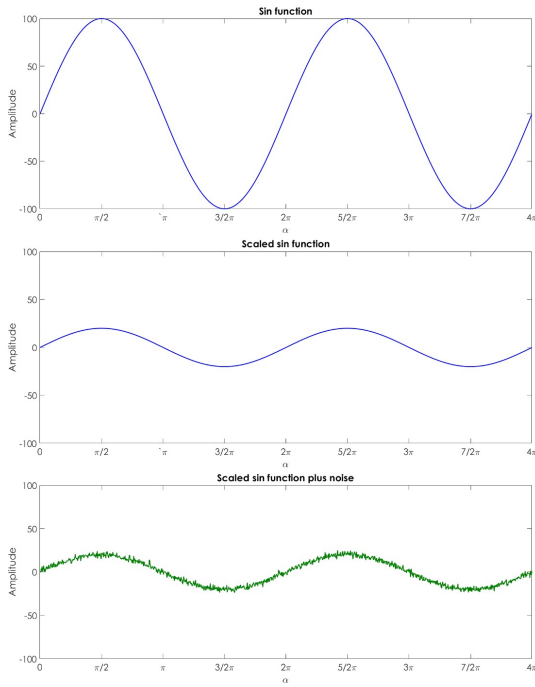


**Figure 1.9:** Sinusoidal analog signal (top), sinusoidal attenuated signal (center), sinusoidal attenuated noisy signal (bottom).

This discussion was mainly related to analog signals. Now, if we take into account the transmission of a digital signal, we have to perform other operations, such as introducing a thresholding operator to discretize the signal. With respect to the previous example, the new transmission block is showed in Figure 1.10 and the output reads:

$$\hat{x}_1(t) = \text{sign} [x(t) + G\sigma(t)] \quad (1.6)$$

which is in practice a square wave.

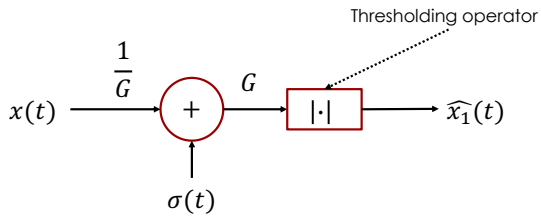


**Figure 1.10:** Scheme of an example of transmission channel for digital signals.

## 1.4 Advantages and disadvantages of digital signals

To conclude this introduction, we have still to present the main advantage of digital signals, but also their drawbacks:

*Pro and cons*

- ✓ noise is easy to control after initial quantization;
- ✓ highly linear (within limited dynamic range);
- ✓ complex algorithms fit into a single chip;
- ✓ flexibility, parameters can easily be varied in software;

- ✓ digital processing is insensitive to component tolerances, aging, environmental conditions, electromagnetic interference;
- ✗ discrete-time processing artifacts (aliasing);
- ✗ a significantly large amount of power can be required (battery, cooling);
- ✗ digital clock and switching cause interference.

# Chapter 2

## Discrete-Time signals

In this Chapter we define more formally the concept of the discrete-time signal and some other properties useful for their description. Historically, discrete-time signals have often been introduced as the discretized version of continuous-time signals, i.e. as the sampled values of analog quantities. For this reason, many of the derivations proceeded within the framework of an underlying continuous-time reality.

**Lecture 2.**  
Thursday 1<sup>st</sup>  
October, 2020.

### 2.1 Time-Domain representation and basic definitions

Signals are represented as **sequences of numbers**, also called **samples**. Typically, the value of a signal sample is denoted as  $x[n]$ , with  $n$  being an integer in the range. So,  $x[n]$  is defined only for  $n \in \mathbb{Z}$  and undefined otherwise, namely for non-integer values of  $n$ .

Sample sequence

In the introduction we have already presented the common notation for discrete-time signals, namely  $\{x[n]\}$ , with  $-\infty < n < \infty$ . Sometimes the numerical values of the samples are explicitly written inside the curly braces, for example:

$$\{x[n]\} = \{\dots, -0.2, \textcolor{red}{2.2}, 1.1, 0.2, -3.7, 2.9, \dots\} \quad (2.1)$$

where the element in red is the sample at time index  $n = 0$ .

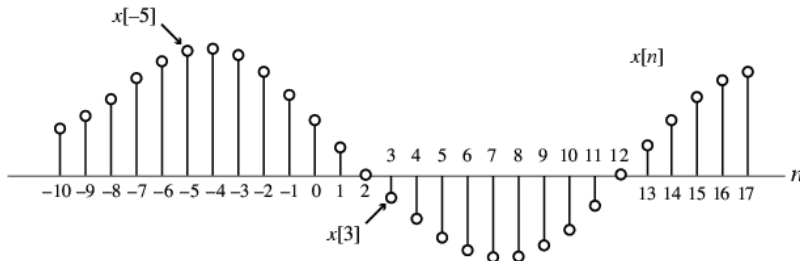


**Figure 2.1:** Example of sample sequence.

In some applications, a discrete-time sequence  $\{x[n]\}$  may be generated by **periodically sampling** a continuous-time signal  $x_a(t)$  at uniform intervals of time. An example is showed in Figure 2.2. Here, the  $n^{\text{th}}$  sample is given by:

Periodic sampling

$$x[n] = x_a(t)_{t=nT} = x_a(nT), \quad n = \dots, -2, -1, 0, 1, 2, \dots \quad (2.2)$$

The spacing  $T$  between two consecutive samples is called the **sampling interval** or **sampling period**. The reciprocal of sampling interval  $T$ , denoted as  $F_T$ , is called the **sampling frequency**:

Sampling period  
and frequency

$$F_T = \frac{1}{T} \quad (2.3)$$

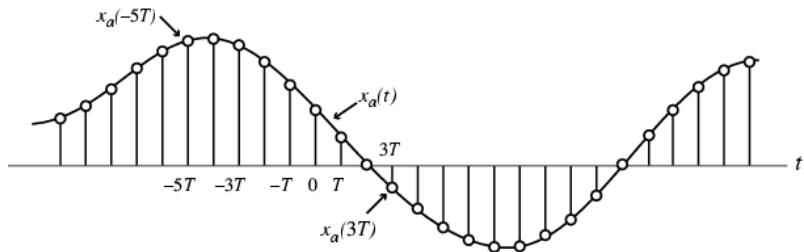


**Figure 2.2:** Example of periodically sampled sequence.

*Real and complex sequences*

The physical unit of the sampling frequency is “cycles per second”, or **Hertz** (Hz), if  $T$  is in seconds. Whether or not the sequence  $\{x[n]\}$  has been obtained by sampling, the quantity  $x[n]$  is called the  $n^{\text{th}}$  sample of the sequence. Moreover,  $\{x[n]\}$  is called **real sequence** if the  $n^{\text{th}}$  sample is real for all values of  $n$ . Otherwise,  $\{x[n]\}$  is called **complex sequence**.

In particular, a complex sequence can be written as:

$$\{x[n]\} = \{x_{\text{re}}[n]\} + j\{x_{\text{im}}[n]\} \quad (2.4)$$

where  $\{x_{\text{re}}[n]\}$  and  $\{x_{\text{im}}[n]\}$  are the real and imaginary parts of  $x[n]$ . The complex conjugate sequence of  $\{x[n]\}$  reads:

$$\{x^*[n]\} = \{x_{\text{re}}[n]\} - j\{x_{\text{im}}[n]\} \quad (2.5)$$

Note that the braces are often ignored to denote a sequence if there is no ambiguity.

#### Example 1: Real and complex sequences

- $\{x[n]\} = \{\cos(0.25n)\}$  is a real sequence;
- $\{y[n]\} = \{e^{j0.3n}\}$  is a complex sequence.

We can write:

$$\{y[n]\} = \underbrace{\{\cos(0.3n)\}}_{\{y_{\text{re}}[n]\}} + j \underbrace{\{\sin(0.3n)\}}_{\{y_{\text{im}}[n]\}} \quad (2.6)$$

Then, we consider the complex conjugate of  $\{y[n]\}$ :

$$\{w[n]\} = \{y^*[n]\} = \{\cos(0.3n)\} - j\{\sin(0.3n)\} = \{e^{-j0.3n}\} \quad (2.7)$$

### 2.1.1 Categorization of discrete-time signals

*Continuous and discrete-valued signals*

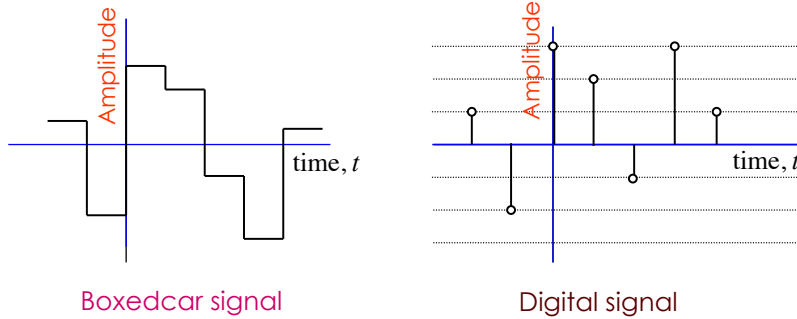
We can have two types of discrete-time signals:

- sampled-data signals in which the samples are **continuous-valued**;
- digital signals in which the samples are **discrete-valued**.

Signals in a practical digital signal processing system are digital signals obtained by quantizing the sample values either by rounding or truncation. An example of visualization is showed in Figure 2.3.

*Finite and infinite-length discrete-time signals*

Again, a discrete-time signal may be a **finite-length** or an **infinite-length** sequence. In the first case, the sequence is defined only for a finite time interval, namely for  $N_1 \leq n \leq N_2$ , where  $-\infty < N_1$ ,  $N_2 < \infty$  and  $N_1 \leq N_2$ . The length or duration of the ladder is  $N = N_2 - N_1 + 1$ .

**Figure 2.3:** Different way to visualize a signal.

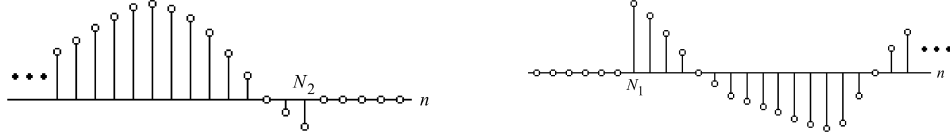
A length- $N$  sequence is often referred to as an  $N$ -point sequence. In general, the length of a finite-length sequence can be increased by using the zero-padding, namely by appending it with zeros. For example:

$$x_p[n] = \begin{cases} n^2 & -3 \leq n \leq 4 \\ 0 & 5 \leq n \leq 8 \end{cases} \quad (2.8)$$

is a finite-length sequence of length 12 obtained by zero-padding  $x[n] = n^2$ ,  $-3 \leq n \leq 4$ , with 4 zero-valued samples.

There is another categorization: a discrete-time signal can be **right-sided** or **left-sided**. A right-sided sequence  $x[n]$  has zero-valued samples for  $n < N_1$ . Moreover, if  $N_1 \geq 0$ , a right-sided sequence is called a **causal sequence**. On the other side, a left-sided sequence  $x[n]$  has zero-valued samples for  $n > N_2$  and if  $N_2 \leq 0$ , it is an **anti-causal sequence**. An example of both the types is showed in Figure 2.4.

*Right and  
left-sided  
discrete-time  
signals and  
(anti)-causal  
sequences*

**Figure 2.4:** Examples of a left-sided sequence (left) and a right-sided sequence (right).

### 2.1.2 Norm of a discrete-time signal

When dealing with the analysis of discrete signal, the concept of norm is frequent. In particular, the  $L_p$ -norm of a signal reads:

$$\|x\|_p = \left( \sum_{n=-\infty}^{\infty} |x[n]|^p \right)^{\frac{1}{p}} \quad (2.9)$$

where  $p$  is a positive integer. The ladder definition provides an estimate of the size of the signal. The value of  $p$  is typically 1, 2 or  $\infty$ :

- $p = 1$ :  $\|x\|_1$  is the absolute value of  $\{x[n]\}$ ;
- $p = 2$ :  $\|x\|_2$  is the Root-Mean-Squared (RMS) value of  $\{x[n]\}$ ;
- $p = \infty$ :  $\|x\|_\infty$  is the peak absolute value of  $\{x[n]\}$ , namely  $\|x\|_\infty = |x|_{\max}$ .

*Norm of a  
discrete-time signal*

We given an example to understand the application of the norm.

**Example 2: Norm of a signal**

Let  $\{y[n]\}$ ,  $0 \leq n \leq N - 1$ , be an approximation of  $\{x[n]\}$ ,  $0 \leq n \leq N - 1$ . An estimate of the relative error is given by the ratio of the  $L_2$ -norm of the difference signal and the  $L_2$ -norm of  $\{x[n]\}$ :

*Relative error*

$$E_{\text{rel}} = \left( \frac{\left( \sum_{n=0}^{N-1} |y[n] - x[n]|^2 \right)^{\frac{1}{p}}}{\left( \sum_{n=0}^{N-1} |x[n]|^2 \right)^{\frac{1}{p}}} \right) \quad (2.10)$$

## 2.2 Operations on sequences

In order to apply a certain operation on a discrete-time signal we can employ a discrete-time system. If the latter is single-input and single-output, it operates on an input sequence, according to some prescribed rules, and develops another sequence, called the output sequence, with more desirable properties. This process is schematized in Figure 2.5.

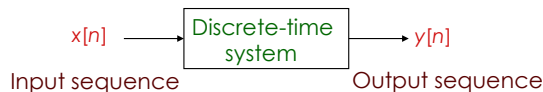


**Figure 2.5:** Scheme of operation on an input sequence, returning an output sequence.

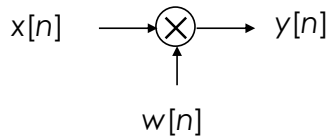
### 2.2.1 Basic operations

In most cases, the operation defining a particular discrete-time system is composed of some basic operations, which we are going to list and study:

*Product operation  
and windowing*

- **product** (modulation) operation:  $y[n] = x[n] \cdot w[n]$

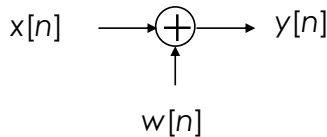
It is employed to form a finite-length sequence from an infinite-length sequence by multiplying the latter with a finite-length sequence called **window sequence**;



**Figure 2.6:** Scheme of product operation.

*Addition operation*

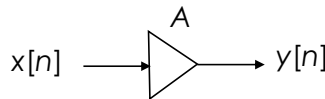
- **addition** operation:  $y[n] = x[n] + w[n]$



**Figure 2.7:** Scheme of addition operation.

*Multiplication  
operation*

- **multiplication** operation:  $y[n] = A \cdot x[n]$

**Figure 2.8:** Scheme of multiplication operation.

- **time-shifting** operation:  $y[n] = x[n - N]$ ,  $N \in \mathbb{Z}$

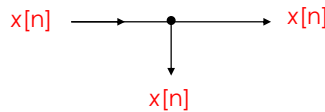
If  $N > 0$ , it is a delaying opeartion. In particular, we have the unit delay with  $y[n] = x[n - 1]$ . If  $N > 0$ , it is an advance operation, with the particular case of unit advance  $y[n] = x[n + 1]$ ;

*Time-shifting operation*

**Figure 2.9:** Schemes of delaying time-shift (left) and delaying time advance (right) operations.

- **time-reversal** operation:  $y[n] = x[-n]$
- **branching** operation: it provides multiple copies of a sequence.

*Time-reversal operation*  
*Branching operation*

**Figure 2.10:** Scheme of branching operation.

When applying these operations, some caution has to be kept. In fact, operations on two or more sequences can be carried out if all sequences involved are of the same length and defined for the same range of the time index  $n$ . However, if the sequences are not of the same length, in some situations, this problem can be circumvented by **appending zero-valued samples** to the sequence(s) of smaller lengths to make all sequences have the same range of the time index.

## 2.2.2 Ensemble averaging

This composite operation is a very simple application of the addition operation, useful to improve the quality of measured data corrupted by an additive random noise. In some cases, actual uncorrupted data vector  $\vec{s}$  remains essentially the same from one mesurement to next, while the additive noise vector is random and not reproducible. Let us denote with  $\vec{d}_i$  the noise vector corrupting the  $i^{\text{th}}$  measurement of the uncorrupted data vector  $\vec{s}$ :

$$\vec{x}_i = \vec{s} + \vec{d}_i \quad (2.11)$$

The average data vector, called the **ensemble average**, obtained after  $k$  measurements is given by:

$$\vec{x}_{\text{avg}} = \frac{1}{k} \sum_{i=1}^k \vec{x}_i = \frac{1}{k} \sum_{i=1}^k (\vec{s} + \vec{d}_i) = \vec{s} + \frac{1}{k} \sum_{i=1}^k \vec{d}_i \quad (2.12)$$

*Ensable averaging to improve data quality*

For large values of  $k$ ,  $\vec{x}_{\text{avg}}$  is usually a reasonable replica of the desired data vector  $\vec{s}$ . An example of results obtained by the application of this operation is showed in the plots in Figure 2.11.

Another more general example of ensable average is showed by the scheme in Figure 2.12, where the figuring block operation reads:

$$y[n] = \alpha_1 x[n] + \alpha_2 x[n - 1] + \alpha_3 x[n - 2] + \alpha_4 x[n - 3] \quad (2.13)$$

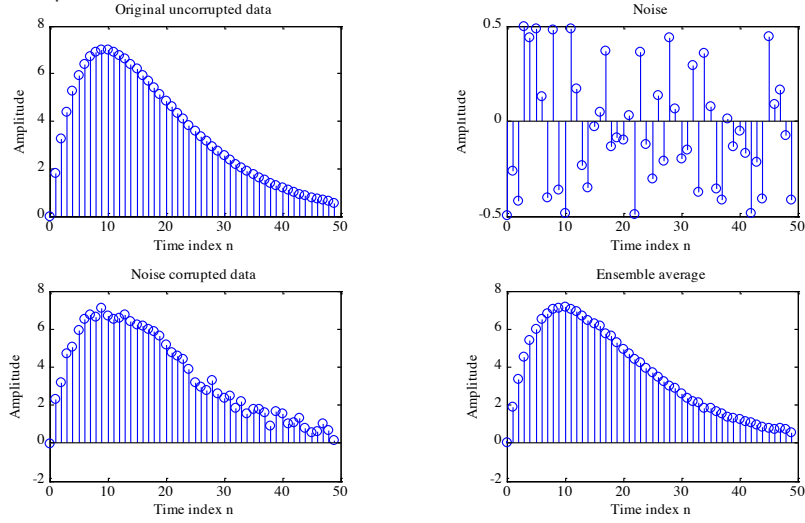


**Figure 2.11:** Example of results obtained by the application of the ensemble average.

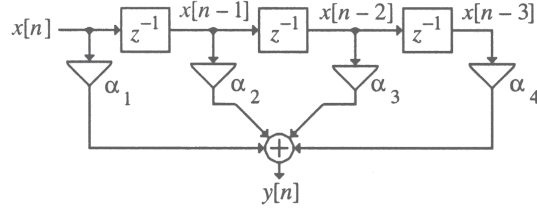


**Figure 2.12:** Ensemble average block, performing the operation in Eq. 2.13.

### 2.2.3 Sampling rate alteration

This is another more complex operation employed to generate a new sequence  $y[n]$  with a sampling rate  $F'_T$  higher or lower than that of the sampling rate  $F_T$  of a given sequence  $x[n]$ . The sampling rate alteration ratio reads:

$$R = \frac{F'_T}{F_T} \quad (2.14)$$

*Sampling rate alteration*

*Interpolation and decimation*

*Up-sampler*

*Down-sampler*

In particular:

- if  $R > 1$ , the process is called **interpolation**;
- if  $R < 1$ , the process is called **decimation**.

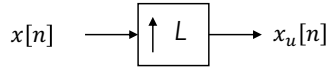
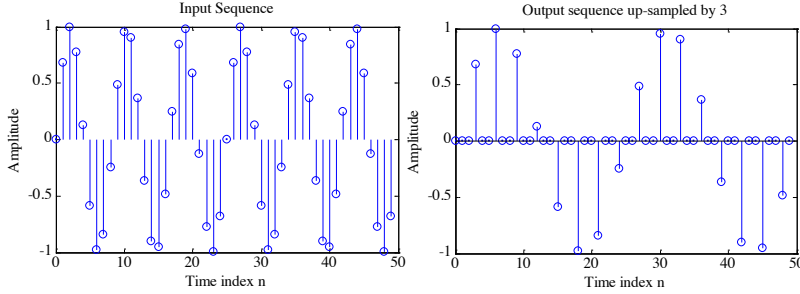
In the case of **up-sampling** by an integer factor  $L > 1$ ,  $L - 1$  equidistant zero-valued samples are inserted by the up-sampler between each two consecutive samples of the input sequence  $x[n]$ :

$$x_u[n] = \begin{cases} x\left[\frac{n}{L}\right] & n = 0, \pm L, \pm 2L, \dots \\ 0 & \text{otherwise} \end{cases} \quad (2.15)$$

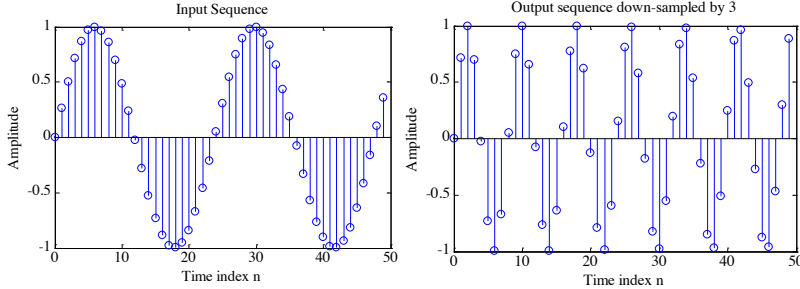
The scheme of this operation is showed in Figure 2.13. An example of the results obtained by the application to a certain input sequence are showed in the plots in Figure 2.14.

On the other hand, in the case of **down-sampling** by an integer factor  $M > 1$ , every  $M^{\text{th}}$  samples of the input sequence are kept and  $M - 1$  in-between samples are removed:

$$y[n] = x[nM] \quad (2.16)$$

**Figure 2.13:** Scheme of up-sampling operation.**Figure 2.14:** Example of results obtained by the application of the up-sampling.

The scheme of this operation is showed in Figure 2.15. An example of the results obtained by the application to a certain input sequence are showed in the plots in Figure 2.16.

**Figure 2.15:** Scheme of down-sampling operation.**Figure 2.16:** Example of results obtained by the application of the down-sampling.

## 2.3 Classification of sequences

Several classifications of discrete-time sequences are possible, based on certain features of the sequences themselves.

A first classification is based on the symmetry of the sequence. In fact, we can have **conjugate-symmetric** sequences, namely satisfying

$$x[n] = x^*[-n] \quad (2.17)$$

If  $x[n]$  is real, then it is an **even sequence**.

Another possibility is a **conjugate-antisymmetric** sequence, namely satisfying:

$$x[n] = -x^*[-n] \quad (2.18)$$

Again, if  $x[n]$  is real, then it is an **odd sequence**.

It follows from the definition that for a conjugate-symmetric sequence  $\{x[n]\}$ ,  $x[0]$  must be a real number. Likewise, for a conjugate antisymmetric sequence  $\{y[n]\}$ ,

*Classification  
based on symmetry*

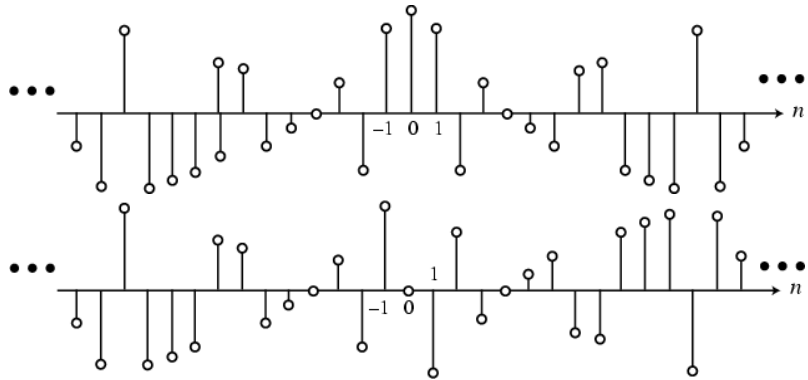


**Figure 2.17:** Example of even (top) and odd (bottom) sequences.

$y[0]$  must be an imaginary number. Another consequence is that for an odd sequence  $\{w[n]\}$ ,  $w[0] = 0$ .

Any complex sequence can be expressed as a sum of its conjugate-symmetric part and its conjugate-antisymmetric part:

$$x[n] = x_{\text{cs}}[n] + x_{\text{ca}}[n] \quad (2.19)$$

where:

$$x_{\text{cs}}[n] = \frac{1}{2}(x[n] + x^*[-n]) \quad (2.20)$$

$$x_{\text{ca}}[n] = \frac{1}{2}(x[n] - x^*[-n]) \quad (2.21)$$

### Example 3: Classification based on symmetry

We consider the length-7 sequence defined for  $-3 \leq n \leq 3$  and its conjugate and time reversed versions:

$$\{g[n]\} = \{0, 1 + j4, -2 + j3, 4 - j2, -5 - j6, -j2, 3\} \quad (2.22)$$

$$\{g^*[n]\} = \{0, 1 - j4, -2 - j3, 4 + j2, -5 + j6, j2, 3\} \quad (2.23)$$

$$\{g^*[-n]\} = \{3, j2, -5 + j6, 4 + j2, -2 - j3, 1 - j4, 0\} \quad (2.24)$$

Therefore:

$$\{g_{\text{cs}}[n]\} = \{1.5, 0.5 + j3, -3.5 + j4.5, 4, -3.5 - j4.5, 0.5 - j3, 1.5\} \quad (2.25)$$

$$\{g_{\text{ca}}[n]\} = \{-1.5, 0.5 + j, 1.5 - j1.5, -j2, -1.5 - j1.5, -0.5 - j, 1.5\} \quad (2.26)$$

It can be easily verified that  $g_{\text{cs}}[n] = g_{\text{cs}}^*[-n]$  and  $g_{\text{ca}}[n] = -g_{\text{ca}}^*[-n]$ .

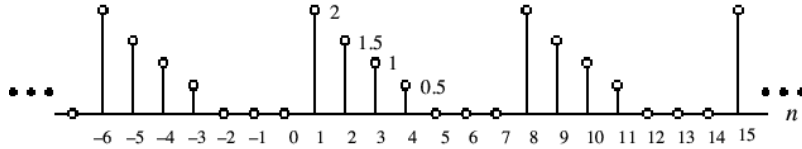
Now, specializing the previous discussion to real sequences, any of them can be expressed as a sum of its even part and its odd part:

$$x[n] = x_{\text{ev}}[n] + x_{\text{od}}[n] \quad (2.27)$$

where:

$$x_{\text{ev}}[n] = \frac{1}{2}(x[n] + x[-n]) \quad (2.28)$$

$$x_{\text{od}}[n] = \frac{1}{2}(x[n] - x[-n]) \quad (2.29)$$

**Figure 2.18:** Example of periodic sequence.

A sequence  $\tilde{x}[n]$  satisfying  $\tilde{x}[n] = \tilde{x}[n + kN]$  is called a **periodic sequence** with a period  $N$  where  $N$  is a positive integer and  $k$  is any integer. The smallest value of  $N$  satisfying  $\tilde{x}[n] = \tilde{x}[n + kN]$  is called the **fundamental period**. A sequence not satisfying the periodicity condition is called an **aperiodic sequence**.

Before introducing the classification based on energy and power of the signal, we have to introduce the previous concepts.

The **total energy** of a sequence  $x[n]$  is defined by:

*Definition of energy*

$$E_x = \sum_{n=-\infty}^{\infty} |x[n]|^2 \quad (2.30)$$

An infinite length sequence with finite sample values may or may not have finite energy. On the other hand, a finite length sequence with finite sample values has finite energy.

The **average power** of an aperiodic sequence is defined by:

*Definition of average power*

$$P_x = \lim_{k \rightarrow \infty} \frac{1}{2k+1} \sum_{n=-k}^k |x[n]|^2 \quad (2.31)$$

We can also define the energy of a sequence  $x[n]$  over a finite interval  $-k \leq n \leq k$  as:

$$E_{x,k} = \sum_{n=-k}^k |x[n]|^2 \quad (2.32)$$

Then, the averaged power reads:

$$P_x = \lim_{k \rightarrow \infty} \frac{1}{2k+1} E_{x,k} \quad (2.33)$$

The average power of a periodic sequence  $\tilde{x}[n]$  with a period  $N$  is given by:

$$P_x = \frac{1}{N} \sum_{n=0}^{N-1} |\tilde{x}[n]|^2 \quad (2.34)$$

The average power of an infinite-length sequence may be finite or infinite.

We come now to the classification based on the energy and the power:

*Classification based on energy and power*

- an infinite energy signal with finite average power is called a **power signal**. As example, one can think about a periodic sequence, which has a finite average power but infinite energy;
- a finite energy signal with zero average power is called an **energy signal**. As example, one can think about a finite-length sequence which has finite energy but zero average power.

**Example 4: Classification based on energy and power**

We consider the causal sequence defined by:

$$x[n] = \begin{cases} 3(-1)^n & n \geq 0 \\ 0 & n < 0 \end{cases} \quad (2.35)$$

Note that  $x[n]$  has infinite energy and its average power is given by:

$$P_x = \lim_{k \rightarrow \infty} \frac{1}{2k+1} \left( 9 \sum_{n=0}^k 1 \right) = \lim_{k \rightarrow \infty} \frac{9(k+1)}{2k+1} = 4.5 \quad (2.36)$$

*Bounded sequences*

We move now to other types of classifications. A sequence  $x[n]$  is said to be **bounded** if:

$$|x[n]| \leq B_x < \infty \quad (2.37)$$

*Absolutely summable sequences*

For example, the sequence  $x[n] = \cos(0.3\pi n)$  is bounded since the cosine is bounded between  $-1$  and  $1$ .

A sequence  $x[n]$  is said to be **absolutely summable** if:

$$\sum_{n=-\infty}^{\infty} |x[n]| < \infty \quad (2.38)$$

**Example 5: Absolute summable sequences**

The sequence:

$$y[n] = \begin{cases} 0.3^n & n \geq 0 \\ 0 & n < 0 \end{cases} \quad (2.39)$$

is absolutely summable since:

$$\sum_{n=0}^{\infty} |0.3^n| = \frac{1}{1-0.3} \approx 1.42857 < \infty \quad (2.40)$$

*Square summable sequences*

A sequence  $x[n]$  is said to be **square summable** if:

$$\sum_{n=-\infty}^{\infty} |x[n]|^2 < \infty \quad (2.41)$$

For example, the sequence:

$$h[n] = \frac{\sin(0.4n)}{\pi n} \quad (2.42)$$

is square summable but no absolutely summable.

## 2.4 Basic signals

In this Section, we list some of the most common discrete-time sequences that we find in this field.

### 2.4.1 Unit sample sequence

The **unit sample** sequence is defined as:

$$\delta[n] = \begin{cases} 0 & n \neq 0 \\ 1 & n = 0 \end{cases} \quad (2.43)$$

and it is visualized in Figure 2.19.

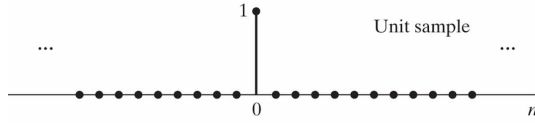


**Figure 2.19:** Unit sample sequence.

The importance of this type of sequence stem from the fact that an arbitrary sequence can be represented as a sum of scaled, delayed impulses:

$$x[n] = \sum_{k=-\infty}^{\infty} x[k]\delta[n-k] \quad (2.44)$$

### 2.4.2 Unit step sequence

The **unit step** sequence is defined as:

*Unit step sequence*

$$u[n] = \begin{cases} 0 & n \geq 0 \\ 1 & n < 0 \end{cases} \quad (2.45)$$

and it is visualized in Figure 2.20.

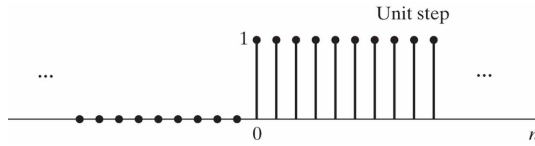


**Figure 2.20:** Unit step sequence.

The unit step can be expressed in terms of unit samples as:

$$u[n] = \sum_{k=0}^{\infty} \delta[n-k] \quad (2.46)$$

### 2.4.3 Real sinusoidal sequence

The **real sinusoidal** sequence is defined as:

*Real sinusoidal sequence*

$$x[n] = A \cos(\omega_0 n + \varphi) \quad (2.47)$$

where  $A$  is the amplitude,  $\omega_0$  is the angular frequency, and  $\varphi$  is the phase of  $x[n]$ . It is visualized in Figure 2.21.

### 2.4.4 Exponential sequence

The **exponential** sequence is defined as:

*Exponential sequence*

$$x[n] = A\alpha^n, \quad -\infty < n < \infty \quad (2.48)$$

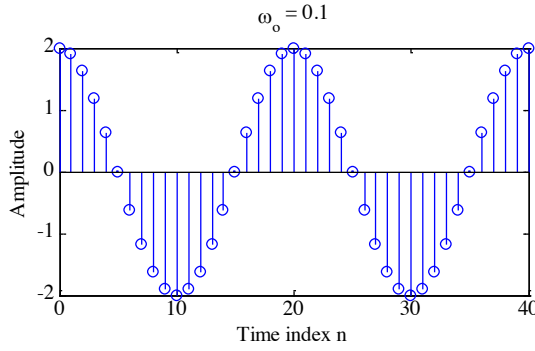


**Figure 2.21:** Real sinusoidal sequence.

where  $A$  and  $\alpha$  are real or complex numbers. If we rewrite:

$$\alpha = e^{\sigma_0 + j\omega_0} \quad (2.49)$$

$$A = |A|e^{j\varphi} \quad (2.50)$$

then we can express:

$$x[n] = |A|e^{j\varphi}e^{(\sigma_0 + j\omega_0)n} = x_{\text{re}}[n] + jx_{\text{im}}[n] \quad (2.51)$$

where:

$$x_{\text{re}}[n] = |A|e^{\sigma_0 n} \cos(\omega_0 n + \varphi) \quad (2.52)$$

$$x_{\text{im}}[n] = |A|e^{\sigma_0 n} \sin(\omega_0 n + \varphi) \quad (2.53)$$

$x_{\text{re}}[n]$  and  $x_{\text{im}}[n]$  of a complex exponential sequence are real sinusoidal sequences with constant ( $\sigma_0 = 0$ ), growing ( $\sigma_0 > 0$ ) and decaying ( $\sigma_0 < 0$ ) amplitudes for  $n > 0$ . This is visualized in Figure 2.22.

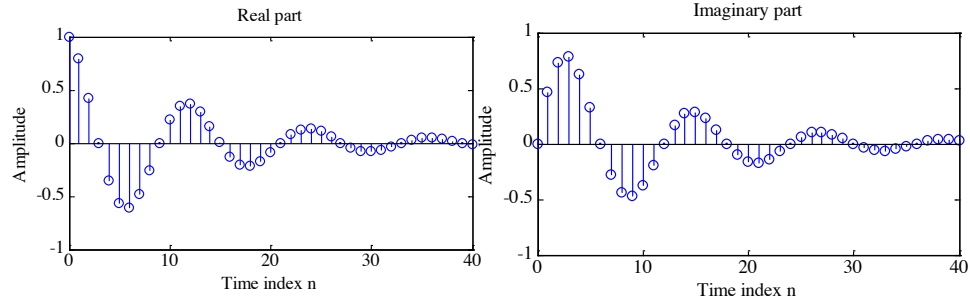


**Figure 2.22:** Real and imaginary part of an exponential sequence.

If we consider a real exponential sequence:

$$x[n] = A\alpha^n, \quad -\infty < n < \infty \quad (2.54)$$

where  $A$  and  $\alpha$  are real numbers, we get results similar to the ones in Figure 2.23. Note that the sinusoidal sequence  $A \cos(\omega_0 n + \varphi)$  and the complex exponential sequence  $B e^{j\omega_0 n}$  are periodic sequences of period  $N$  if  $\omega_0 \pi = 2\pi r$ , where  $N$  and  $r$  are positive integers. The smallest value of  $N$  satisfying the latter equality is the fundamental period of the sequence, as we have already seen previously. To verify this fact, we consider:

$$x_1[n] = \cos(\omega_0 n + \varphi) \quad (2.55)$$

$$x_2[n] = \cos(\omega_0(n + N) + \varphi) \quad (2.56)$$

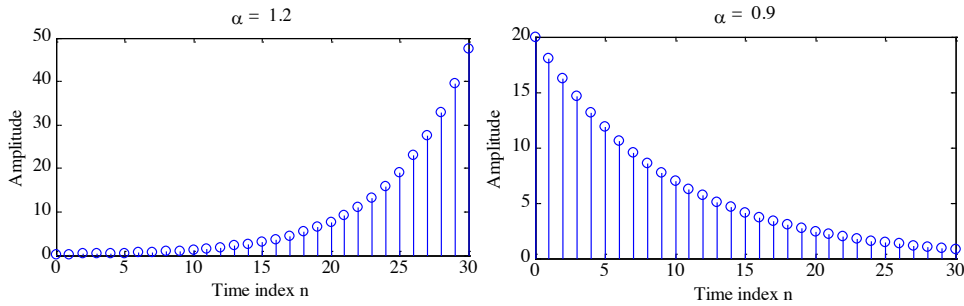


**Figure 2.23:** Amplitude of the real exponential sequence in Eq. 2.54, for  $\alpha = 1.2$  (left) and  $\alpha = 0.9$  (right).

Now:

$$\begin{aligned} x_2[n] &= \cos(\omega_0(n + N) + \varphi) \\ &= \cos(\omega_0n + \varphi) \cos(\omega_0N) - \sin(\omega_0n + \varphi) \sin(\omega_0N) \end{aligned} \quad (2.57)$$

which will be equal to  $\cos(\omega_0n + \varphi) = x_1[n]$  only if  $\sin(\omega_0N) = 0$  and  $\cos(\omega_0N) = 1$ . These two conditions are met if and only if  $\omega_0N = 2\pi r$  or  $\frac{2\pi}{\omega_0} = \frac{N}{r}$ . If  $\frac{2\pi}{\omega_0}$  is a non-integer rational number, then the period will be a multiple of  $\frac{2\pi}{\omega_0}$ , otherwise the sequence is aperiodic.

From the previous discussion, we can extract two properties:

- let us consider  $x[n] = e^{j\omega_1 n}$  and  $y[n] = e^{j\omega_2 n}$ , with  $0 \leq \omega_1 \leq \pi$  and  $2\pi k \leq \omega_2 < 2\pi(k+1)$ , where  $k$  is any positive integer. If  $\omega_2 = \omega_1 + 2\pi k$ , then  $x[n] = y[n]$ . Thus,  $x[n]$  and  $y[n]$  are indistinguishable;
- the frequency of oscillation of  $A \cos(\omega_0)$  increases as  $\omega_0$  increases from 0 to  $\pi$ , and then decreases as  $\omega_0$  increases from  $\pi$  to  $2\pi$ . Thus frequencies in the neighborhood of  $\omega = 0$  are called **low frequencies**, whereas, frequencies in the neighborhood of  $\pi$  are called **high frequencies**.



# Chapter 3

## Discrete-Time systems

In this Chapter we will introduce the concept of discrete-time system in the framework of Hilbert spaces and we will study how linear algebra can be extremely useful when dealing with this kind of systems.

A discrete-time system processes a given input sequence  $x[n]$  to generate an output sequence  $y[n]$  with more desirable properties. In most applicationns, the discrete-time system is a single-input and single-output system, just like in the scheme in Figure 3.1.

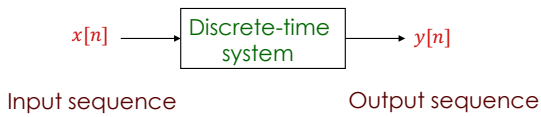


**Figure 3.1:** Scheme of a single-input single-output discrete-time system.

**Lecture 3.**  
Tuesday 6<sup>th</sup>  
October, 2020.  
Discrete-time  
system

### 3.1 Examples of discrete-time systems

Some already seen examples of discrete-time systems are the modulator and the adder, which are 2-input 1-output systems, and the multiplier, the unit delay, the unit advance, which are 1-input 1-output. In this Section, we study other types of systems.

#### 3.1.1 Accumulator system

The output of the **accumulator**  $y[n]$  at time instant  $n$  is the sum of the input sample  $x[n]$  at time instant  $n$  and the previous output  $y[n - 1]$  at time instant  $n - 1$ , which is the sum of all previous input sample values from  $-\infty$  to  $n - 1$ . Mathematically, this reads:

$$\begin{aligned} y[n] &= \sum_{\ell=-\infty}^n x[\ell] = \sum_{\ell=-\infty}^{n-1} x[\ell] \\ &= y[n - 1] + x[n] \end{aligned} \tag{3.1}$$

Accumulator  
system

So, the system cumulatively adds, namely it accumulates all input sample values. The input-output relation can also be rewritten in the form:

$$\begin{aligned} y[n] &= \sum_{\ell=-\infty}^{-1} x[\ell] + \sum_{\ell=0}^n x[\ell] \\ &= y[-1] + \sum_{\ell=0}^n x[\ell], \quad n \geq 0 \end{aligned} \tag{3.2}$$

This form is used for a causal input sequence, in which case  $y[-1]$  is called the initial condition.

### 3.1.2 *M*-point moving average system

*M*-point moving average system

The ***M*-point moving average** is used to smooth random variations in data. In fact, the operation it applies reads:

$$y[n] = \frac{1}{M} \sum_{k=0}^{M-1} x[n - k] \quad (3.3)$$

In most applications, the data  $x[n]$  is a bounded sequence, so also the *M*-point average  $y[n]$  is a bounded sequence. Moreover, if there is no bias in the measurements, an improved estimate of the noisy data is obtained by simply increasing  $M$ .

From a complexity point of view, the direct implementation of this system requires  $M - 1$  additions, 1 division and the storage of the  $M - 1$  past input data samples. However, a more efficient implementation can be developed if we write:

Recursive *M*-point moving average system

$$\begin{aligned} y[n] &= \frac{1}{M} \left( \sum_{\ell=0}^{M-1} x[n - \ell] + x[n - M] - x[n - M] \right) \\ &= \frac{1}{M} \left( \sum_{\ell=1}^M x[n - \ell] + x[n] - x[n - M] \right) \\ &= \frac{1}{M} \left( \sum_{\ell=0}^{M-1} x[n - 1 - \ell] + x[n] - x[n - M] \right) \\ &= y[n - 1] + \frac{1}{M} (x[n] - x[n - M]) \end{aligned} \quad (3.4)$$

In this case, the computation of the *M*-point moving average system is recursive and it requires only 2 additions and 1 division.

Let us consider an application using this system.

#### Example 6: *M*-point moving average system

We consider a signal  $s[n]$  corrupted by a noise  $d[n]$ , namely:

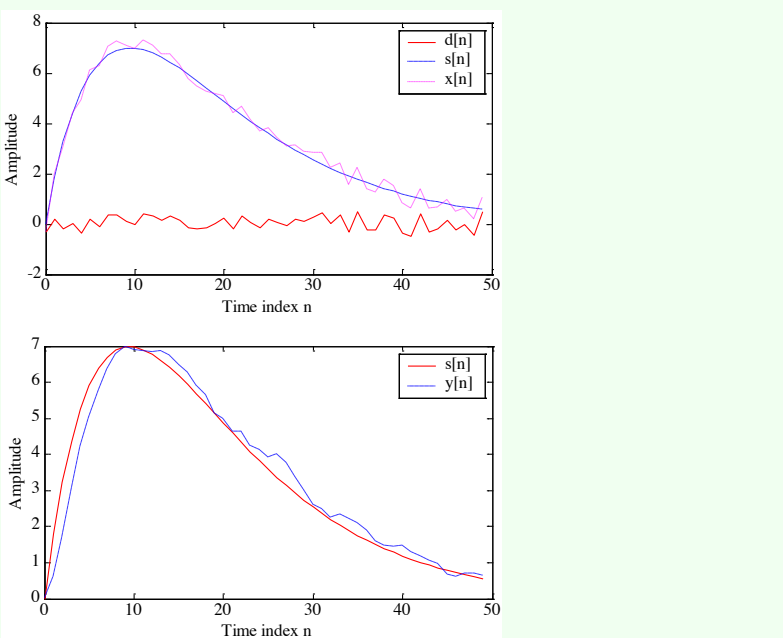
$$x[n] = s[n] + d[n] \quad (3.5)$$

In particular:

$$s[n] = 2[n(0.9)^n] \quad (3.6)$$

$$d[n] = \text{random signal} \quad (3.7)$$

The results obtained by applying the moving average are showed below:



### 3.1.3 Exponentially weighted running average system

In this case, the computation of the **exponentially weighted running average** requires only 2 additions, 1 multiplication and the storage of the previous running average and it does not require the storage of past input data samples. Mathematically, the operation applied reads:

$$y[n] = \alpha y[n - 1] + x[n], \quad 0 < \alpha < 1 \quad (3.8)$$

In particular, for  $0 < \alpha < 1$ , the exponentially weighted average filter places more emphasis on current data samples and less emphasis on past data samples. In fact:

$$\begin{aligned} y[n] &= \alpha(\alpha y[n - 2] + x[n - 1]) + x[n] \\ &= \alpha^2 y[n - 2] + \alpha x[n - 1] + x[n] \\ &= \alpha^2 (\alpha y[n - 3] + x[n - 2]) + \alpha x[n - 1] + x[n] \\ &= \alpha^3 y[n - 3] + \alpha^2 x[n - 2] + \alpha x[n - 1] + x[n] \end{aligned} \quad (3.9)$$

*Exponentially weighted running average system*

### 3.1.4 Linear interpolation system

The **linear interpolation** is employed to estimate the sample values between pairs of adjacent samples of a discrete-time system. A clear example of how this stuff works is showed in Figure 3.2, where the so called factor-of-4 interpolation is employed.

Now, we explain how it works mathematically. If we consider the factor-of-2 interpolator, the operation it performs reads:

$$y[n] = x_u[n] + \frac{1}{2}(x_u[n - 1] + x_u[n + 1]) \quad (3.10)$$

*Linear interpolation system*

Again, the operation performed by a factor-of-3 interpolator reads:

$$y[n] = x_u[n] + \frac{1}{3}(x_u[n - 1] + x_u[n + 2]) + \frac{2}{3}(x_u[n - 2] + x_u[n + 1]) \quad (3.11)$$

and so on and so forth. The application of a factor-of-2 interpolator to an image for can be observed in Figure 3.3. This is a simple example of compression and decompression of informations.

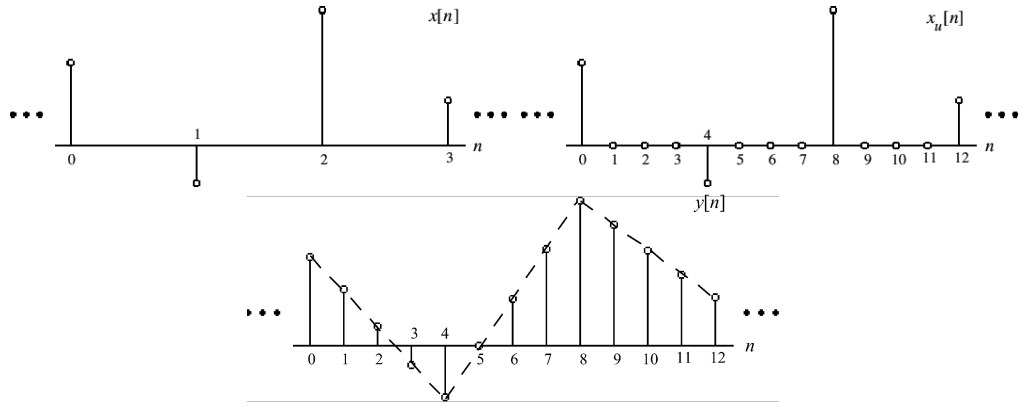


**Figure 3.2:** Result of the factor-of-4 interpolation.

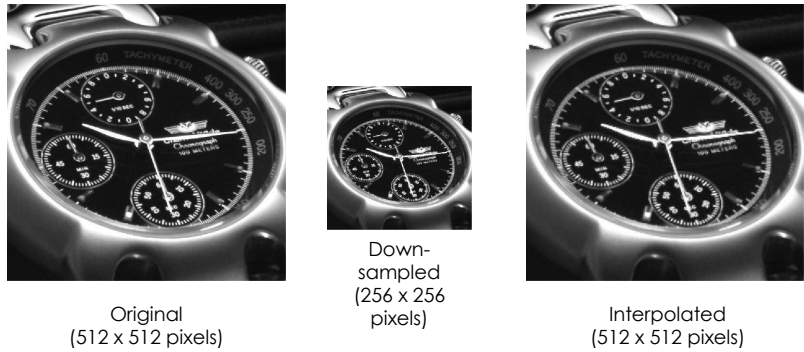


**Figure 3.3:** Application of a factor-of-2 interpolator to a watch image, which is down-sampled before applying the operation.

### 3.1.5 Median system

Median system

The **median** of a set of  $(2k + 1)$  numbers is the number such that  $k$  numbers from the set have values greater than this number and the other  $k$  numbers have smaller values. The median can be determined by rank-ordering the numbers in the set by their values and choosing the number in the middle.

#### Example 7: Median system

If we consider the set of numbers:

$$\{2, -3, 10, 5, -1\} \quad (3.12)$$

the rank-order set is given by:

$$\{-3, -1, 2, 5, 10\} \quad (3.13)$$

and hence, the median is 2

Now, a median filter can be implemented by sliding a window of odd length over the input sequence  $\{x[n]\}$  one sample at a time. The output  $y[n]$  at the instant  $n$  is the median value of the samples inside the window centered at  $n$ . A possible application is found in removing additive random noise, which shows up as sudden large errors in the corrupted signal. Some plots of the result of this application are showed in Figure 3.4.

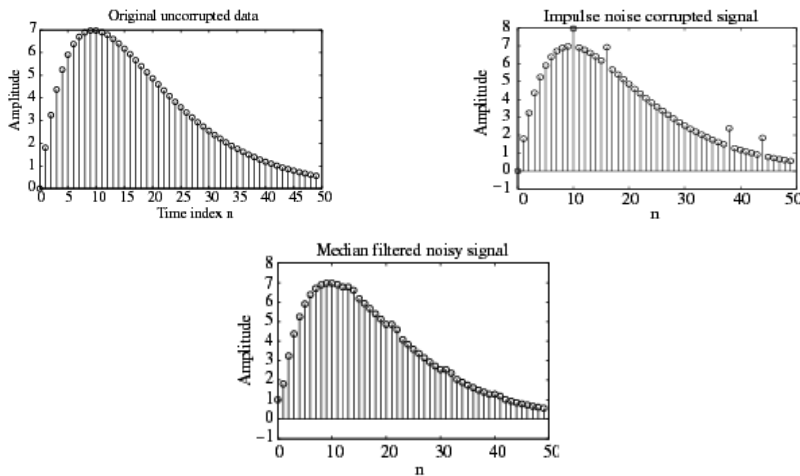


**Figure 3.4:** Example of results of the application of median filtering to a corrupted signal.

## 3.2 Classification of discrete-time systems

After having sketched some common examples, in this Section we present the classification of discrete-system based on their features and we enter into the detail by studying each of them. We can have:

- linear systems;
- shift-invariant systems;
- causal systems;
- stable systems;
- passive and lossless systems.

### 3.2.1 Linear systems

#### Definition 1: Linear systems

*Definition of linear system*

If  $y_1[n]$  is the output due to an input  $x_1[n]$  and  $y_2[n]$  is the output due to an input  $x_2[n]$ , then for an input:

$$x[n] = \alpha x_1[n] + \beta x_2[n] \quad (3.14)$$

the output is given by:

$$y[n] = \alpha y_1[n] + \beta y_2[n] \quad (3.15)$$

This property must hold for any arbitrary constants  $\alpha$  and  $\beta$  and for all possible inputs  $x_1[n]$  and  $x_2[n]$  in order to have a **linear system**.

Let us return to the accumulator example. Here we show that this is a linear system. In fact, if we consider the accumulator outputs for the input sequences  $x_1[n]$  and

*Linear systems:  
the accumulator*

$x_2[n]$ , which read respectively:

$$y_1[n] = \sum_{\ell=-\infty}^n x_1[\ell] \quad (3.16)$$

$$y_2[n] = \sum_{\ell=-\infty}^n x_2[\ell] \quad (3.17)$$

then the output for an input  $x[n] = \alpha x_1[n] + \beta x_2[n]$  reads:

$$\begin{aligned} y[n] &= \sum_{\ell=-\infty}^n (\alpha x_1[\ell] + \beta x_2[\ell]) \\ &= \alpha \sum_{\ell=-\infty}^n x_1[\ell] + \beta \sum_{\ell=-\infty}^n x_2[\ell] \\ &= \alpha y_1[n] + \beta y_2[n] \end{aligned} \quad (3.18)$$

If we consider tha accumulator with causal input applied at  $n = 0$ , the outputs  $y_1[n]$  and  $y_2[n]$  for inputs  $x_1[n]$  and  $x_2[n]$  are given by:

$$y_1[n] = y_1[-1] + \sum_{\ell=0}^n x_1[\ell] \quad (3.19)$$

$$y_2[n] = y_2[-1] + \sum_{\ell=0}^n x_2[\ell] \quad (3.20)$$

Moreover, the output  $y[n]$  for an input  $\alpha x_1[n] + \beta x_2[n]$  is given by:

$$y[n] = y[-1] + \sum_{\ell=0}^n (\alpha x_1[\ell] + \beta x_2[\ell]) \quad (3.21)$$

and, again, for  $\alpha y_1[n] + \beta y_2[n]$ :

$$\begin{aligned} y[n] &= \alpha y_1[n] + \beta y_2[n] \\ &= \alpha \left( y_1[-1] + \sum_{\ell=0}^n x_1[\ell] \right) + \beta \left( y_2[-1] + \sum_{\ell=0}^n x_2[\ell] \right) \\ &= (\alpha y_1[-1] + \beta y_2[-1]) + \left( \alpha \sum_{\ell=0}^n x_1[\ell] + \beta \sum_{\ell=0}^n x_2[\ell] \right) \end{aligned} \quad (3.22)$$

Thus, if  $y[-1] = \alpha y_1[-1] + \beta y_2[-1]$ :

$$y[n] = \alpha y_1[n] + \beta y_2[n] \quad (3.23)$$

For the causal accumulator to be linear, the condition  $y[-1] = \alpha y_1[-1] + \beta y_2[-1]$  must gold for all initial conditions  $y[-1]$ ,  $y_1[-1]$ ,  $y_2[-1]$ , and for all constants  $\alpha$  and  $\beta$ . This condition cannot be satisfied unless the accumulator is initially at rest with zero initial condition. Instead, for non-zero initial condition, the system is non-linear.

*Non-linear systems:  
the median filter*

Let us move to the median filter example in the contest of linear systems discussion. The median filter described earlier is a non-linear dscrete-time system. To show this, we consider an example with a window length of 3. The output of the filter for an input:

$$\{x_1[n]\} = \{3, 4, 5\}, \quad 0 \leq n \leq 2 \quad (3.24)$$

is:

$$\{y_1[n]\} = \{3, 4, 4\}, \quad 0 \leq n \leq 2 \quad (3.25)$$

Again, the output for an input:

$$\{x_2[n]\} = \{2, -1, -1\}, \quad 0 \leq n \leq 2 \quad (3.26)$$

is:

$$\{y_2[n]\} = \{0, -1, -1\}, \quad 0 \leq n \leq 2 \quad (3.27)$$

However, the output for the sum of the previous inputs:

$$\{x[n]\} = \{x_1[n] + x_2[n]\} \quad (3.28)$$

is:

$$\{y[n]\} = \{3, 4, 3\} \neq \{y_1[n] + y_2[n]\} \quad (3.29)$$

Hence, the median filter is a non-linear discrete-time system.

### 3.2.2 Shift-Invariant systems

*Definition of shift-invariant system*

#### Definition 2: Shift-invariant systems

A **shift-invariant system** is a discrete-time system such that, if  $y_1[n]$  is the response to an input  $x_1[n]$ , then the response to an input:

$$x[n] = x_1[n - n_0] \quad (3.30)$$

is:

$$y[n] = y_1[n - n_0] \quad (3.31)$$

where  $n_0$  is any positive or negative integer. This relation must hold for any arbitrary input and its corresponding output.

In the case of sequences and systems with indices  $n$  related to discrete instants of time, the shift-invariance property is called **time-invariance property**. The ladder ensures that for a specified input, the output is independent of the time the input is being applied.

#### Example 8: Shift-invariant system

We consider the up-sampler with an input-output relation given by:

$$x_u[n] \begin{cases} x\left[\frac{n}{L}\right] & n = 0, \pm L, \pm 2L, \dots \\ 0 & \text{otherwise} \end{cases} \quad (3.32)$$

For an input  $x[n] = x_1[n - n_0]$ , the output  $x_{1,u}[n]$  is given by:

$$\begin{aligned} x_{1,u}[n] &= \begin{cases} x\left[\frac{n}{L}\right] & n = 0, \pm L, \pm 2L, \dots \\ 0 & \text{otherwise} \end{cases} \\ &= \begin{cases} x\left[\frac{n-Ln_0}{L}\right] & n = 0, \pm L, \pm 2L, \dots \\ 0 & \text{otherwise} \end{cases} \end{aligned} \quad (3.33)$$

However, from the definition of the up-sampler:

$$x_u[n - n_0] = \begin{cases} x\left[\frac{n-n_0}{L}\right] & n = n_0, n_0 \pm L, n_0 \pm 2L, \dots \\ 0 & \text{otherwise} \end{cases} \neq x_{1,u}[n] \quad (3.34)$$

Hence, the up-sampler is a **time-varying system**.

*Linear  
time-invariant  
(LTI) systems*

Returning to the main discussion, if a system satisfies both the linearity and the time-invariance properties, it is known as **linear time-invariant (LTI) system**. LTI systems are mathematically easy to analyze and characterize, and consequently, easy to design. Indeed, highly useful signal processing algorithms have been developed utilizing this class of systems over the last several decades.

### 3.2.3 Causal systems

*Definition of causal system*

#### Definition 3: Causal systems

A **causal system** is a discrete-time system such that the  $n_0^{\text{th}}$  output sample  $y[n_0]$  depends only on the input samples  $x[n]$  for  $n \leq n_0$  and does not depend on input samples for  $n > n_0$ .

Now, let  $y_1[n]$  and  $y_2[n]$  be the responses of a causal discrete-time system to the inputs  $x_1[n]$  and  $x_2[n]$ , respectively. Then:

$$x_1[n] = x_2[n], \quad n < N \quad (3.35)$$

implies also that:

$$y_1[n] = y_2[n], \quad n < N \quad (3.36)$$

Therefore, for a causal system, changes in output samples do not precede changes in the input samples.

#### Example 9: Causal systems

We give here some examples of causal systems:

$$y[n] = \alpha_1 x[n] + \alpha_2 x[n - 1] + \alpha_3 x[n - 2] + \alpha_4 x[n - 3] \quad (3.37)$$

$$y[n] = b_0 x[n] + b_1 x[n - 1] + b_2 x[n - 2] + \alpha_1 y[n - 1] + \alpha_2 y[n - 2] \quad (3.38)$$

$$y[n] = y[n - 1] + x[n] \quad (3.39)$$

We give here some examples of non-causal systems as well:

$$y[n] = x_u[n] + \frac{1}{2}(x_u[n - 1] + x_u[n + 1]) \quad (3.40)$$

$$y[n] = x_u[n] + \frac{1}{3}(x_u[n - 1] + x_u[n + 2]) + \frac{2}{3}(x_u[n - 2] + x_u[n + 1]) \quad (3.41)$$

Note that a non-causal system can be implemented as a causal system by delaying the output by an appropriate number of samples. For example, a causal implementation of the factor-of-2 interpolator is given by:

$$y[n] = x_u[n - 1] + \frac{1}{2}(x_u[n - 2] + x_u[n]) \quad (3.42)$$

### 3.2.4 Stable systems

#### Definition 4: Stable systems

There are various definitions of stability. We consider here the **bounded-input, bounded-output (BIBO) stability**. If  $y[n]$  is the response to an input  $x[n]$  and if:

$$|x[n]| \leq B_x \quad \forall n \quad (3.43)$$

then:

$$|y[n]| \leq B_y \quad \forall n \quad (3.44)$$

With our conventions, a **stable system** is a discrete-time system satisfying this property.

*Definition of stable system*

#### Example 10: Stable systems

The  $M$ -point moving average filter is BIBO stable. In fact, for a bounded input  $|x[n]| \leq B_x$ , we have:

$$|y[n]| = \left| \frac{1}{M} \sum_{k=0}^{M-1} x[n-k] \right| \leq \frac{1}{M} \sum_{k=0}^{M-1} |x[n-k]| \leq \frac{1}{M} (MB_x) \leq B_x \quad (3.45)$$

### 3.2.5 Passive and lossless systems

#### Definition 5: Passive and lossless systems

A discrete-time system is defined to be **passive** if, for every finite-energy input  $x[n]$ , the output  $y[n]$  has, at most, the same energy, namely:

$$\sum_{n=-\infty}^{\infty} |y[n]|^2 \leq \sum_{n=-\infty}^{\infty} |x[n]|^2 < \infty \quad (3.46)$$

For a **lossless** system, the inequality in Eq. 3.46 is satisfied with an equal sign for every output.

*Definition of passive and lossless system*

#### Example 11: Passive and lossless systems

We consider the discrete-time system defined by  $y[n] = \alpha x[n - N]$  with  $N$  a positive integer. Its output energy is given by:

$$\sum_{n=-\infty}^{\infty} |y[n]|^2 = |\alpha|^2 \sum_{n=-\infty}^{\infty} |x[n]|^2 \quad (3.47)$$

Hence, it is a passive system if  $|\alpha| < 1$  and a lossless system if  $|\alpha| = 1$ .

- 3.3 Impulse and step response
- 3.4 Shift-Invariant systems
- 3.5 Time domain characterizatio of LTI discrete-time system
- 3.6 Convolution sum
- 3.7 Stablility and causality conditions
- 3.8 Correlation and autocorrelation

*Lecture 6.  
Thursday 15<sup>th</sup>  
October, 2020.*

# Chapter 4

## Fourier Analysis

### 4.1 Continuous-time Fourier transform

**Lecture 8.**  
Thursday 22<sup>nd</sup>  
October, 2020.

Let us start with the definition of this very important tool

#### Definition 6: Fourier transform of a continuous-time signal

The CTFT of a continuous-time signal  $x_a(t)$  is given by:

$$X_a(j\Omega) = \int_{-\infty}^{\infty} x_a(t)e^{-j\Omega t} dt \quad (4.1)$$

often referred to as the Fourier spectrum or simply the spectrum of the continuous-time signal.

#### Definition 7: Inverse Fourier transform of a continuous-time signal

The inverse CTFT of a Fourier transform  $X_a(j\Omega)$  is given by:

$$x_a(t) = \frac{1}{2\pi} \int_{-\infty}^{\infty} X_a(j\Omega)e^{+j\Omega t} d\Omega \quad (4.2)$$

often referred to as the Fourier integral.

A CTFT pair will be denoted as:

$$x_a(t) \longleftrightarrow X_a(j\Omega) \quad (4.3)$$

Note that  $\Omega$  is real and denotes the continuous-time angular frequency variable in radians. In general, the CTFT is a complex function of  $\Omega$  in the range  $-\infty < \Omega < \infty$ . It can be expressed in the polar form as:

$$X_a(j\Omega) = |X_a(j\Omega)|e^{j\theta_a(\Omega)} \quad (4.4)$$

where  $\theta_a(\Omega) = \arg X_a(j\Omega)$ . The quantity  $|X_a(j\Omega)|$  is called the magnitude spectrum and the quantity  $\theta_a(\Omega)$  is called the phase spectrum. Both spectra are real function of  $\Omega$  and in general the CTFT  $X_a(j\Omega)$  exists if  $x_a(t)$  satisfies the Dirichlet conditions:

- the signal  $x_a(t)$  has a finite number of discontinuities and a finite number of maxima and minima in any finite interval;
- the signal is absolutely integrable, i.e.:

$$\int_{-\infty}^{\infty} |x_a(t)| dt < \infty \quad (4.5)$$

If the Dirichlet conditions are satisfied, then:

$$\frac{1}{2\pi} \int_{-\infty}^{\infty} X_a(j\Omega) e^{+j\Omega t} d\Omega \quad (4.6)$$

converges to  $x_a(t)$  except at values of  $t$  where  $x_a(t)$  has discontinuities. Moreover, it can be showed that if  $x_a(t)$  is absolutely integrable, then proving the existence of the CTFT reduces to proving:

$$|X_a(t\Omega)| < \infty \quad (4.7)$$

#### 4.1.1 Energy density spectrum

The total energy  $E_x$  of a finite energy continuous-time complex signal  $x_a(t)$  is given by:

$$\begin{aligned} E_x &= \int_{-\infty}^{\infty} |x_a(t)|^2 dt \\ &= \int_{-\infty}^{\infty} x_a(t) x_a^*(t) dt \\ &= \int_{-\infty}^{\infty} x_a(t) \left[ \frac{1}{2\pi} \int_{-\infty}^{\infty} X_a^*(j\Omega) e^{-j\Omega t} d\Omega \right] dt \end{aligned} \quad (4.8)$$

Interchanging the order of the integration we get:

$$\begin{aligned} E_x &= \frac{1}{2\pi} \int_{-\infty}^{\infty} X_a^*(j\Omega) \left[ \int_{-\infty}^{\infty} x_a(t) e^{-j\Omega t} dt \right] d\Omega \\ &= \frac{1}{2\pi} \int_{-\infty}^{\infty} X_a^*(j\Omega) X_a(j\Omega) d\Omega \\ &= \frac{1}{2\pi} \int_{-\infty}^{\infty} |X_a(j\Omega)|^2 d\Omega \end{aligned} \quad (4.9)$$

Hence:

$$\int_{-\infty}^{\infty} |x(t)|^2 dt = \frac{1}{2\pi} \int_{-\infty}^{\infty} |X_a(j\Omega)|^2 d\Omega \quad (4.10)$$

The above relation is more commonly known as the Parseval's relation for finite-energy continuous-time signals. The quantity  $|X_a(j\Omega)|^2$  is called the energy density spectrum of  $x_a(t)$  and it is usually denoted as:

$$S_{xx}(\Omega) = |X_a(j\Omega)|^2 \quad (4.11)$$

The energy over a specified range of frequencies  $\Omega_a \leq \Omega \leq \Omega_b$  can be computed using:

$$E_{x,r} = \frac{1}{2\pi} \int_{\Omega_a}^{\Omega_b} S_{xx}(\Omega) d\Omega \quad (4.12)$$

#### 4.1.2 Band-limited continuous-time signals

A full-band, finite-energy, continuous-time signal has a spectrum occupying the whole frequency range  $-\infty \leq \Omega \leq \infty$ . A band-limited continuous-time signal has a spectrum that is limited to a portion of the frequency range  $-\infty \leq \Omega \leq \infty$ . An ideal band-limited signal has a spectrum that is zero outside a finite frequency range  $\Omega_a \leq |\Omega| \leq \Omega_b$  can be computed using:

$$X_a(j\Omega) = \begin{cases} 0 & 0 \leq |\Omega| < \Omega_a \\ 0 & \Omega_b < |\Omega| < \infty \end{cases} \quad (4.13)$$

However, an ideal band-limited signal cannot be generated in practice.

Band-limited signals are classified according to the frequency range where most of the signal's is concentrated:

- a lowpass, continuous-time signal has a spectrum occupying the frequency range  $0 < |\Omega| \leq \Omega_p < \infty$ , where  $\Omega_p$  is called the bandwidth of the signal;
- a highpass, continuous-time signal has a spectrum occupying the frequency range  $0 < \Omega_p \leq |\Omega| < \infty$ , where the bandwidth of the signal is from  $\Omega_p$  to  $\infty$ ;
- a bandpass, continuous-time signal has a spectrum occupying the frequency range  $0 < \Omega_L \leq |\Omega| \leq \Omega_H < \infty$ , where  $\Omega_H - \Omega_L$  is the bandwidth.

#### 4.1.3 Discrete-time fourier transform

Let us introduce the definition of this concept.

##### Definition 8: Discrete-time Fourier transform

The discrete-time Fourier transform (DTFT)  $X(e^{j\omega})$  of a sequence  $x[n]$  is given by:

$$X(e^{j\omega}) = \sum_{n=-\infty}^{\infty} x[n]e^{-j\omega n} \quad (4.14)$$

where in general  $X(e^{j\omega})$  is a complex function of the real variable  $\omega$  and can be written as:

$$X(e^{j\omega}) = X_{\text{re}}(e^{j\omega}) + jX_{\text{im}}(e^{j\omega}) \quad (4.15)$$

$X_{\text{re}}(e^{j\omega})$  and  $X_{\text{im}}(e^{j\omega})$  are respectively, the real and imaginary parts of  $X(e^{j\omega})$ , and are real functions of  $\omega$ .  $X(e^{j\omega})$  can alternately be expressed as:

$$X(e^{j\omega}) = |X(e^{j\omega})|e^{j\theta(\omega)} \quad (4.16)$$

where  $\theta(\omega) = \arg X(e^{j\omega})$ .  $|X(e^{j\omega})|$  and  $\arg X(e^{j\omega})$  are called respectively magnitude function and phase function. Both quantities are again real functions of  $\omega$ . In many applications, the DTFT is called the Fourier spectrum. Likewise,  $|X(e^{j\omega})|$  and  $\theta(\omega)$  are called respectively the magnitude and phase spectra.

For a real sequence  $x[n]$ ,  $|X(e^{j\omega})|$  and  $X_{\text{re}}(e^{j\omega})$  are even functions of  $\omega$ , whereas,  $\theta(\omega)$  and  $X_{\text{im}}(e^{j\omega})$  are odd functions of  $\omega$ . Note also that  $X(e^{j\omega}) = |X(e^{j\omega})|e^{j\theta(\omega+2\pi k)} = |X(e^{j\omega})|e^{j\theta(\omega)}$  for any integer  $k$ . The phase function  $\theta(\omega)$  cannot be uniquely specified for any DTFT. Unless otherwise stated, we shall assume that the phase function  $\theta(\omega)$  is restricted to the range of values  $-\pi \leq \theta(\omega) < \pi$ , called the principal value.

##### Example 12: DTFT of the unit sample sequence

The DTFT of the unit sample sequence  $\delta[n]$  is given by:

$$\Delta(e^{j\omega}) = \sum_{n=-\infty}^{\infty} \delta[n]e^{-j\omega n} = \delta[0] = 1 \quad (4.17)$$

##### Example 13: DTFT of a causal sequence

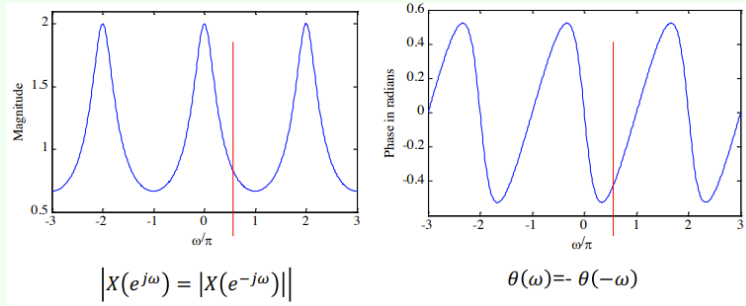
Consider the causal sequence:

$$x[n] = \alpha^n \mu[n], \quad |\alpha| < 1 \quad (4.18)$$

Its DTFT is given by:

$$\begin{aligned}
 X(e^{j\omega}) &= \sum_{n=-\infty}^{\infty} \alpha^n \mu[n] e^{-j\omega n} \\
 &= \sum_{n=0}^{\infty} \alpha^n e^{-j\omega n} \\
 &= \sum_{n=0}^{\infty} (\alpha e^{-j\omega})^n \\
 &= \frac{1}{1 - \alpha e^{-j\omega}}
 \end{aligned} \tag{4.19}$$

as  $|\alpha e^{-j\omega}| = |\alpha| < 1$ . If we take for example  $\alpha = 0.5$ , we get the plot below for the magnitude and phase of the DTFT.



The DTFT  $X(e^{j\omega})$  of a sequence  $x[n]$  is a continuous function of  $\omega$ . It is also a periodic function of  $\omega$  with a period  $2\pi$ :

$$X\left(e^{j(\omega+2\pi k)}\right) = \sum_{n=-\infty}^{\infty} x[n] e^{-j\omega n} e^{-j2\pi kn} = \sum_{n=-\infty}^{\infty} x[n] e^{-j\omega n} = X(e^{j\omega}) \tag{4.20}$$

Therefore:

$$X(e^{j\omega}) = \sum_{n=-\infty}^{\infty} x[n] e^{-j\omega n} \tag{4.21}$$

represents the Fourier series representation of the periodic function. As a result, the Fourier coefficients  $x[n]$  can be computed from  $X(e^{j\omega})$  using the Fourier integral:

$$x[n] = \frac{1}{2\pi} \int_{-\pi}^{\pi} X(e^{j\omega}) e^{j\omega n} d\omega \tag{4.22}$$

**Proof.** Consider:

$$x[n] = \frac{1}{2\pi} \int_{-\pi}^{\pi} \left( \sum_{\ell=-\infty}^{\infty} x[\ell] e^{-j\omega \ell} \right) e^{j\omega n} d\omega \tag{4.23}$$

The order of integration and summation can be interchanged if the summation inside

the brackets converges uniformly, i.e.  $X(e^{j\omega})$  exists. Then:

$$\begin{aligned}
 \frac{1}{2\pi} \int_{-\pi}^{\pi} \left( \sum_{\ell=-\infty}^{\infty} x[\ell] e^{-j\omega\ell} \right) e^{j\omega n} d\omega &= \sum_{\ell=-\infty}^{\infty} x[\ell] \left( \frac{1}{2\pi} \int_{-\pi}^{\pi} e^{j\omega(n-\ell)} d\omega \right) \\
 &= \sum_{\ell=-\infty}^{\infty} x[\ell] \frac{\sin(\pi(n-\ell))}{\pi(n-\ell)} \\
 &= \sum_{\ell=-\infty}^{\infty} x[\ell] \delta[n-\ell] \\
 &= x[n]
 \end{aligned} \tag{4.24}$$

For the convergence condition, an infinite series of the form:

$$X(e^{j\omega}) = \sum_{n=-\infty}^{\infty} x[n] e^{-j\omega n} \tag{4.25}$$

may or may not converge. Therefore, let us consider:

$$X_k(e^{j\omega}) = \sum_{n=-k}^k x[n] e^{-j\omega n} \tag{4.26}$$

Then for uniform convergence of  $X_k(e^{j\omega})$ :

$$\lim_{k \rightarrow \infty} X_k(e^{j\omega}) = X(e^{j\omega}) \tag{4.27}$$

Now, if  $x[n]$  is an absolutely summable sequence, i.e., if  $\sum_{n=-\infty}^{\infty} |x[n]| < \infty$ , then:

$$|X(e^{j\omega})| = \left| \sum_{n=-k}^k x[n] e^{-j\omega n} \right| \leq \sum_{n=-k}^k |x[n]| < \infty \tag{4.28}$$

for all values of  $\omega$ . Thus, the absolute summability of  $x[n]$  is a sufficient condition for the existence of the DTFT  $X(e^{j\omega})$ . ■

#### Example 14: Absolute summability condition

The sequence  $x[n] = \alpha^n \mu[n]$  for  $|\alpha| < 1$  is absolutely summable as:

$$\sum_{n=-k}^k |\alpha^n| \mu[n] = \sum_{n=0}^{\infty} |\alpha^n| = \frac{1}{1 - |\alpha|} < \infty \tag{4.29}$$

and its DTFT  $X(e^{j\omega})$  therefore converges to  $\frac{1}{1 - \alpha e^{j\omega}}$  uniformly.

Note that since:

$$\sum_{n=-\infty}^{\infty} |x[n]|^2 \leq \left( \sum_{n=-\infty}^{\infty} |x[n]| \right)^2 \tag{4.30}$$

an absolutely summable sequence has always a finite energy. However, a finite-energy sequence is not necessarily absolutely summable.

**Example 15: Absolute summability**

The sequence:

$$x[n] = \begin{cases} \frac{1}{n} & n \geq 1 \\ 0 & n \leq 0 \end{cases} \quad (4.31)$$

has finite energy equal to:

$$E_x = \sum_{n=1}^{\infty} \left( \frac{1}{n} \right)^2 = \frac{\pi^2}{6} \quad (4.32)$$

but  $x[n]$  is not absolutely summable.

In order to represent a finite energy sequence  $x[n]$  that is not absolutely summable by a DTFT  $X(e^{j\omega})$ , it is necessary to consider a mean-square convergence of  $X(e^{j\omega})$ :

$$\lim_{k \rightarrow \infty} \int_{-\pi}^{\pi} |X(e^{j\omega}) - X_k(e^{j\omega})|^2 d\omega = 0 \quad (4.33)$$

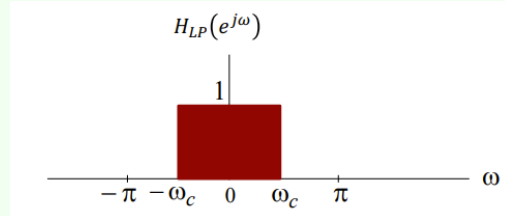
The total energy of the error  $X(e^{j\omega}) - X_k(e^{j\omega})$  must approach zero at each value of  $\omega$  as  $k$  goes to  $\infty$ . In such a case, the absolute value of the error  $|X(e^{j\omega}) - X_k(e^{j\omega})|$  may not go to zero as  $k$  goes to  $\infty$  and the DTFT is no longer bounded.

**Example 16: Mean-square convergence**

Consider the DTFT:

$$H_{LP}(e^{j\omega}) = \begin{cases} 1 & 0 \leq |\omega| \leq \omega_c \\ 0 & \omega < |\omega| \leq \pi \end{cases} \quad (4.34)$$

showed in the plot below.



The inverse DTFT of  $H_{LP}(e^{j\omega})$  is given by:

$$h_{LP}[n] = \frac{1}{2\pi} \int_{-\omega_c}^{\omega_c} e^{j\omega n} d\omega = \frac{1}{2\pi} \left( \frac{e^{j\omega_c n}}{jn} - \frac{e^{-j\omega_c n}}{jn} \right) = \frac{\sin(\omega_c n)}{\pi n} \quad (4.35)$$

for  $-\infty < n < \infty$ . The energy of  $h_{LP}[n]$  is given by  $\frac{\omega_c}{\pi}$ .  $h_{LP}[n]$  is a finite-energy sequence, but it is not absolutely summable. In fact, the result:

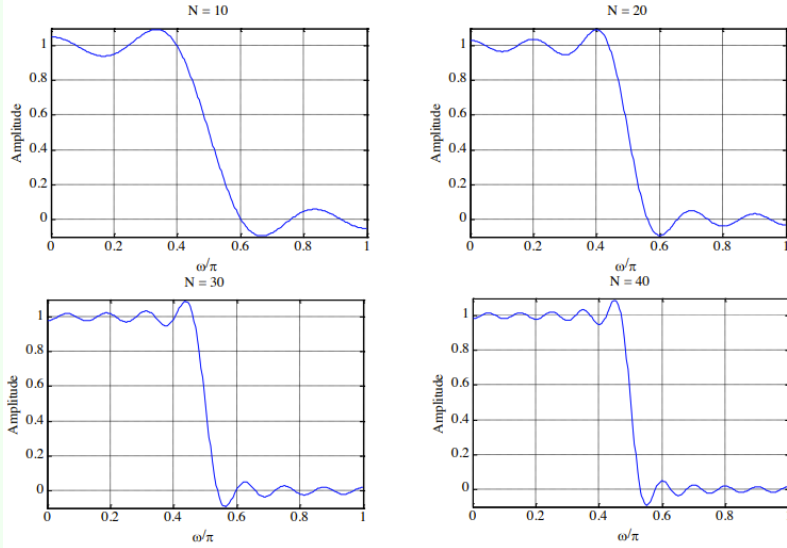
$$\sum_{n=-k}^{n=k} h_{LP}[n] e^{-j\omega n} = \sum_{n=-k}^{n=k} \frac{\sin(\omega_c n)}{\pi n} e^{-j\omega n} \quad (4.36)$$

does not uniformly converge to  $H_{LP}(e^{j\omega})$  for all values of  $\omega$ , but converges to  $H_{LP}(e^{j\omega})$  in the mean-square sense.

The mean-square convergence property of the sequence  $h_{LP}[n]$  can be further illustrated by examining the plot of the function:

$$H_{LP,k}(e^{j\omega}) = \sum_{n=-k}^k \frac{\sin(\omega_c n)}{\pi n} e^{-j\omega n} \quad (4.37)$$

for various values of  $k$ , as showed below.



As can be seen from these plots, independently of the value of  $k$  there are ripples in the plot of  $H_{LP,k}(e^{j\omega})$  around both sides of the point  $\omega = \omega_c$ . The number of ripples increases as  $k$  increases with the height of the largest ripple remaining the same for all values of  $k$ . As  $k$  goes to  $\infty$ , the condition:

$$\lim_{k \rightarrow \infty} \int_{-\pi}^{\pi} |H_{LP}(e^{j\omega}) - H_{LP,k}(e^{j\omega})|^2 d\omega = 0 \quad (4.38)$$

holds indicating the convergence of  $H_{LP,k}(e^{j\omega})$  to  $H_{LP}(e^{j\omega})$ .

The oscillatory behaviour of  $H_{LP,k}(e^{j\omega})$  approximating  $H_{LP}(e^{j\omega})$  in the mean-square sense at a point of discontinuity is known as the Gibbs phenomenon

The DTFT can also be defined for a certain class of sequences which are neither absolutely summable nor square summable. Examples of such sequences are the unit step sequence  $\mu[n]$ , the sinusoidal sequence  $\cos(\omega_0 n + \varphi)$  and the exponential sequence  $A\alpha^n$ . For this type of sequences, a DTFT representation is possible using the Dirac delta function  $\delta(\omega)$ .

A Dirac delta function  $\delta(\omega)$  is a function of  $\omega$  with infinite height, zero width, and unit area. It is the limiting form of a unit area pulse function  $p_\Delta$  as  $\Delta$  goes to zero satisfying:

$$\lim_{\Delta \rightarrow 0} \int_{-\infty}^{\infty} p_\Delta(\omega) d\omega = \int_{-\infty}^{\infty} \delta(\omega) d\omega \quad (4.39)$$

### Example 17: Dirac $\delta$ application

Consider the complex exponential sequence:

$$x[n] = e^{j\omega_0 n} \quad (4.40)$$

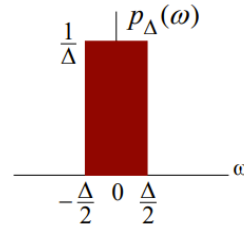


**Figure 4.1:** Plot and area of  $p_{\Delta}(\omega)$  function.

Its DTFT is given by:

$$X(e^{j\omega}) = \sum_{k=-\infty}^{\infty} 2\pi\delta(\omega - \omega_0 + 2k\pi) \quad (4.41)$$

where  $\delta(\omega)$  is an impulse function of  $\omega$  and  $-\pi \leq \omega_0 \leq \pi$ . The function in Eq. 4.41 is periodic in  $\omega$  with a period  $2\pi$  and it is called periodic impulse train. In order to verify that  $X(e^{j\omega})$  given above is indeed the DTFT of  $x[n] = e^{j\omega_0 n}$  we compute the inverse DTFT of  $X(e^{j\omega})$ :

$$\begin{aligned} x[n] &= \frac{1}{2\pi} \int_{-\pi}^{\pi} \sum_{k=-\infty}^{\infty} 2\pi\delta(\omega - \omega_0 + 2\pi k) e^{j\omega n} d\omega \\ &= \int_{-\pi}^{\pi} \delta(\omega - \omega_0) e^{j\omega n} d\omega \\ &= e^{j\omega_0 n} \end{aligned} \quad (4.42)$$

where we have used the sampling property of the impulse function  $\delta(\omega)$ .

Last but not least, we list in Table 4.1 a set of commonly used DTFT pairs.

| Sequence                               | DTFT  |
|--|---|
| $\delta[n]$                            | 1   |
| 1                                      | $\sum_{k=-\infty}^{\infty} 2\pi\delta(\omega + 2\pi k)$                             |
| $e^{j\omega_0 n}$                      | $\sum_{k=-\infty}^{\infty} 2\pi\delta(\omega - \omega_0 + 2\pi k)$                  |
| $\mu[n]$                               | $\frac{1}{1 - e^{-j\omega}} + \sum_{k=-\infty}^{\infty} \pi\delta(\omega + 2\pi k)$ |
| $\alpha^n \mu[n] \quad ( \alpha  < 1)$ | $\frac{1}{1 - \alpha e^{-j\omega}}$   |

**Table 4.1:** Commonly used DTFT pairs.

#### 4.1.4 DTFT properties

There are a number of important properties of the DTFT that are useful in signal processing applications. These are listed here in Figures 4.2, 4.3, 4.4 without proof, since it is quite straightforward to derive them. We illustrate the applications of some of the DTFT properties.

| Sequence                     | Discrete-Time Fourier Transform  |
|------------------------------|--|
| $x[n]$                       | $X(e^{j\omega})$   |
| $x[-n]$                      | $X(e^{-j\omega})$  |
| $x^*[-n]$                    | $X^*(e^{j\omega})$   |
| $\operatorname{Re}\{x[n]\}$  | $X_{\text{cs}}(e^{j\omega}) = \frac{1}{2}\{X(e^{j\omega}) + X^*(e^{-j\omega})\}$ |
| $j\operatorname{Im}\{x[n]\}$ | $X_{\text{ca}}(e^{j\omega}) = \frac{1}{2}\{X(e^{j\omega}) - X^*(e^{-j\omega})\}$ |
| $x_{\text{cs}}[n]$           | $X_{\text{re}}(e^{j\omega})$   |
| $x_{\text{ca}}[n]$           | $jX_{\text{im}}(e^{j\omega})$  |

**Figure 4.2:** DTFT symmetry relations for a complex sequence  $x[n]$ .

| Sequence  | Discrete-Time Fourier Transform   |
|---|---|
| $x[n]$  | $X(e^{j\omega}) = X_{\text{re}}(e^{j\omega}) + jX_{\text{im}}(e^{j\omega})$ |
| $x_{\text{ev}}[n]$  | $X_{\text{re}}(e^{j\omega})$  |
| $x_{\text{od}}[n]$  | $jX_{\text{im}}(e^{j\omega})$   |
| Symmetry relations  |   |
| $X(e^{j\omega}) = X^*(e^{-j\omega})$                        |   |
| $X_{\text{re}}(e^{j\omega}) = X_{\text{re}}(e^{-j\omega})$  |   |
| $X_{\text{im}}(e^{j\omega}) = -X_{\text{im}}(e^{-j\omega})$ |   |
| $ X(e^{j\omega})  =  X(e^{-j\omega}) $                      |   |
| $\arg\{X(e^{j\omega})\} = -\arg\{X(e^{-j\omega})\}$         |   |

**Figure 4.3:** DTFT symmetry realtions for a real sequence  $x[n]$ .**Example 18: DTFT properties**

We determine the DTFT  $Y(e^{j\omega})$  of:

$$y[n] = (n+1)\alpha^n \mu[n], \quad |\alpha| < 1 \quad (4.43)$$

Let  $x[n] = \alpha^n \mu[n]$ , with  $\alpha < 1$ . We can therefore write:

$$y[n] = nx[n] + x[n] \quad (4.44)$$

The DTFT of  $x[n]$  is given by:

$$X(e^{j\omega}) = \frac{1}{1 - \alpha e^{-j\omega}} \quad (4.45)$$

Using the differentiation property of the DTFT, we observe that the DTFT of  $nx[n]$  is given by:

$$j \frac{dX(e^{j\omega})}{d\omega} = j \frac{d}{d\omega} \left( \frac{1}{1 - \alpha e^{-j\omega}} \right) = \frac{\alpha e^{-j\omega}}{(1 - \alpha e^{-j\omega})^2} \quad (4.46)$$

| Type of Property                | Sequence                               | Discrete-Time Fourier Transform   |
|---------------------------------|--|---|
|                                 | $g[n]$<br>$h[n]$                       | $G(e^{j\omega})$<br>$H(e^{j\omega})$  |
| Linearity                       | $\alpha g[n] + \beta h[n]$             | $\alpha G(e^{j\omega}) + \beta H(e^{j\omega})$                                      |
| Time-shifting                   | $g[n - n_0]$                           | $e^{-j\omega n_0} G(e^{j\omega})$   |
| Frequency-shifting              | $e^{j\omega_0 n} g[n]$                 | $G(e^{j(\omega - \omega_0)})$   |
| Differentiation<br>in frequency | $ng[n]$                                | $j \frac{dG(e^{j\omega})}{d\omega}$   |
| Convolution                     | $g[n] \circledast h[n]$                | $G(e^{j\omega}) H(e^{j\omega})$   |
| Modulation                      | $g[n]h[n]$                             | $\frac{1}{2\pi} \int_{-\pi}^{\pi} G(e^{j\theta}) H(e^{j(\omega - \theta)}) d\theta$ |
| Parseval's relation             | $\sum_{n=-\infty}^{\infty} g[n]h^*[n]$ | $\frac{1}{2\pi} \int_{-\pi}^{\pi} G(e^{j\omega}) H^*(e^{j\omega}) d\omega$          |

**Figure 4.4:** DTFT general properties.

Next, using the linearity property of the DTFT, we arrive at:

$$Y(e^{j\omega}) = \frac{\alpha e^{-j\omega}}{(1 - \alpha e^{-j\omega})^2} + \frac{1}{1 - \alpha e^{-j\omega}} = \frac{1}{(1 - \alpha e^{-j\omega})^2} \quad (4.47)$$

#### Example 19: DTFT properties

We determine the DTFT  $V(e^{j\omega})$  of the sequence  $v[n]$ , defined by:

$$d_0 v[n] + d_1 v[n - 1] = p_0 \delta[n] + p_1 \delta[n - 1] \quad (4.48)$$

The DTFT of  $\delta[n]$  is 1. Using the time-shifting property of the DTFT, we observe that the DTFT of  $\delta[n-1]$  is  $e^{-j\omega}$  and the DTFT of  $v[n-1]$  is  $e^{-j\omega} V(e^{j\omega})$ . Using the linearity property we then obtain the frequency-domain representation of  $d_0 v[n] + d_1 v[n - 1]$  as:

$$d_0 V(e^{j\omega}) + d_1 e^{-j\omega} V(e^{j\omega}) = p_0 + p_1 e^{-j\omega} \quad (4.49)$$

Solving the above equation we get:

$$V(e^{j\omega}) = \frac{p_0 + p_1 e^{-j\omega}}{d_0 + d_1 e^{-j\omega}} \quad (4.50)$$

#### 4.1.5 Energy density spectrum

The total energy of a finite-energy sequence  $g[n]$  is given by:

$$E_g = \sum_{n=-\infty}^{\infty} |g[n]|^2 \quad (4.51)$$

From Parseval's relation we observe that:

$$E_g = \sum_{n=-\infty}^{\infty} |g[n]|^2 = \frac{1}{2\pi} \int_{-\pi}^{\pi} |G(e^{j\omega})|^2 d\omega \quad (4.52)$$

The quantity:

$$S_{gg}(\omega) = |G(e^{j\omega})|^2 \quad (4.53)$$

is called the energy density spectrum. The area under this curve in the range  $-\pi \leq \omega \leq \pi$  divided by  $2\pi$  is the energy of the sequence.

#### 4.1.6 Band-limited discrete-time signals

Since the spectrum of a discrete-time signal is a periodic function of  $\omega$  with a period  $2\pi$ , a full-band signal has a spectrum occupying the frequency range  $-\pi \leq \omega \leq \pi$ . A band-limited discrete-time signal has a spectrum that is limited to a portion of the frequency range  $-\pi \leq \omega \leq \pi$ .

An ideal band-limited signal has a spectrum that is zero outside a frequency range  $0 < \omega_a \leq |\omega| \leq \omega_b < \pi$ , that is:

$$X(e^{j\omega}) = \begin{cases} 0 & 0 \leq |\omega| < \omega_a \\ 0 & \omega_b < |\omega| < \pi \end{cases} \quad (4.54)$$

However, an ideal band-limited discrete-time signal cannot be generated in practice. A classification of a band-limited discrete-time signal is based on the frequency range where most of the signal energy is concentrated. A lowpass discrete-time real signal has a spectrum occupying the frequency range  $0 < |\omega| \leq \omega_p < \pi$  and has a bandwidth of  $\omega_p$ .

A highpass discrete-time real signal has a spectrum occupying the frequency range  $0 < \omega_p \leq |\omega| < \pi$  and has a bandwidth of  $\pi - \omega_p$ .

A bandpass discrete-time real signal has a spectrum occupying the frequency range  $0 < \omega_L \leq |\omega| \leq \omega_H < \pi$  and has a bandwidth of  $\omega_H - \omega_L$ .

#### Example 20: Band-limited discrete-time signals

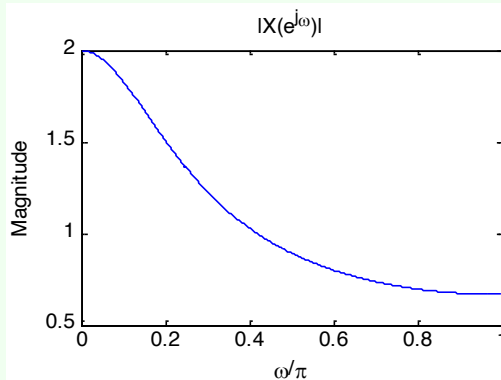
Consider the sequence:

$$x[n] = (0.5)^n \mu[n] \quad (4.55)$$

The DTFT is:

$$X(e^{j\omega}) = \frac{1}{1 - 0.5e^{-j\omega}} \quad (4.56)$$

and the magnitude spectrum is showed below.



It can be showed that 80% of the energy of this lowpass signal is contained in the frequency range  $0 \leq |\omega| \leq 0.5081\pi$ . Hence, we can define the 80% bandwidth to be  $0.5081\pi$  radians.

Returning to the energy density spectrum, we consider some other examples introducing also the concept of band-limited signals.

**Example 21: Energy density spectrum**

We compute the energy of the sequence:

$$h_{LP}[n] = \frac{\sin(\omega_c n)}{\pi n}, \quad -\infty < n < \infty \quad (4.57)$$

Here:

$$\sum_{n=-\infty}^{\infty} |h_{LP}[n]|^2 = \frac{1}{2\pi} \int_{-\pi}^{\pi} |H_{LP}(e^{j\omega})|^2 d\omega \quad (4.58)$$

where:

$$H_{LP}(e^{j\omega}) = \begin{cases} 1 & 0 \leq |\omega| \leq \omega_c \\ 0 & \omega_c < |\omega| \leq \pi \end{cases} \quad (4.59)$$

Therefore:

$$\sum_{n=-\infty}^{\infty} |h_{LP}[n]|^2 = \frac{1}{2\pi} \int_{-\omega_c}^{\omega_c} d\omega = \frac{\omega_c}{\pi} < \infty \quad (4.60)$$

Hence,  $h_{LP}[n]$  is a finite-energy lowpass sequence.

## 4.2 Linear convolution using DTFT

An important property of the DTFT is given by the convolution theorem. It states that if  $y[n] = x[n] * h[n]$ , then the DTFT  $Y(e^{j\omega})$  of  $y[n]$  is given by:

$$Y(e^{j\omega}) = X(e^{j\omega})H(e^{j\omega}) \quad (4.61)$$

An implication of this result is that the linear convolution  $y[n]$  of the sequences  $x[n]$  and  $h[n]$  can be performed as follows:

- compute the DTFTs  $X(e^{j\omega})$  and  $H(e^{j\omega})$  of the sequences  $x[n]$  and  $h[n]$ , respectively;
- form the DTFT  $Y(e^{j\omega}) = X(e^{j\omega})H(e^{j\omega})$ ;
- compute the IDFT  $y[n]$  of  $Y(e^{j\omega})$ .

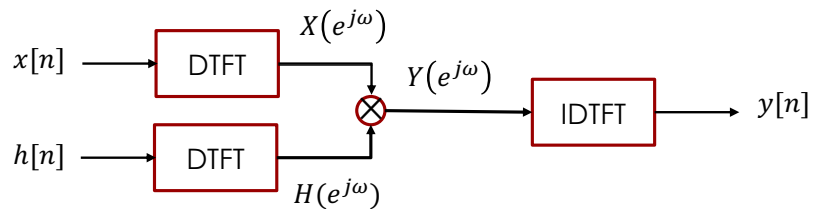


**Figure 4.5:** Scheme of the computation of linear convolution  $y[n]$  of the sequences  $x[n]$  and  $h[n]$ .

Note that in numerical computation, when the computed phase function is outside the range  $[-\pi, \pi]$ , the phase is computed modulo  $2\pi$ , to bring the computed value to this range. Thus, the phase functions of some sequences exhibit discontinuities of  $2\pi$  radians in the plot. For example, there is a discontinuity of  $2\pi$  at  $\omega = 0.72$  in the

phase response below:

$$X(e^{j\omega}) = \frac{0.008 - 0.033e^{-j\omega} + 0.05e^{-2j\omega} - 0.033e^{-3j\omega} + 0.008e^{-4j\omega}}{1 + 2.37e^{-j\omega} + 2.7e^{-2j\omega} + 1.6e^{-3j\omega} + 0.41e^{-4j\omega}} \quad (4.62)$$

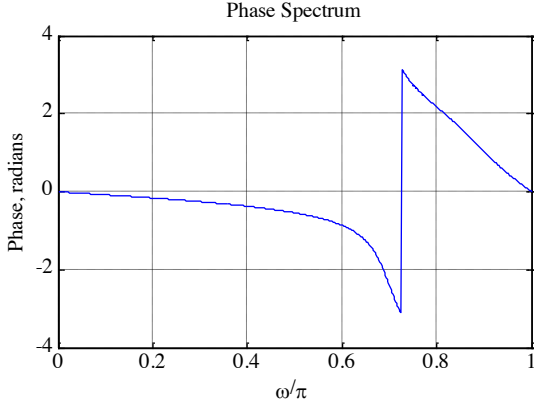


**Figure 4.6:** Discontinuity in the phase response of Eq. 4.62.

In such cases, often an alternate type of phase function that is continuous function of  $\omega$  is derived from the original phase function by removing the discontinuities of  $2\pi$ . Process of discontinuity removal is called unwrapping the phase and the unwrapped phase function will be denoted as  $\theta_c(\omega)$ .

For example, the unwrapped phase function of the DTFT in Eq. 4.62 is showed in Figure 4.7.

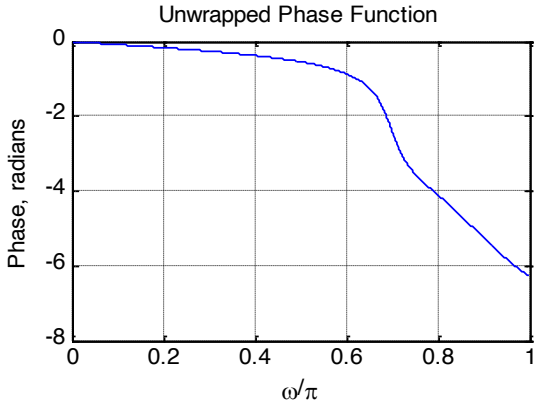


**Figure 4.7:** Unwrapped phase function of Eq. 4.62.

The conditions under which the phase function will be a continuous function of  $\omega$  is next derived. Now consider:

$$\ln X(e^{j\omega}) = \ln |X(e^{j\omega})| + j\theta(\omega) \quad (4.63)$$

where:

$$\theta(\omega) = \arg \{X(e^{j\omega})\} \quad (4.64)$$

From  $\ln X(e^{j\omega})$  we can also compute  $\frac{d \ln X(e^{j\omega})}{d\omega}$ :

$$\frac{d \ln X(e^{j\omega})}{d\omega} = \frac{d \ln |X(e^{j\omega})|}{d\omega} + j \frac{d\theta(\omega)}{d\omega} \quad (4.65)$$

Thus,  $\frac{d\theta(\omega)}{d\omega}$  is given by the imaginary part of:

$$\frac{1}{X(e^{j\omega})} \left[ \frac{dX_{\text{re}}(e^{j\omega})}{d\omega} + j \frac{dX_{\text{im}}(e^{j\omega})}{d\omega} \right] \quad (4.66)$$

Hence:

$$\frac{d\theta(\omega)}{d\omega} = \frac{1}{|X(e^{j\omega})|^2} \left[ X_{\text{re}}(e^{j\omega}) \frac{dX_{\text{im}}(e^{j\omega})}{d\omega} - X_{\text{im}}(e^{j\omega}) \frac{dX_{\text{re}}(e^{j\omega})}{d\omega} \right] \quad (4.67)$$

The phase function can thus be defined unequivocally by its derivative:

$$\theta(\omega) = \int_0^\omega \left[ \frac{d\theta(\eta)}{d\eta} \right] d\eta \quad (4.68)$$

with the constraint  $\theta(0) = 0$ .

The phase function defined by Eq. 4.68 is called the unwrapped phase function of  $X(e^{j\omega})$  and it is a continuous function of  $\omega$ . Therefore,  $\ln X(e^{j\omega})$  exists. Moreover, the phase function will be an odd function of  $\omega$  if:

$$\frac{1}{\pi} \int_0^{2\pi} \left[ \frac{d\theta(\eta)}{d\eta} \right] d\eta = 0 \quad (4.69)$$

If the above constraint is not satisfied, then the computed phase function will exhibit absolute jumps greater than  $\pi$ .

### 4.3 The frequency response

Most discrete-time signals encountered in practice can be represented as a linear combination of a very large, maybe infinite, number of sinusoidal discrete-time signals of different angular frequencies. Thus, knowing the response of the LTI system to a single sinusoidal signal, we can determine its response to more complicated signals by making use of the superposition property.

An important property of an LTI system is that for certain types of input signals, called eigen functions, the output signal is the input signal multiplied by a complex constant. We consider here one such eigen function as the input.

Consider the LTI discrete-time system with an impulse response  $\{h[n]\}$ . Its input-output relationship in the time-domain is given by the convolution sum:

$$y[n] = \sum_{k=-\infty}^{\infty} h[k]x[n-k] \quad (4.70)$$

If the input is of the form:

$$x[n] = e^{j\omega n}, \quad -\infty < n < \infty \quad (4.71)$$

then it follows that the output is given by:

$$y[n] = \sum_{k=-\infty}^{\infty} h[k]x[n-k] = \left( \sum_{k=-\infty}^{\infty} h[k]e^{-j\omega k} \right) e^{j\omega n} \quad (4.72)$$

Now, let:

$$H(e^{j\omega}) = \sum_{k=-\infty}^{\infty} h[k]e^{-j\omega k} \quad (4.73)$$

Then we can write:

$$y[n] = H(e^{j\omega})e^{j\omega n} \quad (4.74)$$

Thus for a complex exponential input signal  $e^{j\omega n}$ , the output of an LTI discrete-time system is also a complex exponential signal of the same frequency multiplied by a complex constant  $H(e^{j\omega})$ . Thus  $e^{j\omega n}$  is an eigen function of the system.

The quantity  $H(e^{j\omega})$  is called the frequency response of the LTI discrete-time system.  $H(e^{j\omega})$  provides a frequency-domain description of the system and is precisely the DTFT of the impulse response  $\{h[n]\}$  of the system.  $H(e^{j\omega})$ , in general, is a complex function of  $\omega$  with a period  $2\pi$ . It can be expressed in terms of its real and imaginary parts:

$$H(e^{j\omega}) = H_{\text{re}}(e^{j\omega}) + jH_{\text{im}}(e^{j\omega}) \quad (4.75)$$

or, in terms of its magnitude and phase:

$$H(e^{j\omega}) = |H(e^{j\omega})|e^{j\theta(\omega)} \quad (4.76)$$

where:

$$\theta(\omega) = \arg\{H(e^{j\omega})\} \quad (4.77)$$

The function  $|H(e^{j\omega})|$  is called the magnitude response and the function  $\theta(\omega)$  is called the phase response of the LTI discrete-time system. Design specifications for the LTI discrete-time system, in many applications, are given in terms of the magnitude response or the phase response or both.

In some cases, the magnitude function is specified in decibels as:

$$g(\omega) = 20 \log_{10} |H(e^{j\omega})| \text{dB} \quad (4.78)$$

where  $G(\omega)$  is called the gain function. The negative of the gain function  $A(\omega) = -G(\omega)$  is called the attenuation or loss function.

Note that magnitude and phase functions are real functions of  $\omega$ , whereas the frequency response is a complex function of  $\omega$ . If the impulse response  $h[n]$  is real then it follows that the magnitude function is an even function of  $\omega$ :

$$|H(e^{j\omega})| = |H(e^{-j\omega})| \quad (4.79)$$

and the phase function is an odd function of  $\omega$ :

$$\theta(\omega) = -\theta(-\omega) \quad (4.80)$$

Likewise, for a real impulse response  $h[n]$ ,  $H_{\text{re}}(e^{j\omega})$  is even and  $H_{\text{im}}(e^{j\omega})$  is odd.

### Example 22: M-point moving average filter

Consider the  $M$ -point moving average filter with an impulse response given by:

$$h[n] = \begin{cases} \frac{1}{M} & 0 \leq n \leq M-1 \\ 0 & \text{otherwise} \end{cases} \quad (4.81)$$

Its frequency response is then given by:

$$H(e^{j\omega}) = \frac{1}{M} \sum_{n=0}^{M-1} e^{-j\omega n} \quad (4.82)$$

Performing all the calculations:

$$\begin{aligned}
 H(e^{j\omega}) &= \frac{1}{M} \left( \sum_{n=0}^{\infty} e^{-j\omega n} - \sum_{n=M}^{\infty} e^{-j\omega n} \right) \\
 &= \frac{1}{M} \left( \sum_{n=0}^{\infty} e^{-j\omega n} \right) (1 - e^{-jM\omega}) \\
 &= \frac{1}{M} \frac{1 - e^{-jM\omega}}{1 - e^{-j\omega}} \\
 &= \frac{1}{M} \frac{\sin(\frac{M\omega}{2})}{\sin(\frac{\omega}{2})} e^{-j\frac{(M-1)\omega}{2}}
 \end{aligned} \tag{4.83}$$

Thus, the magnitude response of the  $M$ -point moving average filter is given by:

$$|H(e^{j\omega})| = \left| \frac{1}{M} \frac{\sin(\frac{M\omega}{2})}{\sin(\frac{\omega}{2})} \right| \tag{4.84}$$

and the phase response is given by

$$\theta(\omega) = -\frac{(M-1)\omega}{2} + \pi \sum_{k=1}^{\lfloor \frac{M}{2} \rfloor} \mu \left[ \omega - \frac{2\pi k}{M} \right] \tag{4.85}$$

Note that the frequency response also determines the steady-state response of an LTI discrete-time system to a sinusoidal input.

### Example 23: Steady-state response

We determine the steady-state output  $y[n]$  of a real coefficient LTI discrete-time system with a frequency response  $H(e^{j\omega})$  for an input:

$$x[n] = A \cos(\omega_0 n + \varphi), \quad -\infty < n < \infty \tag{4.86}$$

We can express the input  $x[n]$  as:

$$x[n] = g[n] + g^*[n] \tag{4.87}$$

where:

$$g[n] = \frac{1}{2} A e^{j\varphi} e^{j\omega_0 n} \tag{4.88}$$

Now the output of the system for an input  $e^{j\omega_0 n}$  is simply  $H(e^{j\omega_0})e^{j\omega_0 n}$ . Because of linearity, the response  $v[n]$  to an input  $g[n]$  is given by:

$$v[n] = \frac{1}{2} A e^{j\varphi} H(e^{j\omega_0}) e^{j\omega_0 n} \tag{4.89}$$

Likewise, the output  $v^*[n]$  to the input  $g^*[n]$  is:

$$v^*[n] = \frac{1}{2} A e^{-j\varphi} H(e^{-j\omega_0}) e^{-j\omega_0 n} \tag{4.90}$$

Combining the last two equations we get:

$$\begin{aligned}
 y[n] &= v[n] + v^*[n] \\
 &= \frac{1}{2}Ae^{j\varphi}H(e^{j\omega_0})e^{j\omega_0 n} + \frac{1}{2}Ae^{-j\varphi}H(e^{-j\omega_0})e^{-j\omega_0 n} \\
 &= \frac{1}{2}A|H(e^{j\omega_0})|\left\{e^{j\theta(\omega_0)}e^{j\varphi}e^{j\omega_0 n} + e^{-j\theta(\omega_0)}e^{-j\varphi}e^{-j\omega_0 n}\right\} \\
 &= A|H(e^{j\omega_0})|\cos(\omega_0 n + \theta(\omega_0) + \varphi)
 \end{aligned} \tag{4.91}$$

Thus, the output  $y[n]$  has the same sinusoidal waveform as the input with two differences:

- the amplitude is multiplied by  $|H(e^{j\omega_0})|$ , the value of the magnitude function at  $\omega = \omega_0$ ;
- the output has a phase lag relative to the input by an amount  $\theta(\omega_0)$ , the value of the phase function at  $\omega = \omega_0$ .

The expression for the steady-state response developed earlier assumes that the system is initially relaxed before the application of the input  $x[n]$ . In practice, excitation  $x[n]$  to a discrete-time system is usually a right-sided sequence applied at some sample index  $n = n_0$ . Now, we develop the expression for the output for such an input.

Without any loss of generality, assume  $x[n] = 0$  for  $n < 0$ . From the input-output relation in Eq. 4.70, we observe that for an input:

$$x[n] = e^{j\omega n} \mu[n] \tag{4.92}$$

the output is given by:

$$y[n] = \left( \sum_{k=-\infty}^{\infty} h[k]e^{j\omega(n-k)} \right) \mu[n] = \left( \sum_{k=-\infty}^{\infty} h[k]e^{-j\omega k} \right) e^{j\omega n} \mu[n] \tag{4.93}$$

The output for  $n < 0$  is  $y[n] = 0$ , while for  $n \geq 0$  it is given by:

$$\begin{aligned}
 y[n] &= \left( \sum_{k=0}^{\infty} h[k]e^{-j\omega k} \right) e^{j\omega n} - \left( \sum_{k=n+1}^{\infty} h[k]e^{-j\omega k} \right) e^{j\omega n} \\
 &= H(e^{j\omega})e^{j\omega n} - \left( \sum_{k=n+1}^{\infty} h[k]e^{-j\omega k} \right) e^{j\omega n}
 \end{aligned} \tag{4.94}$$

The first term on the RHS is the same as that obtained when the input is applied at  $n = 0$  to an initially relaxed system and it is the steady-state response:

$$y_{\text{sr}}[n] = H(e^{j\omega})e^{j\omega n} \tag{4.95}$$

The second term on the RHS is called the transient response:

$$y_{\text{tr}}[n] = - \left( \sum_{k=n+1}^{\infty} h[k]e^{-j\omega k} \right) e^{j\omega n} \tag{4.96}$$

To determine the effect of the above term on the total output response, we observe:

$$|y_{\text{tr}}[n]| = \left| \sum_{k=n+1}^{\infty} h[k]e^{-j\omega(k-n)} \right| \leq \sum_{k=n+1}^{\infty} |h[k]| \leq \sum_{k=0}^{\infty} |h[k]| \tag{4.97}$$

For a causal, stable LTI IIR discrete-time system,  $h[n]$  is absolutely summable. As a result, the transient response  $y_{\text{tr}}[n]$  is a bounded sequence. Moreover, as  $n \rightarrow \infty$ :

$$\sum_{k=n+1}^{\infty} |h[k]| \rightarrow 0 \quad (4.98)$$

and hence, the transient response decays to zero as  $n$  gets very large.

For a causal FIR LTI discrete-time system with an impulse response  $h[n]$  of length  $N + 1$ ,  $h[n] = 0$  for  $n > N$ . Hence,  $y_{\text{tr}}[n] = 0$  for  $n > N - 1$ . Here the output reaches the steady-state value  $y_{\text{sr}}[n] = H(e^{j\omega})e^{j\omega n}$  at  $n = N$ .

## 4.4 The concept of filtering

One application of an LTI discrete-time system is to pass certain frequency components in an input sequence without any distortion (if possible) and to block other frequency components. Such systems are called digital filters and one of the main subjects of discussion in this course.

The key to the filtering process is the Fourier transform

$$x[n] = \frac{1}{2\pi} \int_{-\pi}^{\pi} H(e^{j\omega}) e^{j\omega n} d\omega \quad (4.99)$$

It expresses an arbitrary input as a linear weighted sum of an infinite number of exponential sequences, or equivalently, as a linear weighted sum of sinusoidal sequences. Thus, by appropriately choosing the values of the magnitude function  $|H(e^{j\omega})|$  of the LTI digital filter at frequencies corresponding to the frequencies of the sinusoidal components of the input, some of these components can be selectively heavily attenuated or filtered with respect to the others.

To understand the mechanism behind the design of frequency-selective filters, consider a real-coefficient LTI discrete-time system characterized by a magnitude function:

$$|H(e^{j\omega})| \approx \begin{cases} 1 & |\omega| \leq \omega_c \\ 0 & \omega_c < |\omega| \leq \pi \end{cases} \quad (4.100)$$

We apply to the system an input:

$$x[n] = A \cos(\omega_1 n) + B \cos(\omega_2 n), \quad 0 < \omega_1 < \omega_c < \omega_2 < \pi \quad (4.101)$$

Because of linearity, the output of this system is of the form:

$$y[n] = A |H(e^{j\omega_1})| \cos(\omega_1 n + \theta(\omega_1)) + B |H(e^{j\omega_2})| \cos(\omega_2 n + \theta(\omega_2)) \quad (4.102)$$

As  $|H(e^{j\omega_1})| \approx 1$  and  $|H(e^{j\omega_2})| \approx 0$ , the output reduces to:

$$y[n] \approx A |H(e^{j\omega_1})| \cos(\omega_1 n + \theta(\omega_1)) \quad (4.103)$$

Thus, the system acts like a lowpass filter.

Now we consider an example of design of a very simple digital filter.

### Example 24: Design of a simple digital filter

The input consists of a sum of two sinusoidal sequences of angular frequencies 0.1 rad/sample and 0.4 rad/sample. We need to design a highpass filter that will pass the high-frequency component of the input but block the low-frequency component.

For simplicity, assume the filter to be an FIR filter of length 3 with an impulse response:

$$h[0] = h[2] = \alpha \quad (4.104)$$

$$h[1] = \beta \quad (4.105)$$

The convolution sum description of this filter is then given by:

$$\begin{aligned} y[n] &= h[0]x[n]h[1]x[n-1] + h[2]x[n-2] \\ &= \alpha x[n] + \beta x[n-1] + \alpha x[n-2] \end{aligned} \quad (4.106)$$

$y[n]$  and  $x[n]$  are, respectively, the output and the input sequences.

The design objective is to choose suitable values of  $\alpha$  and  $\beta$  so that the output is a sinusoidal sequence with a frequency of 0.4 rad/sample.

Now, the frequency response of the FIR filter is given by:

$$\begin{aligned} H(e^{j\omega}) &= h[0] + h[1]e^{-j\omega} + h[2]e^{-j2\omega} \\ &= \alpha(1 + e^{-j2\omega}) + \beta e^{-j\omega} \\ &= 2\alpha \left( \frac{e^{j\omega} + e^{-j\omega}}{2} \right) e^{-j\omega} + \beta e^{-j\omega} \\ &= (2\alpha \cos \omega + \beta) e^{-j\omega} \end{aligned} \quad (4.107)$$

The magnitude and phase functions are:

$$|H(e^{j\omega})| = 2\alpha \cos \omega + \beta \quad (4.108)$$

$$\theta(\omega) = -\omega \quad (4.109)$$

In order to block the low-frequency component, the magnitude function at  $\omega = 0.1$  should be equal to zero. Likewise, to pass the high-frequency component, the magnitude function at  $\omega = 0.4$  should be equal to one. Thus, the two conditions that must be satisfied are:

$$|H(e^{j0.1})| = 2\alpha \cos(0.1) + \beta = 0 \quad (4.110)$$

$$|H(e^{j0.4})| = 2\alpha \cos(0.4) + \beta = 1 \quad (4.111)$$

Solving the above two equations we get:

$$\alpha = -6.76195 \quad (4.112)$$

$$\beta = 13.456335 \quad (4.113)$$

$$(4.114)$$

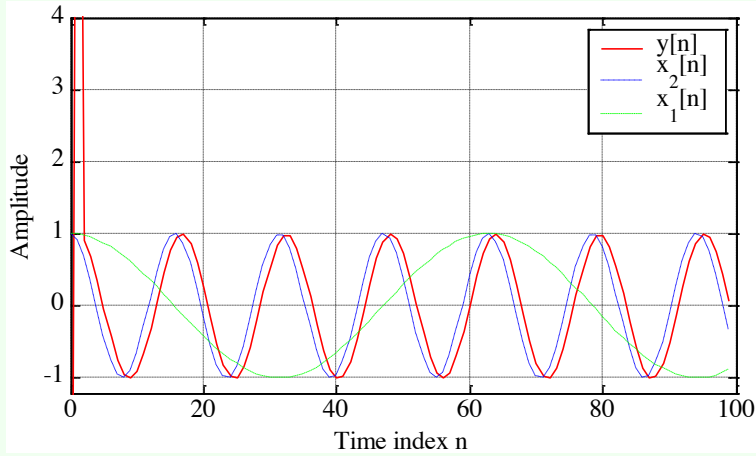
Thus the output-input relation of the FIR filter is given by:

$$y[n] = -6.76195(x[n] + x[n-2]) + 13.456335x[n-1] \quad (4.115)$$

where the input is:

$$x[n] = \{\cos(0.1n) + \cos(0.4n)\}\mu[n] \quad (4.116)$$

A plot of the signals of interests is showed below.



The first seven samples of the output are showed below as well.

| $n$ | $\cos(0.1n)$ | $\cos(0.4n)$ | $x[n]$    | $y[n]$     |
|-----|--------------|--------------|-----------|------------|
| 0   | 1.0          | 1.0          | 2.0       | -13.52390  |
| 1   | 0.9950041    | 0.9210609    | 1.9160652 | 13.956333  |
| 2   | 0.9800665    | 0.6967067    | 1.6767733 | 0.9210616  |
| 3   | 0.9553364    | 0.3623577    | 1.3176942 | 0.6967064  |
| 4   | 0.9210609    | -0.0291995   | 0.8918614 | 0.3623572  |
| 5   | 0.8775825    | -0.4161468   | 0.4614357 | -0.0292002 |
| 6   | 0.8253356    | -0.7373937   | 0.0879419 | -0.4161467 |

From this table, it can be seen that, neglecting the least significant digit:

$$y[n] = \cos(0.4(n-1)), \quad n \geq 2 \quad (4.117)$$

Computation of the present value of the output requires the knowledge of the present and two previous input samples. Hence, the first two output samples,  $y[0]$  and  $y[1]$ , are the result of assumed zero input sample values at  $n = -1$  and  $n = -2$ . Therefore, first two output samples constitute the transient part of the output. Since the impulse response is of length 3, the steady-state is reached at  $n = N = 2$ . Note also that the output is delayed version of the high-frequency component  $\cos(0.4n)$  of the input, and the delay is one sample period.

**Lecture 12.**  
Thursday 5<sup>th</sup>  
November, 2020.

## 4.5 Discrete Fourier Transform

We have discussed the DTFT for a discrete-time function given by:

$$X(e^{j\omega}) = \sum_{n=-\infty}^{\infty} x[n]e^{-j\omega n} \quad (4.118)$$

and the IDTFT:

$$x[n] = \frac{1}{2\pi} \int_{-\pi}^{\pi} X(e^{j\omega})e^{j\omega n} d\omega \quad (4.119)$$

The pair and their properties and applications have some limitations. The input signal is usually aperiodic and may be finite in length.

Moreover, we often do not have an infinite amount of data which is required by DTFT. For example in a computer we cannot calculate uncountable infinite (continuum) of

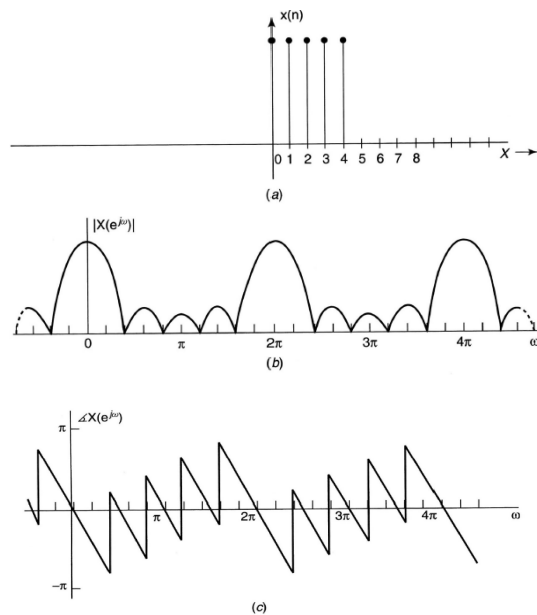


**Figure 4.8:** In order from top to bottom, a finite-length signal, its magnitude spectrum, its phase spectrum.

frequencies as required by DTFT. Thus, we use DTF to look at finite segment of data. We only observe the data through a window:

$$x_0[n] = x[n]w_R[n] \quad (4.120)$$

$$w_R[n] = \begin{cases} 1 & n = 0, 1, \dots, N-1 \\ 0 & \text{otherwise} \end{cases} \quad (4.121)$$

In this case, the  $x_0[n]$  is just a sampled data between  $n = 0, n = N-1$  (so,  $N$  points). The solution to our problems is given by the Discrete Fourier Transform (DFT).

#### Definition 9: Discrete Fourier Transform (DFT)

The simplest relation between a length- $N$  sequence  $x[n]$ , defined for  $0 \leq n \leq N-1$ , and its DTFT  $X(e^{j\omega})$  is obtained by uniformly sampling on the  $\omega$ -axis between  $0 \leq \omega \leq 2\pi$  at  $\omega_k = \frac{2\pi k}{N}$ , for  $0 \leq k \leq N-1$ . From the definition of the DTFT we thus have:

$$X[k] = [X(e^{j\omega})]_{\omega=\frac{2\pi k}{N}} = \sum_{n=0}^{N-1} x[n]e^{-j2\pi k \frac{n}{N}} \quad (4.122)$$

Note that  $X[k]$  is also a length- $N$  sequence in the frequency domain and it is called the Discrete Fourier Transform (DFT) of the sequence  $x[n]$ . Using the notation  $W_N = e^{-j\frac{2\pi}{N}}$ , the DFT is usually expressed as:

$$X[k] = \sum_{n=0}^{N-1} x[n]W_N^{kn}, \quad 0 \leq k \leq N-1 \quad (4.123)$$

**Definition 10: Inverse Discrete Fourier Transform (IDFT)**

The Inverse Discrete Fourier Transform (IDFT) is given by:

$$x[n] = \frac{1}{N} \sum_{k=0}^{N-1} X[k] W_N^{-kn}, \quad 0 \leq n \leq N-1 \quad (4.124)$$

To verify the above expression we multiply both sides of the above equation by  $W_N^{\ell n}$  and sum the result from  $n = 0$  to  $n = N - 1$ , resulting in:

$$\begin{aligned} \sum_{n=0}^{N-1} x[n] W_N^{\ell n} &= \sum_{n=0}^{N-1} \left( \frac{1}{N} \sum_{k=0}^{N-1} X[k] W_N^{-kn} \right) W_N^{\ell n} \\ &= \frac{1}{N} \sum_{n=0}^{N-1} \sum_{k=0}^{N-1} X[k] W_N^{-(k-\ell)n} \\ &= \frac{1}{N} \sum_{k=0}^{N-1} \sum_{n=0}^{N-1} X[k] W_N^{-(k-\ell)n} \end{aligned} \quad (4.125)$$

Making use of the identity:

$$\sum_{n=0}^{N-1} W_N^{-(k-\ell)n} = \begin{cases} N & k - \ell = rN, \quad n \in \mathbb{Z} \\ 0 & \text{otherwise} \end{cases} \quad (4.126)$$

we observe that the right-hand-side of the last equation is equal to  $X[\ell]$ . Hence:

$$\sum_{n=0}^{N-1} x[n] W_N^{\ell n} = X[\ell] \quad (4.127)$$

**Example 25: Discrete Fourier Transform**

Consider the length- $N$  sequence:

$$x[n] = \begin{cases} 1 & n = 0 \\ 0 & 1 \leq n \leq N-1 \end{cases} \quad (4.128)$$

Its  $N$ -point DFT is given by:

$$X[k] = \sum_{n=0}^{N-1} x[n] W_N^{kn} = x[0] W_N^0 = 1 \quad (4.129)$$

with  $0 \leq k \leq N-1$ .

**Example 26: Discrete Fourier Transform**

Consider the length- $N$  sequence:

$$y[n] = \begin{cases} 1 & n = m \\ 0 & 0 \leq n \leq m-1, \quad m+1 \leq n \leq N-1 \end{cases} \quad (4.130)$$

Its  $N$ -point DFT is given by:

$$Y[k] = \sum_{n=0}^{N-1} y[n] W_N^{kn} = y[m] W_N^{km} = W_N^{km} \quad (4.131)$$

with  $0 \leq k \leq N - 1$ .

### Example 27: Discrete Fourier Transform

Consider the length- $N$  sequence defined for  $0 \leq n \leq N - 1$ :

$$g[n] = \cos\left(\frac{2\pi rn}{N}\right), \quad 0 \leq r \leq N - 1 \quad (4.132)$$

Using trigonometric identities, we can rewrite:

$$g[n] = \frac{1}{2} \left( e^{j2\pi r \frac{n}{N}} + e^{-j2\pi r \frac{n}{N}} \right) = \frac{1}{2} (W_N^{-rn} + W_N^{rn}) \quad (4.133)$$

The  $N$ -point DFT of  $g[n]$  is thus given by:

$$G[k] = \sum_{n=0}^{N-1} g[n] W_N^{kn} = \frac{1}{2} \left( \sum_{n=0}^{N-1} W_N^{-(r-k)n} + \sum_{n=0}^{N-1} W_N^{(r+k)n} \right) \quad (4.134)$$

with  $0 \leq k \leq N - 1$ . Making use of the identity:

$$\sum_{n=0}^{N-1} W_N^{-(k-\ell)n} = \begin{cases} N & k - \ell = rN, \quad r \in \mathbb{Z} \\ 0 & \text{otherwise} \end{cases} \quad (4.135)$$

we get:

$$\begin{cases} \frac{N}{2} & k = r \\ \frac{N}{2} & k = N - r \\ 0 & \text{otherwise} \end{cases} \quad (4.136)$$

with  $0 \leq k \leq N - 1$ .

#### 4.5.1 Matrix relations

The DFT samples defined by:

$$X[k] = \sum_{n=0}^{N-1} x[n] W_N^{kn}, \quad 0 \leq k \leq N - 1 \quad (4.137)$$

can be expressed in matrix form as:

$$\mathbf{X} = \mathbf{D}_N \mathbf{x} \quad (4.138)$$

where:

$$\mathbf{X} = [X[0] \ X[1] \ \dots \ X[N - 1]]^T \quad (4.139)$$

$$\mathbf{x} = [x[0] \ x[1] \ \dots \ x[N - 1]]^T \quad (4.140)$$

and  $\mathbf{D}_N$  is the  $N \times N$  DFT matrix given by:

$$\mathbf{D}_N = \begin{bmatrix} 1 & 1 & 1 & \dots & 1 \\ 1 & W_N^1 & W_N^2 & \dots & W_N^{(N-1)} \\ 1 & W_N^2 & W_N^4 & \dots & W_N^{2(N-1)} \\ \vdots & \vdots & \vdots & \ddots & \vdots \\ 1 & W_N^{(N-1)} & W_N^{2(N-1)} & \dots & W_N^{(N-1)^2} \end{bmatrix} \quad (4.141)$$

Likewise, the IDFT relation given by:

$$x[n] = \frac{1}{N} \sum_{k=0}^{N-1} X[k] W_N^{-kn}, \quad 0 \leq n \leq N-1 \quad (4.142)$$

can be expressed in matrix form as:

$$\mathbf{x} = \mathbf{D}_N^{-1} \mathbf{X} \quad (4.143)$$

where  $\mathbf{D}_N^{-1}$  is the  $N \times N$  IDFT matrix, given by:

$$\mathbf{D}_N^{-1} = \begin{bmatrix} 1 & 1 & 1 & \cdots & 1 \\ 1 & W_N^{-1} & W_N^{-2} & \cdots & W_N^{-(N-1)} \\ 1 & W_N^{-2} & W_N^{-4} & \cdots & W_N^{-2(N-1)} \\ \vdots & \vdots & \vdots & \ddots & \vdots \\ 1 & W_N^{-(N-1)} & W_N^{-2(N-1)} & \cdots & W_N^{-(N-1)^2} \end{bmatrix} = \frac{1}{N} \mathbf{D}_N^* \quad (4.144)$$

#### 4.5.2 DTFT from DFT by interpolation

The  $N$ -point DFT  $X[k]$  of a length- $N$  sequence  $x[n]$  is simply the frequency samples of its DTFT  $X(e^{j\omega})$  evaluated at  $N$  uniformly spaced frequency points:

$$\omega = \omega_k = \frac{2\pi k}{N}, \quad 0 \leq k \leq N-1 \quad (4.145)$$

Given the  $N$ -point DFT  $X[k]$  of a length- $N$  sequence  $x[n]$ , its DTFT  $X(e^{j\omega})$  can be uniquely determined from  $X[k]$ . Thus:

$$\begin{aligned} X(e^{j\omega}) &= \sum_{n=0}^{N-1} x[n] e^{-j\omega n} \\ &= \sum_{n=0}^{N-1} \left[ \frac{1}{N} \sum_{k=0}^{N-1} X[k] W_N^{-kn} \right] e^{-j\omega n} \\ &= \frac{1}{N} \sum_{k=0}^{N-1} X[k] \underbrace{\sum_{n=0}^{N-1} e^{-j(\omega - \frac{2\pi k}{N})n}}_S \end{aligned} \quad (4.146)$$

To develop a compact expression for the sum  $S$ , let  $r = e^{-j(\omega - \frac{2\pi k}{N})}$ . Then:

$$S = \sum_{n=0}^{N-1} r^n \quad (4.147)$$

From the above:

$$\begin{aligned} rS &= \sum_{n=1}^N r^n = 1 + \sum_{n=1}^{N-1} r^n r^N - 1 \\ &= \sum_{n=0}^{N-1} r^n + r^N - 1 = S + r^N - 1 \end{aligned} \quad (4.148)$$

or, equivalently:

$$S - rS = (1 - r)S = 1 - r^N \quad (4.149)$$

Hence:

$$\begin{aligned} S &= \frac{1 - r^N}{1 - r} \\ &= \frac{1 - e^{-j(\omega n - 2\pi k)}}{1 - e^{-j(\omega - \frac{2\pi k}{N})}} \\ &= \frac{\sin\left(\frac{\omega N 2\pi k}{2}\right)}{\sin\left(\frac{\omega N - 2\pi k}{2N}\right)} e^{-j\left(\frac{\omega - 2\pi k}{N}\right)\left(\frac{N-1}{2}\right)} \end{aligned} \quad (4.150)$$

Therefore:

$$X(e^{j\omega}) = \frac{1}{N} \sum_{k=0}^{N-1} X[k] \frac{\sin\left(\frac{\omega N 2\pi k}{2}\right)}{\sin\left(\frac{\omega N - 2\pi k}{2N}\right)} e^{-j\left(\frac{\omega - 2\pi k}{N}\right)\left(\frac{N-1}{2}\right)} \quad (4.151)$$

### 4.5.3 Sampling the DTFT

Consider a sequence  $x[n]$  with a DTFT  $X(e^{j\omega})$ . We sample  $X(e^{j\omega})$  at  $N$  equally spaced points  $\omega_k = \frac{2\pi k}{N}$ ,  $0 \leq k \leq N-1$ , developing the  $N$  frequency samples  $\{X(e^{j\omega_k})\}$ . These  $N$  frequency samples can be considered as an  $N$ -point DFT  $Y[k]$  whose  $N$ -point IDFT is a length- $N$  sequence  $y[n]$ . Now:

$$X(e^{j\omega}) = \sum_{\ell=-\infty}^{\infty} x[\ell] e^{-j\omega\ell} \quad (4.152)$$

Thus:

$$Y[k] = X(e^{j\omega_k}) = X(e^{j\frac{2\pi k}{N}}) = \sum_{\ell=-\infty}^{\infty} x[\ell] e^{-j2\pi k \frac{\ell}{N}} = \sum_{\ell=-\infty}^{\infty} x[\ell] W_N^{k\ell} \quad (4.153)$$

An IDFT of  $Y[k]$  yields:

$$\begin{aligned} y[n] &= \frac{1}{N} \sum_{k=0}^{N-1} Y[k] W_N^{-kn} \\ &= \frac{1}{N} \sum_{k=0}^{N-1} \sum_{\ell=-\infty}^{\infty} x[\ell] W_N^{k\ell} W_N^{-kn} \\ &= \sum_{\ell=-\infty}^{\infty} x[\ell] \left[ \sum_{k=0}^{N-1} W_N^{-k(n-\ell)} \right] \\ &= \sum_{m=-\infty}^{\infty} x[n+mN] \end{aligned} \quad (4.154)$$

with  $0 \leq n \leq N-1$ , where in the last passage the identity in Eq. 4.135 is employed. Thus,  $y[n]$  is obtained from  $x[n]$  by adding an infinite number of shifted replicas of  $x[n]$ , with each replica shifted by an integer multiple of  $N$  sampling instants, and observing the sum only for the interval  $0 \leq n \leq N-1$ .

To apply the last result to finite-length sequences, we assume that the samples outside the specified range are zeros. Thus, if  $x[n]$  is a length- $M$  sequence with  $M \leq N$ , then  $y[n] = x[n]$  for  $0 \leq n \leq N-1$ . If  $M > N$ , there is a time-domain aliasing of samples of  $x[n]$  in generating  $y[n]$ , and  $x[n]$  cannot be recovered from  $y[n]$ .

**Example 28: Aliasing**

Let  $x[n] = \{0, 1, 2, 3, 4, 5\}$ . By sampling its DTFT  $X(e^{j\omega})$  at  $\omega_k = \frac{2\pi k}{4}$ , with  $0 \leq k \leq 3$ , and then applying a 4-point IDFT to these samples, we arrive at the sequence  $y[n]$  given by:

$$y[n] = x[n] + x[n+4] + x[n-4], \quad 0 \leq n \leq 3 \quad (4.155)$$

We get  $y[n] = \{4, 6, 2, 3\}$ .  $x[n]$  cannot be recovered from  $y[n]$ .

#### 4.5.4 DFT properties

Like the DTFT, the DFT also satisfies a number of properties that are useful in signal processing applications. Some of these properties are essentially identical to those of the DTFT, while some others are somewhat different. A summary of the DFT properties are given in Figures 4.9, 4.10 and 4.11.

| Length- $N$ Sequence  | $N$ -point DFT  |
|-----------------------|---|
| $x[n]$                | $X[k]$  |
| $x^*[n]$              | $X^*[(-k)_N]$   |
| $x^*[(-n)_N]$         | $X^*[k]$  |
| $\text{Re}\{x[n]\}$   | $X_{\text{pcs}}[k] = \frac{1}{2}\{X[(k)_N] + X^*[(-k)_N]\}$ |
| $j \text{Im}\{x[n]\}$ | $X_{\text{pca}}[k] = \frac{1}{2}\{X[(k)_N] - X^*[(-k)_N]\}$ |
| $x_{\text{pcs}}[n]$   | $\text{Re}\{X[k]\}$   |
| $x_{\text{pca}}[n]$   | $j \text{Im}\{X[k]\}$                                       |

Note:  $x_{\text{pcs}}[n]$  and  $x_{\text{pca}}[n]$  are the periodic conjugate-symmetric and periodic conjugate-antisymmetric parts of  $x[n]$ , respectively. Likewise,  $X_{\text{pcs}}[k]$  and  $X_{\text{pca}}[k]$  are the periodic conjugate-symmetric and periodic conjugate-antisymmetric parts of  $X[k]$ , respectively.

**Figure 4.9:** Symmetry relations of DFT for a complex sequence  $x[n]$ .

| Length- $N$ Sequence | $N$ -point DFT  |
|----------------------|---|
| $x[n]$               | $X[k] = \text{Re}\{X[k]\} + j \text{Im}\{X[k]\}$  |
| $x_{\text{pe}}[n]$   | $\text{Re}\{X[k]\}$   |
| $x_{\text{po}}[n]$   | $j \text{Im}\{X[k]\}$   |
| Symmetry relations   | $\begin{aligned} X[k] &= X^*[(-k)_N] \\ \text{Re } X[k] &= \text{Re } X[(-k)_N] \\ \text{Im } X[k] &= -\text{Im } X[(-k)_N] \\  X[k]  &=  X[(-k)_N]  \\ \arg X[k] &= -\arg X[(-k)_N] \end{aligned}$ |

Note:  $x_{\text{pe}}[n]$  and  $x_{\text{po}}[n]$  are the periodic even and periodic odd parts of  $x[n]$ , respectively.

**Figure 4.10:** Symmetry relations of DFT for a real sequence  $x[n]$ .

#### 4.5.5 Circular shift of a sequence

This property is analogous to the time-shifting property of the DTFT but with a difference. Consider length- $N$  sequences defined for  $0 \leq n \leq N-1$ . Sample values

| Type of Property                | Length- $N$ Sequence                              | $N$ -point DFT  |
|---------------------------------|---|---|
|                                 | $\frac{g[n]}{h[n]}$                               | $\frac{G[k]}{H[k]}$   |
| Linearity                       | $\alpha g[n] + \beta h[n]$                        | $\alpha G[k] + \beta H[k]$                                    |
| Circular time-shifting          | $g[(n - n_0)_N]$                                  | $W_N^{kn_0} G[k]$   |
| Circular frequency-shifting     | $W_N^{-k_0 n} g[n]$                               | $G[\langle k - k_0 \rangle_N]$                                |
| Duality                         | $G[n]$  | $N g[\langle -k \rangle_N]$                                   |
| $N$ -point circular convolution | $\sum_{m=0}^{N-1} g[m]h[\langle n - m \rangle_N]$ | $G[k]H[k]$  |
| Modulation                      | $g[n]h[n]$  | $\frac{1}{N} \sum_{m=0}^{N-1} G[m]H[\langle k - m \rangle_N]$ |

|                     |   |
|---------------------|---|
| Parseval's relation | $\sum_{n=0}^{N-1}  x[n] ^2 = \frac{1}{N} \sum_{k=0}^{N-1}  X[k] ^2$ |
|---------------------|---|

**Figure 4.11:** General properties of DFT.

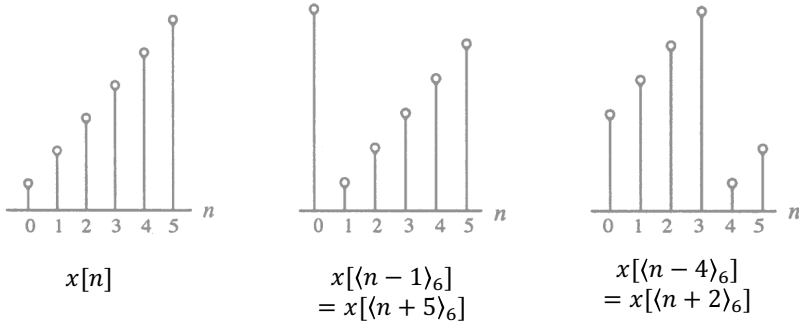
of such sequences are equal to zero for values of  $n < 0$  and  $n \geq N$ . If  $x[n]$  is such a sequence, then for any arbitrary integer  $n_0$ , the shifted sequence  $x_1[n] = x[n - n_0]$  is no longer defined for the range  $0 \leq n \leq N - 1$ . We thus need to define another type of shift that will always keep the shifted sequence in the range  $0 \leq n \leq N - 1$ . The desired shift, called the circular shift, is defined using a modulo operation:

$$x_c[n] = x[\langle n - n_0 \rangle_N] \quad (4.156)$$

For  $n_0 > 0$  (right circular shift), the above equation implies:

$$x_c[n] = \begin{cases} x[n - n_0] & n_0 \leq n \leq N - 1 \\ x[N - n_0 + n] & 0 \leq n \leq n_0 \end{cases} \quad (4.157)$$

An illustration of the concept of circular shift is showed in Figure 4.12. As it is possible to observe, a right circular shift by  $n_0$  is equivalent to a left circular shift by  $N - n_0$  sample periods. A circular shift by an integer number  $n_0$  greater than  $N$  is equivalent to a circular shift by  $\langle n_0 \rangle_N$ .

**Figure 4.12:** Illustration of circular shift.

#### 4.5.6 Circular convolution

This operation is analogous to linear convolution, but with a difference. Consider two length- $N$  sequences,  $g[n]$  and  $h[n]$ , respectively. Their linear convolution results in a length- $(2N - 1)$  sequence  $y_L[n]$  given by:

$$y_L[n] = \sum_{m=0}^{N-1} g[m]h[n - m], \quad 0 \leq n \leq 2N - 2 \quad (4.158)$$

In computing  $y_L[n]$  we have assumed that both length- $N$  sequences have been zero-padded to extend their lengths to  $2N - 1$ . The longer form of  $y_L[n]$  results from the time-reversal of the sequence  $h[n]$  and its linear shift to the right. The first nonzero value of  $y_L[n]$  is  $y_L[0] = g[0]h[0]$  and the last nonzero value is  $y_L[2N - 2] = g[N - 1]h[N - 1]$ .

To develop a convolution-like operation resulting in a length- $N$  sequence  $y_C[n]$ , we need to define a circular time-reversal, and then apply a circular time-shift. Resulting operation, called a circular convolution, is defined by:

$$y_C[n] = \sum_{m=0}^{N-1} g[m]h[\langle n-m \rangle_N], \quad 0 \leq n \leq N-1 \quad (4.159)$$

Since the operation defined involves two length- $N$  sequences, it is often referred to as an  $N$ -point circular convolution, denoted as:

**Lecture 13.**  
Tuesday 10<sup>th</sup>  
November, 2020.

#### 4.5.7 DFT of real sequences

In most practical applications, sequences of interest are real. In such cases, the symmetry properties of the DFT can be exploited to make the DFT computations more efficient.

Let  $g[n]$  and  $h[n]$  be two length- $N$  real sequences with  $G[k]$  and  $H[k]$  denoting their respective  $N$ -point DFTs. These two  $N$ -point DFTs can be computed efficiently using a single  $N$ -point DFT. Now, define a complex length- $N$  sequence:

$$x[n] = g[n] + jh[n] \quad (4.160)$$

Hence,  $g[n] = \text{Re}\{x[n]\}$  and  $h[n] = \text{Im}\{x[n]\}$ . Let  $X[k]$  denote the  $N$ -point DFT of  $x[n]$ . Then, we arrive at:

$$G[k] = \frac{1}{2}\{X[k] + X^*[\langle -k \rangle_N]\} \quad (4.161)$$

$$H[k] = \frac{1}{2j}\{X[k] - X^*[\langle -k \rangle_N]\} \quad (4.162)$$

Note that for  $0 \leq k \leq N-1$ :

$$X^*[\langle -k \rangle_N] = X^*[\langle N-k \rangle_N] \quad (4.163)$$

#### Example 29: DFT of real sequences

We compute the 4-point DFTs of the two real sequences  $g[n]$  and  $h[n]$ :

$$g[n] = \{1, 2, 0, 1\} \quad (4.164)$$

$$h[n] = \{2, 2, 1, 1\} \quad (4.165)$$

Then  $x[n] = g[n] + jh[n]$  is given by:

$$x[n] = \{1 + j2, 2 + j2, 1 + j\} \quad (4.166)$$

Its DFT  $X[k]$  is:

$$\begin{bmatrix} X[0] \\ X[1] \\ X[2] \\ X[3] \end{bmatrix} = \begin{bmatrix} 1 & 1 & 1 & 1 \\ 1 & -j & -1 & j \\ 1 & -1 & 1 & -1 \\ 1 & j & -1 & -1 \end{bmatrix} \begin{bmatrix} 1+j2 \\ 2+j2 \\ j \\ 1+j \end{bmatrix} = \begin{bmatrix} 4+j6 \\ 2 \\ -2 \\ j2 \end{bmatrix} \quad (4.167)$$

From the above:

$$X^*[k] = [4 - j6, 2, -2, -j2] \quad (4.168)$$

Hence:

$$X^*[\langle 4 - k \rangle_4] = [4 - j6, -j2, -2, 2] \quad (4.169)$$

Therefore:

$$G[k] = [4, 1 - j, -2, 1 + j] \quad (4.170)$$

$$H[k] = [6, 1 - j, 0, 1 + j] \quad (4.171)$$

verifying the results derived in Lecture 12

Now, let  $v[n]$  be a length- $2N$  real sequence with a  $2N$ -point DFT  $V[k]$ . Define two length- $N$  real sequences  $g[n]$  and  $h[n]$  as follows. Let  $G[k]$  and  $H[k]$  denote their respective  $N$ -point DFTs:

$$\begin{cases} g[n] = v[2n] \\ h[n] = v[2n + 1] \end{cases} \quad 0 \leq n \leq N \quad (4.172)$$

We define a length- $N$  complex sequence  $x[n] = g[n] + jh[n]$  with an  $N$ -point DFT  $X[k]$ . Then, as showed earlier:

$$G[k] = \frac{1}{2}\{X[k] + X^*[\langle -k \rangle_N]\} \quad (4.173)$$

$$H[k] = \frac{1}{2j}\{X[k] - X^*[\langle -k \rangle_N]\} \quad (4.174)$$

Now, for  $0 \leq k \leq 2N - 1$ :

$$\begin{aligned} V[k] &= \sum_{n=0}^{2N-1} v[n]W_{2N}^{nk} \\ &= \sum_{n=0}^{N-1} v[2n]W_{2N}^{2nk} + \sum_{n=0}^{N-1} v[2n+1]W_{2N}^{(2n+1)k} \\ &= \sum_{n=0}^{N-1} g[n]W_N^{nk} + \sum_{n=0}^{N-1} W_N^{nk}W_{2N}^k \\ &= \sum_{n=0}^{N-1} g[n]W_N^{nk} + W_{2N}^k \sum_{n=0}^{N-1} h[n]W_N^{nk} \\ &= G[\langle k \rangle_N] + W_{2N}^k H[\langle k \rangle_N] \end{aligned} \quad (4.175)$$

### Example 30: DFT of real sequences

Let us determine the 8-point DFT  $V[k]$  of the length-8 real sequence:

$$v[n] = \{1, 2, 2, 2, 0, 1, 1, 1\} \quad (4.176)$$

We form two length-4 real sequences as follows:

$$g[n] = v[2n] = \{1, 2, 0, 1\} \quad (4.177)$$

$$h[n] = v[2n+1] = \{2, 2, 1, 1\} \quad (4.178)$$

Now:

$$V[k] = G[\langle k \rangle_4] + W_8^k H[\langle k \rangle_4] \quad 0 \leq k \leq 7 \quad (4.179)$$

Substituting the values of the 4-point DFTs  $G[k]$  and  $H[k]$  computed earlier, we get:

$$V[0] = G[0] + H[0] = 4 + 6 = 10 \quad (4.180)$$

$$V[1] = G[1] + W_1^0 H[1] = (1 - j) + e^{-j\frac{\pi}{4}}(1 - j) = 1 - j2.4142 \quad (4.181)$$

$$V[2] = G[2] + W_2^0 H[2] = -2 + e^{-j\frac{3\pi}{4}} \cdot 0 = -2 \quad (4.182)$$

$$V[3] = G[3] + W_3^0 H[3] = (1 + j) + e^{-j\frac{3\pi}{4}}(1 + j) = 1 - j0.4142 \quad (4.183)$$

$$V[4] = G[0] + W_4^0 H[0] = 4 + e^{-j\pi} \cdot 6 = -2 \quad (4.184)$$

$$V[5] = G[1] + W_5^0 H[1] = (1 - j) + e^{-j\frac{5\pi}{4}}(1 - j) = 1 + j0.4142 \quad (4.185)$$

$$V[6] = G[2] + W_6^0 H[2] = -2 + e^{-j\frac{3\pi}{2}} \cdot 0 = -2 \quad (4.186)$$

$$V[7] = G[3] + W_7^0 H[3] = (1 + j) + e^{-j\frac{7\pi}{4}}(1 + j) = 1 + j2.4142 \quad (4.187)$$

## 4.6 Linear convolution using the DFT

Linear convolution is a key operation in many signal processing applications. Since a DFT can be efficiently implemented using FFT algorithms, it is of interest to develop methods for the implementation of linear convolution using the DFT.

Let  $g[n]$  and  $h[n]$  be two finite-length sequences of length  $N$  and  $M$ , respectively. Moreover, we denote with  $L = N + M + 1$ . Then, we define two length- $L$  sequences:

$$g_e[n] = \begin{cases} g[n] & 0 \leq n \leq N - 1 \\ 0 & N \leq n \leq L - 1 \end{cases} \quad (4.188)$$

$$h_e[n] = \begin{cases} h[n] & 0 \leq n \leq M - 1 \\ 0 & M \leq n \leq L - 1 \end{cases} \quad (4.189)$$

Then:

$$y_L[n] = g[n] * h[n] = y_C[n] = g_e[n] \overset{L}{*} h_e[n] \quad (4.190)$$

The corresponding implementation scheme is illustrated in Figure 4.13.

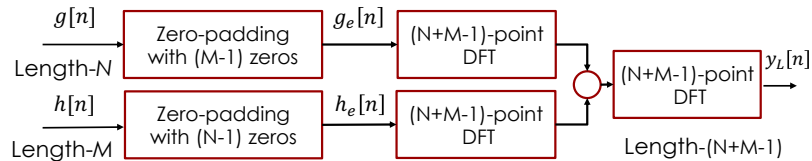


**Figure 4.13:** Scheme of linear convolution of two finite-length sequences.

We next consider the DFT-based implementation of:

$$y[n] = \sum_{\ell=0}^{M-1} h[\ell]x[n-\ell] = h[n] * x[n] \quad (4.191)$$

where  $h[n]$  is a finite-length sequence of length  $M$  and  $x[n]$  is an infinite length (or a finite length sequence of length much greater than  $M$ ). We first segment  $x[n]$ , assumed to be a causal sequence here without any loss of generality, into a set of contiguous finite-length subsequences  $x_m[n]$  of length  $N$  each:

$$x[n] = \sum_{m=0}^{\infty} x_m[n - mN] \quad (4.192)$$

where:

$$x_m[n] = \begin{cases} x[n + mN] & 0 \leq n \leq N - 1 \\ 0 & \text{otherwise} \end{cases} \quad (4.193)$$

Thus, we can write:

$$y[n] = h[n] * x[n] = \sum_{m=0}^{\infty} y_m[n - mN] \quad (4.194)$$

where:

$$y_m = h[n] * x_m[n] \quad (4.195)$$

Since  $h[n]$  is of length  $M$  and  $x_m[n]$  is of length  $N$ , the linear convolution  $h[n] * x_m[n]$  is of length  $N + M - 1$ .

As a result, the desired linear convolution  $y[n] = h[n] * x[n]$  has been broken up into a sum of infinite numbers of short-length linear convolutions of length  $N + M - 1$  each:

$$y_m[n] = h[n] * x_m[n] \quad (4.196)$$

Each of these short convolutions can be implemented using the DFT-based method discussed earlier, where now the DFTs (and the IDFT) are computed on the basis of  $N + M - 1$  points.

There is one more subtlety to take care of before we can implement:

$$y[n] = \sum_{m=0}^{\infty} y_m[n - mN] \quad (4.197)$$

using the DFT-based approach. Now the first convolution in Eq. 4.197, namely  $y_0 = h[n] * x_0[n]$ , is of length  $N + M - 1$  and is defined for  $0 \leq n \leq N + M - 2$ . The second short convolution, namely  $y_1[n] = h[n] * x_1[n]$ , is also of length  $N + M - 1$  but it is defined for  $N \leq n \leq 2N + M - 2$ . There is an overlap of  $M - 1$  samples between these two short linear convolutions. Likewise the third short convolution, namely  $y_2[n] = h[n] * x_2[n]$ , is also of length  $N + M - 1$  but is defined for  $2N \leq n \leq 3N + M - 2$ . Thus, there is an overlap of  $M - 1$  samples between  $h[n] * x_1[n]$  and  $h[n] * x_2[n]$ .

In general, there will be an overlap of  $M - 1$  samples between the samples of the short convolutions  $h[n] * x_{r-1}[n]$  and  $h[n] * x_r[n]$  for  $(r-1)N \leq n \leq rN + M - 1$ . This process is illustrated in Figures 4.14 and 4.15 for  $M = 5$  and  $N = 7$ .

Therefore,  $y[n]$  obtained by a linear convolution of  $x[n]$  and  $h[n]$  is given by:

$$y[n] = y_0[n] \quad 0 \leq n \leq 6 \quad (4.198)$$

$$y[n] = y_0[n] + y_1[n - 7] \quad 7 \leq n \leq 10 \quad (4.199)$$

$$y[n] = y_1[n - 7] \quad 11 \leq n \leq 13 \quad (4.200)$$

$$y[n] = y_1[n - 7] + y_2[n - 14] \quad 14 \leq n \leq 17 \quad (4.201)$$

$$y[n] = y_2[n - 14] \quad 18 \leq n \leq 20 \quad (4.202)$$

$$\vdots \quad \vdots$$

The above procedure is called the overlap-add method since the results of the short linear convolutions overlap and the overlapped portions are added to get the correct final result.

In implementing the overlap-add method using the DFT, we need to compute two  $(N + M - 1)$ -point DFTs and one  $(N + M - 1)$ -point IDFT since the overall linear

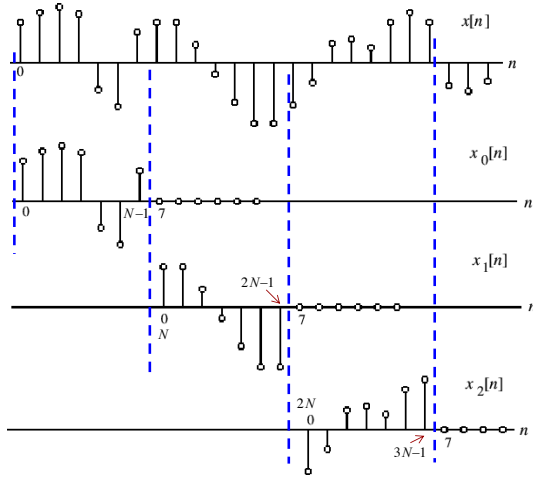


**Figure 4.14:** Overlap-add method for  $M = 5$  and  $N = 7$ .

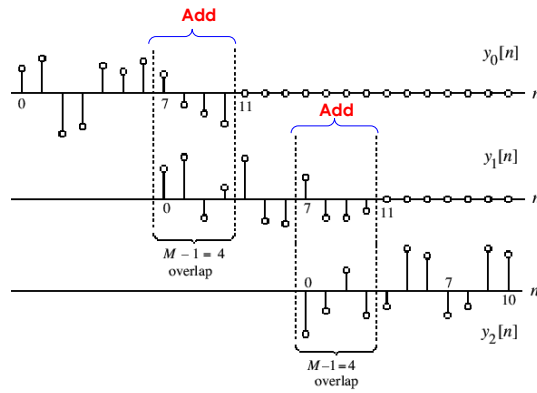


**Figure 4.15:** Overlap-add method for  $M = 5$  and  $N = 7$ .

convolution was expressed as a sum of short-length linear convolutions of length  $N + M - 1$  each. It is possible to implement the overall linear convolution by performing instead circular convolution of length shorter than  $N + M - 1$ . To this end, it is necessary to segment  $x[n]$  into overlapping blocks  $x_m[n]$ , keep the terms of the circular convolution of  $h[n]$  with  $x_m[n]$  that corresponds to the terms obtained by a linear convolution of  $h[n]$  and  $x_m[n]$ , and throw away the other parts of the circular convolution.

To understand the correspondence between the linear and circular convolutions, consider a length-4 sequence  $x[n]$  and a length-3 sequence  $h[n]$ . Let  $y_L[n]$  denote the result of a linear convolution of  $x[n]$  with  $h[n]$ . The six samples of  $y_L[n]$  are given by:

$$y_L[0] = h[0]x[0] \quad (4.203)$$

$$y_L[1] = h[0]x[1] + h[1]x[0] \quad (4.204)$$

$$y_L[2] = h[0]x[2] + h[1]x[1] + h[2]x[0] \quad (4.205)$$

$$y_L[3] = h[0]x[3] + h[1]x[2] + h[2]x[1] \quad (4.206)$$

$$y_L[4] = h[1]x[3] + h[2]x[2] \quad (4.207)$$

$$y_L[5] = h[2]x[3] \quad (4.208)$$

If we append  $h[n]$  with a single zero-valued sample and convert it into a length-4

sequence  $h_e[n]$ , the 4-point circular convolution  $y_C[n]$  of  $h_e[n]$  and  $x[n]$  is given by:

$$y_C[0] = h[0]x[0] + h[1]x[3] + h[2]x[2] \quad (4.209)$$

$$y_C[1] = h[0]x[1] + h[1]x[0] + h[2]x[3] \quad (4.210)$$

$$y_C[2] = h[0]x[2] + h[1]x[1] + h[2]x[0] \quad (4.211)$$

$$y_C[3] = h[0]x[3] + h[1]x[2] + h[2]x[1] \quad (4.212)$$

If we compare the expressions for the samples of  $y_L[n]$  with the samples of  $y_C[n]$ , we observe that the first 2 terms of  $y_C[n]$  do not correspond to the first 2 terms of  $y_L[n]$ , whereas the last 2 terms of  $y_C[n]$  are precisely the same as the third and the forth terms of  $y_L[n]$ .

In general, if we consider the  $N$ -point circular convolution of a length- $M$  sequence  $h[n]$  with a length- $N$  sequence  $x[n]$  with  $N > M$ , the first  $M - 1$  samples of the circular convolution are incorrect and are rejected. The remaining  $N - M + 1$  samples correspond to the correct samples of the linear convolution of  $h[n]$  with  $x[n]$ .

Now we consider an infinitely long or very long sequence  $x[n]$ . We break it up as a collection of smaller length (length-4) overlapping sequences  $x_m[n]$  as  $x_m[n] = x[n + 2m]$ , with  $0 \leq n \leq 3$ ,  $0 \leq m \leq \infty$ . Next, we form:

$$w_m[n] = h[n] \stackrel{4}{\ast} x_m[n] \quad (4.213)$$

or, equivalently

$$w_m[0] = h[0]x_m[0] + h[1]x_m[3] + h[2]x_m[2] \quad (4.214)$$

$$w_m[1] = h[0]x_m[1] + h[1]x_m[0] + h[2]x_m[3] \quad (4.215)$$

$$w_m[2] = h[0]x_m[2] + h[1]x_m[1] + h[2]x_m[0] \quad (4.216)$$

$$w_m[3] = h[0]x_m[3] + h[1]x_m[2] + h[2]x_m[1] \quad (4.217)$$

Computing the above for  $m = 0, 1, 2, 3, \dots$ , and substituting the values of  $x_m[n]$ , we arrive at:

|  |          |
|--|----------|
| $w_0[0] = h[0]x[0] + h[1]x[3] + h[2]x[2]$        | ← Reject |
| $w_0[1] = h[0]x[1] + h[1]x[0] + h[2]x[3]$        | ← Reject |
| $w_0[2] = h[0]x[2] + h[1]x[1] + h[2]x[0] = y[2]$ | ← Save   |
| $w_0[3] = h[0]x[3] + h[1]x[2] + h[2]x[1] = y[3]$ | ← Save   |
| $w_1[0] = h[0]x[2] + h[1]x[5] + h[2]x[4]$        | ← Reject |
| $w_1[1] = h[0]x[3] + h[1]x[2] + h[2]x[5]$        | ← Reject |
| $w_1[2] = h[0]x[4] + h[1]x[3] + h[2]x[2] = y[4]$ | ← Save   |
| $w_1[3] = h[0]x[5] + h[1]x[4] + h[2]x[3] = y[5]$ | ← Save   |
| $w_2[0] = h[0]x[4] + h[1]x[5] + h[2]x[6]$        | ← Reject |
| $w_2[1] = h[0]x[5] + h[1]x[4] + h[2]x[7]$        | ← Reject |
| $w_2[2] = h[0]x[6] + h[1]x[5] + h[2]x[4] = y[6]$ | ← Save   |
| $w_2[3] = h[0]x[7] + h[1]x[6] + h[2]x[5] = y[7]$ | ← Save   |

It should be noted that to determine  $y[0]$  and  $y[1]$  we need to form  $x_{-1}[n]$ , setting  $x_{-1}[0] = x_{-1}[1] = 0$ ,  $x_{-1}[2] = x[0]$ ,  $x_{-1}[3] = x[1]$ , and compute:

$$w_{-1}[n] = h[n] \stackrel{4}{\ast} x_{-1}[n] \quad 0 \leq n \leq 3 \quad (4.218)$$

then reject  $w_{-1}[0]$  and  $w_{-1}[1]$ , and save  $w_{-1}[2] = y[0]$  and  $w_{-1}[3] = y[1]$ .

In general, let  $h[n]$  be a length- $N$  sequence. Let  $x_m[n]$  denote the  $m^{\text{th}}$  section of an infinitely long sequence  $x[n]$  of length  $N$  and defined by:

$$x_m[n] = x[n + m(N - m + 1)] \quad 0 \leq n \leq N - 1 \quad (4.219)$$

with  $M < N$ . Let  $w_m[n] = h[n] * x_m[n]$ . Then, we reject the first  $M - 1$  samples of  $w_m[n]$  and “about” the remaining  $M - M + 1$  samples of  $w_m[n]$  to form  $y_L[n]$ , namely the linear convolution of  $h[n]$  and  $x[n]$ . If  $y_m[n]$  denotes the saved portion of  $w_m[n]$ , i.e.:

$$y_m[n] = \begin{cases} 0 & 0 \leq n \leq M - 2 \\ w_m[n] & M - 1 \leq n \leq N - 2 \end{cases} \quad (4.220)$$

then:

$$y_L[n + m(N - M + 1)] = y_m[n] \quad M - 1 \leq n \leq N - 1 \quad (4.221)$$

The approach is called overlap-save method since the input is segmented into overlapping sections and parts of the results of the circular convolutions are saved and abutted to determine the linear convolution result. The process is illustrated in Figure 4.16.

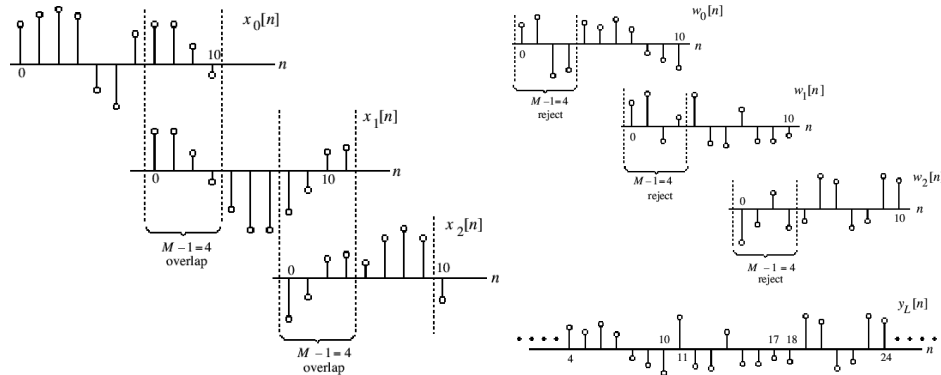


**Figure 4.16:** Illustration of the overlap-save method.

# Chapter 5

## The Z transform

We have seen that the DTFT provides a frequency-domain representation of discrete-time signals and LTI discrete-time systems. However, because of the convergence condition, in many cases, the DTFT of a sequence may not exist. As a result, it is not possible to make use of such frequency-domain characterization in these cases. A possible solution and alternative is a generalization of the DTFT, which leads to the z-transform. The ladder may exist for many sequences for which the DTFT does not exist. Moreover, use of z-transform techniques permits simple but powerful algebraic manipulations. Consequently, z-transform has become an important tool in the analysis and design of digital filters

**Lecture 14.**  
Thursday 12<sup>th</sup>  
November, 2020.

### 5.1 The definition

#### Definition 11: Z-transform

For a given sequence  $g[n]$ , its z-transform  $G(z)$  is defined as:

$$G(z) = \sum_{n=-\infty}^{\infty} g[n]z^{-n} \quad (5.1)$$

where  $z = \text{Re}[z] + j \text{Im}[z]$  is a complex variable.

If we let  $z = re^{j\omega}$ , then the z-transform reduces to:

$$G(re^{j\omega}) = \sum_{n=-\infty}^{\infty} g[n]r^{-n}e^{-j\omega n} \quad (5.2)$$

The above can be interpreted as the DTFT of the modified sequence  $\{g[n]r^{-n}\}$ . For  $r = 1$  (i.e.,  $|z| = 1$ ), the z-transform reduces to its DTFT, provided the ladder exists. Like the DTFT, there are conditions on the convergence of the infinite series like:

$$\sum_{n=-\infty}^{\infty} g[n]z^{-n} \quad (5.3)$$

For a given sequence, the set  $R$  of values of  $z$  for which its z-transform converges is called the region of convergence (ROC).

From our earlier discussion on the uniform convergence of the DTFT, it follows that the series:

$$G(re^{j\omega}) = \sum_{n=-\infty}^{\infty} g[n]r^{-n}e^{-j\omega n} \quad (5.4)$$

converges if  $\{g[n]r^{-n}\}$  is absolutely summable, i.e. if:

$$\sum_{n=-\infty}^{\infty} |g[n]r^{-n}| < \infty \quad (5.5)$$

In general, the ROC  $R$  of a z-transform of a sequence  $g[n]$  is an annular region of the z-plane, namely:

$$R_{g^-} < |z| < R_{g^+} \quad (5.6)$$

where  $0 \leq R_{g^-} < R_{g^+} < \infty$ .

### Example 31: Z-transform calculation

We determine the z-transform  $X(z)$  of the causal sequence  $x[n] = \alpha^n \mu[n]$  and its ROC. Now:

$$X(z) = \alpha^n \mu[n] z^{-n} = \sum_{n=0}^{\infty} \alpha^n z^{-n} \quad (5.7)$$

The above power series converges to:

$$X(z) = \frac{1}{1 - \alpha z^{-1}} \quad |\alpha z^{-1}| < 1 \quad (5.8)$$

ROC is the annular region  $|z| > |\alpha|$ .

### Example 32: Z-transform calculation

The z-transform  $\mu(z)$  of the unit step sequence  $\mu[n]$  can be obtained from:

$$X(z) = \frac{1}{1 - \alpha z^{-1}} \quad |\alpha z^{-1}| < 1 \quad (5.9)$$

By setting  $\alpha = 1$ :

$$\mu(z) = \frac{1}{1 - z^{-1}} \quad |z^{-1}| < 1 \quad (5.10)$$

ROC is the annular region  $1 < |z| < \infty$ . Note that the unit step sequence  $\mu[n]$  is not absolutely summable, and hence its DTFT does not converge uniformly.

### Example 33: Z-transform calculation

Consider the anti-causal sequence:

$$y[n] = -\alpha^n \mu[-n - 1] \quad (5.11)$$

Its z-transform is given by:

$$\begin{aligned} Y(z) &= - \sum_{n=-\infty}^{-1} \alpha^n z^{-n} = - \sum_{m=1}^{\infty} \alpha^{-m} z^m \\ &= -\alpha^{-1} z \sum_{m=0}^{\infty} \alpha^{-m} z^m = -\frac{-\alpha^{-1} z}{1 - \alpha z^{-1}} \\ &= \frac{1}{1 - \alpha z^{-1}} \end{aligned} \quad (5.12)$$

for  $|\alpha^{-1} z| < 1$ . ROC is the annular region  $|z| < |\alpha|$ .

Note that the z-transforms of the two sequences  $\alpha^n \mu[n]$  and  $-\alpha^n \mu[-n-1]$  are identical even though the two parent sequences are different. The only way a unique sequence can be associated with a z-transform is by specifying its ROC.

Another important point is that the DTFT  $G(e^{j\omega})$  of a sequence  $g[n]$  converges uniformly if and only if the ROC of the z-transform  $G(z)$  of  $g[n]$  includes the unit circle. However, the existence of the DTFT does not always imply the existence of the z-transform.

**Example 34: Z-transform**

The finite energy sequence:

$$h_{LP}[n] = \frac{\sin(\omega_c n)}{\pi n} \quad -\infty < n < \infty \quad (5.13)$$

has a DTFT given by:

$$H_{LP}(e^{j\omega}) = \begin{cases} 1 & 0 \leq |\omega| \leq \omega_c \\ 0 & \omega_c < |\omega| \leq \pi \end{cases} \quad (5.14)$$

which converges in the mean-square sense. However,  $h_{LP}[n]$  does not have a z-transform as it is not absolutely summable for any value of  $r$ .

Some commonly used z-transform pairs are listed in Figure 5.1.

| Sequence                       | $z$ -Transform  | ROC               |
|--------------------------------|---|-------------------|
| $\delta[n]$                    | 1   | All values of $z$ |
| $\mu[n]$                       | $\frac{1}{1-z^{-1}}$  | $ z  > 1$         |
| $\alpha^n \mu[n]$              | $\frac{1}{1-\alpha z^{-1}}$   | $ z  >  \alpha $  |
| $(r^n \cos \omega_o n) \mu[n]$ | $\frac{1-(r \cos \omega_o) z^{-1}}{1-(2r \cos \omega_o) z^{-1} + r^2 z^{-2}}$ | $ z  > r$         |
| $(r^n \sin \omega_o n) \mu[n]$ | $\frac{(r \sin \omega_o) z^{-1}}{1-(2r \cos \omega_o) z^{-1} + r^2 z^{-2}}$   | $ z  > r$         |

Figure 5.1: Common z-transform pairs.

## 5.2 Rational z-transforms

In the case of LTI discrete-time systems we are concerned with in this course, all pertinent z-transforms are rational functions of  $z^{-1}$ , that is, they are ratios of two polynomials in  $z^{-1}$ :

$$G(z) = \frac{P(z)}{D(z)} = \frac{p_0 + p_1 z^{-1} + \cdots + p_{M-1} z^{-(M-1)} + p_M z^{-M}}{d_0 + d_1 z^{-1} + \cdots + d_{N-1} z^{-(N-1)} + d_N z^{-N}} \quad (5.15)$$

The degree of the numerator polynomial  $P(z)$  is  $M$  and the degree of the denominator polynomial  $D(z)$  is  $N$ . An alternate representation of a rational z-transform is as a

ratio of two polynomials in  $z$ :

$$G(z) = z^{(N-M)} \frac{p_0 z^M + \cdots + p_{M-1} z + p_M}{d_0 z^N + \cdots + d_{N-1} z + d_N} \quad (5.16)$$

Again, a rational z-transform can be alternately written in factored form as:

$$G(z) = \frac{p_0 \prod_{\ell=1}^M (1 - \xi_\ell z^{-1})}{d_0 \prod_{\ell=1}^N (1 - \lambda_\ell z^{-1})} = z^{(N-M)} \frac{p_0 \prod_{\ell=1}^M (z - \xi_\ell)}{d_0 \prod_{\ell=1}^N (z - \lambda_\ell)} \quad (5.17)$$

We have as roots:

- $z = \xi_\ell$ , roots of the numerator polynomial. These values of  $z$  are known as the zeros of  $G(z)$ ;
- $z = \lambda_\ell$ , roots of the denominator polynomial. These values of  $z$  are known as the poles of  $G(z)$ .

#### Example 35: Zeros and poles

The z-transform:

$$\mu(z) = \frac{1}{1 - z^{-1}} \quad |z| > 1 \quad (5.18)$$

has a zero at  $z = 0$  and a pole at  $z = 1$ .

#### Example 36: ROC of a rational z-transform

The z-transform  $H(z)$  of the sequence  $h[n] = (-0.6)^n \mu[n]$  is given by:

$$H(z) = \frac{1}{1 + 0.6z^{-1}} \quad |z| > 0.6 \quad (5.19)$$

Here the ROC is just outside the circle going through the point  $z = -0.6$ .

A physical interpretation of the concepts of poles and zeros can be given by plotting the log-magnitude  $20 \log_{10} |G(z)|$  as showed in Figure 5.2 for:

$$G(z) = \frac{1 - 2.4z^{-1} + 2.88z^{-2}}{1 - 0.8z^{-1} + 0.64z^{-2}} \quad (5.20)$$

Observe that the magnitude plot exhibits very large peaks around the points  $z = 0.4 \pm j0.6928$ , which are the poles of  $G(z)$ . It also exhibits very narrow and deep wells around the location of the zeros at  $z = 1.2 \pm j1.2$ .

ROC of a z-transform is an important concept. Without its knowledge, there is no unique relationship between a sequence and its z-transform. Hence, the z-transform must always be specified with its ROC. Moreover, there is a relationship between the ROC of the z-transform of the impulse response of a causal LTI discrete-time system and its BIBO stability.

Another important distinction is that a sequence can be one of the following types: finite-length, right-sided, left-sided and two-sided. In general, the ROC depends on the type of the sequence of interest.

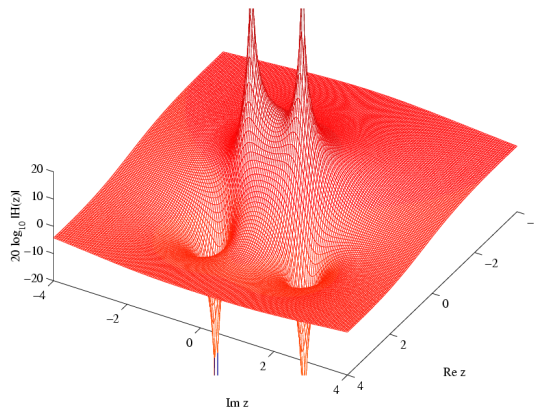


**Figure 5.2:** Log-magnitude plot for  $G(z)$  in Eq. 5.20.

#### Example 37: Finite-length sequence z-transform

Consider a finite-length sequence  $g[n]$  defined for  $-M \leq n \leq N$ , where  $M$  and  $N$  are non-negative integers and  $|g[n]| < \infty$ . Its z-transform is given by:

$$G(z) = \sum_{n=-M}^N g[n]z^{-n} = \frac{\sum_{n=0}^{N+M} g[n-M]z^{N+M-n}}{z^N} \quad (5.21)$$

Note that  $G(z)$  has  $M$  zeros and  $N$  poles. As can be seen from the expression for  $G(z)$ , the z-transform of a finite-length bounded sequence converges everywhere in the z-plane except possibly at  $z = 0$  and/or at  $z = \infty$ .

#### Example 38: Right-sided sequence z-transform

A right-sided sequence with nonzero sample values for  $n \geq 0$  is sometimes called a causal sequence. So, consider a causal sequence  $u_1[n]$ . Its z-transform is given by:

$$U_1(z) = \sum_{n=0}^{\infty} u_1[n]z^{-n} \quad (5.22)$$

It can be showed that  $U_1(z)$  converges exterior to a circle with  $|z| = R_1$ , including the point  $z = \infty$ .

On the other hand, a right-sided sequence  $u_2[n]$  with nonzero sample values only for  $n \geq -M$  with  $M$  non-negative has a z-transform  $U_2(z)$  with  $M$  poles at  $z = \infty$ . The ROC of  $U_2(z)$  is exterior to a circle  $|z| = R_2$ , excluding the point  $z = \infty$ .

#### Example 39: Left-sided sequence z-transform

A left-sided sequence with nonzero sample values for  $n \leq 0$  is sometimes called anticausal sequence. So, consider an anticausal sequence  $v_1[n]$ . Its z-transform is given by:

$$V_1(z) = \sum_{n=-\infty}^0 v_1[n]z^{-n} \quad (5.23)$$

It can be showed that  $V_1(z)$  converges interior to a circle  $|z| = R_3$ , including the

point  $z = 0$ .

On the other hand, a left-sided sequence with nonzero sample values only for  $n \leq N$  with  $N$  non-negative has a z-transform  $V_2(z)$  with  $N$  poles at  $z = 0$ . The ROC of  $V_2(z)$  is interior to a circle  $|z| = R_4$ , excluding the point  $z = 0$ .

#### Example 40: Two-sided sequence z-transform

The z-transform of a two-sided sequence  $w[n]$  can be expressed as:

$$W(z) = \sum_{n=-\infty}^{\infty} w[n]z^{-n} = \sum_{n=0}^{\infty} w[n]z^{-n} + \sum_{n=-\infty}^{-1} w[n]z^{-n} \quad (5.24)$$

The first term on the RHS can be interpreted as the z-transform of a right-sided sequence and it thus converges exterior to the circle  $|z| = R_5$ . The second term of the RHS can be interpreted as the z-transform of a left-sided sequence and it thus converges interior to the circle  $|z| = R_6$ . If  $R_5 < R_6$ , there is an overlapping ROC given by  $R_5 < |z| < R_6$ . If  $R_5 > R_6$ , there is no overlap and the z-transform does not exist.

In particular, let us consider as example the two-sided sequence:

$$u[n] = \alpha^n \quad (5.25)$$

where  $\alpha$  can be either real or complex. Its z-transform is given by:

$$U(z) = \sum_{n=-\infty}^{\infty} \alpha^n z^{-n} = \sum_{n=0}^{\infty} \alpha^n z^{-n} + \sum_{n=-\infty}^{-1} \alpha^n z^{-n} \quad (5.26)$$

The first term on the RHS converges for  $|z| > |\alpha|$ , whereas the second term converges for  $|z| < |\alpha|$ . There is no overlap between these two regions, hence the z-transform of  $u[n] = \alpha^n$  does not exist.

The ROC of a rational z-transform cannot contain any pole (since it is infinite at a pole) and is bounded by the poles. To show that the z-transform is bounded by the poles, assume that the z-transform  $X(z)$  has simple poles at  $z = \alpha$  and  $z = \beta$ . Assume that the corresponding sequence  $x[n]$  is a right-sided sequence. Then,  $x[n]$  has the form:

$$x[n] = (r_1 \alpha^n + r_2 \beta^n) \mu[n - N_0] \quad |\alpha| < |\beta| \quad (5.27)$$

where  $N_0$  is a positive or negative integer. Now, the z-transform of the right-sided sequence  $\gamma^n \mu[n - N_0]$  exists if:

$$\sum_{n=N_0}^{\infty} |\gamma^n z^{-n}| < \infty \quad (5.28)$$

for some  $z$ . The condition in Eq. 5.28 holds for  $|z| > |\gamma|$ , but not for  $|z| \leq |\gamma|$ . Therefore, the z-transform of Eq. 5.27 has a ROC defined by  $|\beta| < |z| \leq \infty$ . Likewise, the z-transform of a left-sided sequence:

$$x[n] = (r_1 \alpha^n + r_2 \beta^n) \mu[-n - N_0] \quad |\alpha| < |\beta| \quad (5.29)$$

has a ROC define by  $0 \leq |z| < |\alpha|$ .

### 5.3 Inverse z-transform

Firstly, we recall that, for  $z = re^{j\omega}$ , the z-transform  $G(z)$  given by:

$$G(z) = \sum_{n=-\infty}^{\infty} g[n]z^{-n} = \sum_{n=-\infty}^{\infty} g[n]r^{-n}e^{-j\omega n} \quad (5.30)$$

is the DTFT of the modified sequence  $g[n]r^{-n}$ . Accordingly, the inverse DTFT is thus given by:

$$g[n]r^{-n} = \frac{1}{2\pi} \int_{-\pi}^{\pi} G(re^{j\omega})e^{j\omega n} d\omega \quad (5.31)$$

By making a change of variable  $z = re^{j\omega}$ , the previous equation can be converted into a contour integral given by:

$$g[n] = \frac{1}{2\pi j} \oint_{C'} G(z)z^{n-1} dz \quad (5.32)$$

where  $C'$  is a counterclockwise contour of integration defined by  $|z| = r$ . But the integral remains unchanged when is replaced with any contour  $C$  encircling the point  $z = 0$  in the ROC of  $G(z)$ . The contour integral can be evaluated using the Cauchy's residue theorem resulting in:

$$g[n] = \sum \text{Res}_C [G(z)z^{n-1}] \quad (5.33)$$

Eq. 5.33 needs to be evaluated at all values of  $n$  and is not pursued here.

A rational z-transform  $G(z)$  with a causal inverse transform  $g[n]$  has an ROC that is exterior to a circle. Here, it is more convenient to express  $G(z)$  in a partial-fraction expansion form and then determine  $g[n]$  by summing the inverse transform of the individual simpler terms in the expansion. A rational  $G(z)$  can be expressed as:

$$G(z) = \frac{P(z)}{D(z)} = \frac{\sum_{i=0}^M p_i z^{-i}}{\sum_{i=0}^N d_i z^{-i}} \quad (5.34)$$

If  $M \geq N$ , then  $G(z)$  can be re-expressed as:

$$G(z) = \sum_{\ell=0}^{M-N} \eta_\ell z^{-\ell} + \frac{P_1(z)}{D(z)} \quad (5.35)$$

where the degree of  $P_1(z)$  is less than  $N$ . The rational function  $\frac{P_1(z)}{D(z)}$  is called a proper fraction. To develop the proper fraction part  $\frac{P_1(z)}{D(z)}$  from  $G(z)$ , a long division of  $P(z)$  by  $D(z)$  should be carried out in a reverse order until the remainder polynomial  $P_1(z)$  is of lower degree than that of the denominator  $D(z)$ .

#### Example 41: Inverse transform by partial-fraction expansion

Consider:

$$G(z) = \frac{2 + 0.8z^{-1} + 0.5z^{-2} + 0.3z^{-3}}{1 + 0.8z^{-1} + 0.2z^{-2}} \quad (5.36)$$

By long division in reverse order we arrive at:

$$G(z) = -3.5 + 1.5z^{-1} + \underbrace{\frac{5.5 + 2.1z^{-1}}{1 + 0.8z^{-1} + 0.2z^{-2}}}_{\text{Proper fraction}} \quad (5.37)$$

In most practical cases, the rational z-transform of interest  $G(z)$  is a proper fraction with simple poles. Let the poles of  $G(z)$  be at  $z = \lambda_k$ , with  $1 \leq k \leq N$ . A partial-fraction expansion of  $G(z)$  is then of the form:

$$G(z) = \sum_{\ell=1}^N \left( \frac{\rho_\ell}{1 - \lambda_\ell z^{-1}} \right) \quad (5.38)$$

The constants  $\rho_\ell$  in the partial-fraction expansion are called the residues and are given by:

$$\rho_\ell = [(1 - \lambda_\ell z^{-1})G(z)]_{z=\lambda_\ell} \quad (5.39)$$

Each term of the sum in partial-fraction expansion has a ROC given by  $|z| > |\lambda_\ell|$  and thus has an inverse transform of the form  $\rho_\ell(\lambda_\ell)^n \mu[n]$ . Therefore, the inverse transform  $g[n]$  of  $G(z)$  is given by:

$$g[n] = \sum_{\ell=1}^N \rho_\ell (\lambda_\ell)^n \mu[n] \quad (5.40)$$

Note that the approach in Eq. 5.40 with a slight modification can also be used to determine the inverse of a rational z-transform of a noncausal sequence.

#### Example 42: Inverse transfrom of a causal sequence

Let the z-transform  $H(z)$  of a causal sequence  $h[n]$  be given by:

$$H(z) = \frac{z(z+2)}{(z-0.2)(z+0.6)} = \frac{1+2z^{-1}}{(1-0.2z^{-1})(1+0.6z^{-1})} \quad (5.41)$$

A partial-fraction expansion of  $H(z)$  is then of the form:

$$H(z) = \frac{\rho_1}{1-0.2z^{-1}} + \frac{\rho_2}{1+0.6z^{-1}} \quad (5.42)$$

Now:

$$\rho_1 = [(1-0.2z^{-1})H(z)]_{z=0.2} = \left[ \frac{1+2z^{-1}}{1+0.6z^{-1}} \right]_{z=0.2} = 2.75 \quad (5.43)$$

$$\rho_2 = [(1+0.6z^{-1})H(z)]_{z=-0.6} = \left[ \frac{1+2z^{-1}}{1-0.2z^{-1}} \right]_{z=-0.6} = -1.75 \quad (5.44)$$

Hence:

$$H(z) = \frac{2.75}{1-0.2z^{-1}} - \frac{1.75}{1+0.6z^{-1}} \quad (5.45)$$

The inverse transform of the above is therefore given by:

$$h[n] = 2.75(0.2)^n \mu[n] - 1.75(-0.6)^n \mu[n] \quad (5.46)$$

In case  $G(z)$  has multiple poles, the partial-fraction expansion is of slightly different form. Let the pole at  $z = v$  be of multiplicity  $L$  and the remaining  $N - L$  poles be simple and at  $z = \lambda_\ell$ , for  $1 \leq \ell \leq N - L$ . Then, the partial-fraction expansion of  $G(z)$  is of the form:

$$G(z) = \sum_{\ell=0}^{M-N} \eta_\ell z^{-\ell} + \sum_{\ell=1}^{N-L} \frac{\rho_\ell}{1 - \lambda_\ell z^{-1}} + \sum_{i=1}^L \frac{\gamma_i}{(1 - vz^{-1})^i} \quad (5.47)$$

where the constants  $\gamma_i$  are computed using:

$$\gamma_i = \frac{1}{(L-i)!(-v)^{L-i}} \frac{d^{L-i}}{dz^{L-i}} [(1-vz^{-1})G(z)]_{z=v} \quad 1 \leq i \leq L \quad (5.48)$$

The residues  $\rho_\ell$  are calculated as before.

## 5.4 Z-transform properties

A list of properties of the z-transform is showed in Figure 5.3.

| Property                                  | Sequence                   | $z$ -Transform  | ROC   |
|---|----------------------------|---|---|
|   | $g[n]$<br>$h[n]$           | $G(z)$<br>$H(z)$  | $\mathcal{R}_g$<br>$\mathcal{R}_h$                              |
| Conjugation                               | $g^*[n]$                   | $G^*(z^*)$  | $\mathcal{R}_g$   |
| Time-reversal                             | $g[-n]$                    | $G(1/z)$  | $1/\mathcal{R}_g$   |
| Linearity                                 | $\alpha g[n] + \beta h[n]$ | $\alpha G(z) + \beta H(z)$  | Includes $\mathcal{R}_g \cap \mathcal{R}_h$                     |
| Time-shifting                             | $g[n - n_o]$               | $z^{-n_o} G(z)$   | $\mathcal{R}_g$ , except possibly the point $z = 0$ or $\infty$ |
| Multiplication by an exponential sequence | $\alpha^n g[n]$            | $G(z/\alpha)$   | $ \alpha  \mathcal{R}_g$  |
| Differentiation of $G(z)$                 | $ng[n]$                    | $-z \frac{dG(z)}{dz}$   | $\mathcal{R}_g$ , except possibly the point $z = 0$ or $\infty$ |
| Convolution                               | $g[n] \otimes h[n]$        | $G(z)H(z)$  | Includes $\mathcal{R}_g \cap \mathcal{R}_h$                     |
| Modulation                                | $g[n]h[n]$                 | $\frac{1}{2\pi j} \oint_C G(v)H(z/v)v^{-1} dv$  | Includes $\mathcal{R}_g \mathcal{R}_h$                          |
| Parseval's relation                       |                            | $\sum_{n=-\infty}^{\infty} g[n]h^*[n] = \frac{1}{2\pi j} \oint_C G(v)H^*(1/v^*)v^{-1} dv$ |   |

Note: If  $\mathcal{R}_g$  denotes the region  $R_{g-} < |z| < R_{g+}$  and  $\mathcal{R}_h$  denotes the region  $R_{h-} < |z| < R_{h+}$ , then  $1/\mathcal{R}_g$  denotes the region  $1/R_{g+} < |z| < 1/R_{g-}$  and  $\mathcal{R}_g \mathcal{R}_h$  denotes the region  $R_{g-} R_{h-} < |z| < R_{g+} R_{h+}$ .

Figure 5.3: Properties of the z-transform.

### Example 43: Z-transform properties

Consider the two-sided sequence:

$$v[n] = \alpha^n \mu[n] - \beta^n \mu[-n-1] \quad (5.49)$$

Let  $x[n] = \alpha^n \mu[n]$  and  $y = -\beta^n \mu[-n-1]$  with  $X(z)$  and  $Y(z)$  denoting, respectively, their z-transforms. Now:

$$X(z) = \frac{1}{1 - \alpha z^{-1}} \quad |z| > |\alpha| \quad (5.50)$$

$$Y(z) = \frac{1}{1 - \beta z^{-1}} \quad |z| < |\beta| \quad (5.51)$$

Using the linearity property we arrive at:

$$V(z) = X(z) + Y(z) = \frac{1}{1 - \alpha z^{-1}} + \frac{1}{1 - \beta z^{-1}} \quad (5.52)$$

The ROC of  $V(z)$  is given by the overlap regions of  $|z| > |\alpha|$  and  $|z| < |\beta|$ . We have that:

- if  $|\alpha| < |\beta|$ , then there is an overlap and the ROC is an annular region  $|\alpha| < |z| < |\beta|$ ;
- if  $|\alpha| > |\beta|$ , then there is no overlap and  $V(z)$  does not exist.

#### Example 44: Z-transform properties

We determine the z-transform and its ROC of the causal sequence:

$$x[n] = r^n (\cos(\omega_0 n)) \mu[n] \quad (5.53)$$

We can express  $x[n] = v[n] + v^*[n]$ , where:

$$v[n] = \frac{1}{2} r^n e^{j\omega_0 n} \mu[n] = \frac{1}{2} \alpha^n \mu[n] \quad (5.54)$$

The z-transform of  $v[n]$  is given by:

$$V(z) = \frac{1}{2} \frac{1}{1 - \alpha z^{-1}} = \frac{1}{2} \frac{1}{1 - re^{j\omega_0 z^{-1}}} \quad |z| > |\alpha| = r \quad (5.55)$$

Using the conjugation property, we obtain the z-transform of  $v^*[n]$  as:

$$V^*(z^*) = \frac{1}{2} \frac{1}{1 - \alpha^* z^{-1}} = \frac{1}{2} \frac{1}{1 - re^{-j\omega_0 z^{-1}}} \quad |z| > |\alpha| \quad (5.56)$$

Finally, using the linearity property we get:

$$X(z) = V(z) + V^*(z^*) = \frac{1}{2} \left( \frac{1}{1 - re^{j\omega_0 z^{-1}}} + \frac{1}{1 - re^{-j\omega_0 z^{-1}}} \right) \quad (5.57)$$

or:

$$X(z) = \frac{1 - (r \cos \omega_0) z^{-1}}{1 - (2r \cos \omega_0) z^{-1} + r^2 z^{-2}} \quad |z| > r \quad (5.58)$$

#### Example 45: Z-transform properties

We determine the z-transform  $Y(z)$  and the ROC of the sequence:

$$y[n] = (n + 1) \alpha^n \mu[n] \quad (5.59)$$

We can write  $y[n] = nx[n] + x[n]$  where:

$$x[n] = \alpha^n \mu[n] \quad (5.60)$$

Now, the z-transform  $X(z)$  of  $x[n] = \alpha^n \mu[n]$  is given by:

$$X(z) = \frac{1}{1 - \alpha z^{-1}} \quad |z| > |\alpha| \quad (5.61)$$

Using the differentiation property, we arrive at the z-transform of  $nx[n]$  as:

$$-z \frac{dX(z)}{dz} = \frac{\alpha z^{-1}}{1 - \alpha z^{-1}} \quad |z| > |\alpha| \quad (5.62)$$

Using the linearity property we finally obtain:

$$Y(z) = \frac{1}{1 - \alpha z^{-1}} + \frac{\alpha z^{-1}}{(1 - \alpha z^{-1})^2} = \frac{1}{(1 - \alpha z^{-1})^2} \quad |z| > |\alpha| \quad (5.63)$$

**Lecture 17.**  
Tuesday 24<sup>th</sup>  
November, 2020.

## 5.5 Stability condition

A causal LTI digital filter is BIBO stable if and only if its impulse response  $h[n]$  is absolutely summable, i.e.:

$$S = \sum_{n=-\infty}^{\infty} |h[n]| < \infty \quad (5.64)$$

We now develop a stability condition in terms of the pole locations of the transfer function  $H(z)$ .

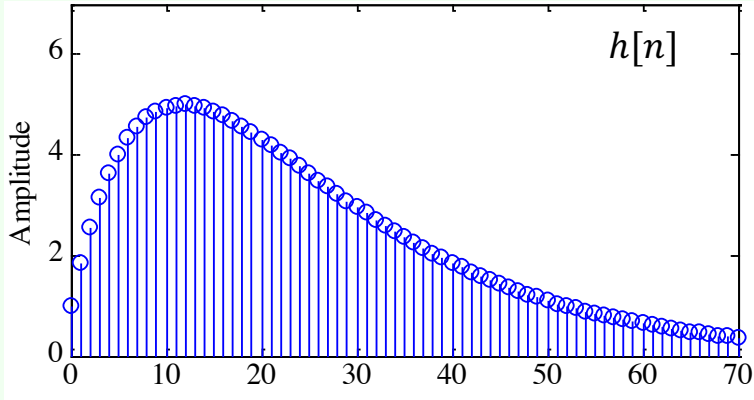
The ROC of the z-transform  $H(z)$  of the impulse response sequence  $h[n]$  is defined by values of  $|z| = r$  for which  $h[n]r^{-n}$  is absolutely summable. Thus, if the ROC includes the unit circle  $|z| = 1$ , then the digital filter is stable, and viceversa. In addition, for a stable and causal digital filter for which  $h[n]$  is a right-sided sequence, the ROC will include the unit circle and entire z-plane including the point  $z = \infty$ . Note that a FIR digital filter with bounded impulse response is always stable. On the other hand, a IIR filter may be unstable if not designed properly. In addition, an originally stable IIR filter characterized by infinite precision coefficients may become unstable when coefficients get quantized due to implementation.

### Example 46: Stability condition

Consider the causal IIR transfer function:

$$H(z) = \frac{1}{1 - 1.845z^{-1} + 0.850586z^{-2}} \quad (5.65)$$

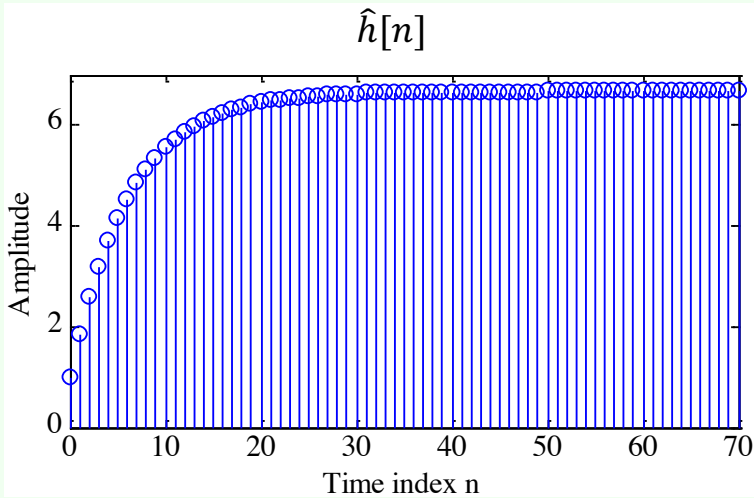
The plot of the impulse response coefficients is showed below. As can be seen from the plot, the impulse response coefficient  $h[n]$  decays rapidly to zero value as  $n$  increases.



The absolute summability condition of  $h[n]$  is satisfied. Hence,  $H(z)$  is a stable transfer function. Now, consider the case when the transfer function coefficients are rounded to values with 2 digits after the decimal point:

$$\hat{H}(z) = \frac{1}{1 - 1.85z^{-1} + 0.85z^{-2}} \quad (5.66)$$

A plot of the impulse response of  $\hat{h}[n]$  is showed below.



In this case, the impulse coefficient  $\hat{h}[n]$  increases rapidly to a constant value as  $n$  increases. Hence, the absolute summability condition of  $\hat{h}[n]$  is violated. Thus,  $\hat{H}[z]$  is an unstable transfer function.

The stability testing of a IIR transfer function is therefore an important problem. In most cases it is difficult to compute the infinite sum in Eq. 5.64. For a causal IIR transfer function, the sum  $S$  can be computed approximately as:

$$S_k = \sum_{n=0}^{k-1} |h[n]| \quad (5.67)$$

The partial sum is computed for increasing values of  $k$  until the difference between a series of consecutive values of  $S_k$  is smaller than some arbitrarily chosen small number, which is typically  $10^{-6}$ . For a transfer function of very high order this approach may not be satisfactory. An alternate, easy-to-test, stability condition is developed next. Let us consider the causal IIR digital filter with a rational transfer function  $H(z)$

given by:

$$H(z) = \frac{\sum_{k=0}^M p_k z^{-k}}{\sum_{k=0}^N d_k z^{-k}} \quad (5.68)$$

Its impulse response  $\{h[n]\}$  is a right-sided sequence. The ROC of  $H(z)$  is exterior to a circle going through the pole furthest from  $z = 0$ . But stability requires that  $\{h[n]\}$  is absolutely summable. This in turn implies that the DTFT  $H(e^{j\omega})$  of  $\{h[n]\}$  exists. Now, if the ROC of the x-transform  $H(z)$  includes the unit circle, then:

$$H(e^{j\omega}) = [H(z)]_{z=e^{j\omega}} \quad (5.69)$$

In conclusion, all the poles of a causal stable transfer function  $H(z)$  must be strictly inside the unit circle, as showed in Figure 5.4.

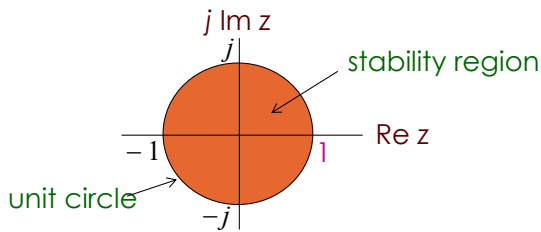


**Figure 5.4:** Stability condition (shaded area).

#### Example 47: Stability condition

The factored form of the previous example transfer function is:

$$H(z) = \frac{1}{1 - 1.845z^{-1} + 0.850586z^{-2}} = \frac{1}{(1 - 0.902z^{-1})(1 - 0.943z^{-1})} \quad (5.70)$$

which has a real pole at  $z = 0.902$  and a real pole at  $z = 0.943$ . Since both poles are inside the unit circle,  $H(z)$  is BIBO stable.

On the other hand, the factored form of  $\hat{H}(z)$  is:

$$\hat{H}(z) = \frac{1}{1 - 1.85z^{-1} + 0.85z^{-2}} = \frac{1}{(1 - z^{-1})(1 - 0.85z^{-1})} \quad (5.71)$$

which has a real pole on the unit circle at  $z = 1$  and the other pole inside the unit circle. Since not both the poles are inside the unit circle,  $\hat{H}(z)$  is unstable.



# Chapter 6

## Filter design

Before starting with the discussion of filter design, we have to go some steps backward and introduce some concepts

### 6.1 Phase and group delay

#### 6.1.1 Phase delay

If the input  $x[n]$  to an LTI system  $H(e^{j\omega})$  is a sinusoidal signal of frequency  $\omega_0$ , i.e.:

$$x[n] = A \cos(\omega_0 n + \varphi), \quad -\infty < n < \infty \quad (6.1)$$

then the output  $y[n]$  is also a sinusoidal signal of the same frequency  $\omega_0$ , but lagging in phase by  $\theta(\omega_0)$  radians:

$$y[n] = A |H(e^{j\omega_0})| \cos(\omega_0 n + \theta(\omega_0) + \varphi), \quad -\infty < n < \infty \quad (6.2)$$

We can rewrite the output expression as:

$$y[n] = A |H(e^{j\omega_0})| \cos(\omega_0(n - \tau_p(\omega_0) + \varphi)) \quad (6.3)$$

where:

$$\tau_p(\omega_0) = -\frac{\theta(\omega_0)}{\omega_0} \quad (6.4)$$

is called the phase delay. The minus sign in front indicates phase lag. Thus, the output  $y[n]$  is a time-delayed version of the input  $x[n]$ . In general,  $y[n]$  will not be a delayed replica of  $x[n]$  unless the phase delay  $\tau_p(\omega_0)$  is an integer.

#### 6.1.2 Group delay

When the input is composed of many sinusoidal components with different frequencies that are not harmonically related, each component will go through different phase delays. In this case, the signal delay is determined using the group delay defined by:

$$\tau_g(\omega) = -\frac{d\theta(\omega)}{d\omega} \quad (6.5)$$

In defining the group delay, it is assumed that the phase function is unwrapped so that its derivatives exist.

**Example 48: Phase and group delay**

The phase function of the FIR filter:

$$y[n] = \alpha x[n] + \beta x[n - 1] + \gamma x[n - 2] \quad (6.6)$$

is:

$$\theta(\omega) = -\omega \quad (6.7)$$

Hence, its group delay is given by  $\tau_g(\omega) = 1$ .

## 6.2 Type of transfer functions

The time-domain classification of an LTI digital transfer function sequence is based on the length of its impulse response. We can have:

- Finite Impulse Response (FIR) transfer function;
- Infinite Impulse Response (IIR) transfer function.

In the case of digital transfer functions with frequency-selective frequency responses, there are two types of classifications:

- a classification based on the shape of the magnitude function  $|H(e^{j\omega})|$ ;
- a classification based on the form of the phase function  $\theta(\omega)$ .

One common classification is based on an ideal magnitude response. A digital filter designed to pass signal components of certain frequencies without distortion should have a frequency response equal to one at these frequencies, and should have a frequency response equal to zero at all other frequencies.

### 6.2.1 Ideal filters

The range of frequencies where the frequency response takes the value of one is called the passband. The range of frequencies where the frequency response takes the value of zero is called the stopband.

Frequency responses of the four popular types of ideal digital filters with real impulse response coefficients are showed in Figure 6.1.

In particular, the passband and stopband of those filters are listed in Table 6.1. The frequencies  $\omega_c$ ,  $\omega_{c_1}$  and  $\omega_{c_2}$  are called the cutoff frequencies. An ideal filter has a magnitude response equal to one in the passband and zero in the stopband, and has a zero phase everywhere.

| Type     | Passband  | Stopband  |
|----------|---|---|
| Lowpass  | $0 \leq \omega \leq \omega_c$   | $\omega_c < \omega \leq \pi$  |
| Highpass | $\omega_c \leq \omega \leq \pi$   | $0 \leq \omega < \omega_c$  |
| Bandpass | $\omega_{c_1} \leq \omega \leq \omega_{c_2}$                              | $0 \leq \omega < \omega_{c_1}$ and $\omega_{c_2} < \omega \leq \pi$ |
| Stopband | $0 \leq \omega \leq \omega_{c_1}$ and $\omega_{c_2} \leq \omega \leq \pi$ | $\omega_{c_1} < \omega < \omega_{c_2}$                              |

**Table 6.1:** Passband and stopband of the four popular types of ideal digital filters

Earlier in the course we derived the inverse DTFT of the frequency response  $H_{LP}(e^{j\omega})$  of the ideal lowpass filter:

$$h_{LP}[n] = \frac{\sin(\omega_c n)}{\pi n}, \quad -\infty < n < \infty \quad (6.8)$$

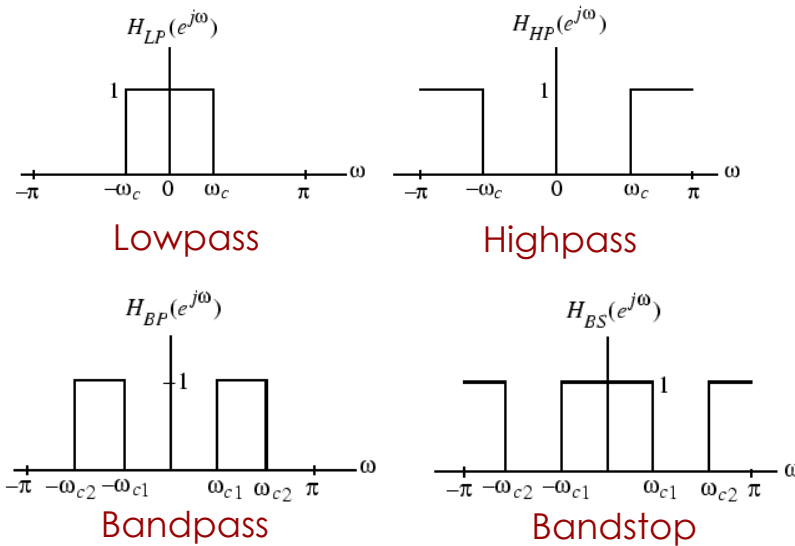


**Figure 6.1:** Frequency responses of the four popular types of ideal digital filters with real impulse response coefficients.

We have also shown that the above impulse response is not absolutely summable, and hence, the corresponding transfer function is not BIBO stable. Also,  $h_{LP}[n]$  is not causal and is of doubly infinite length. The remaining three ideal filters are also characterized by doubly infinite, noncausal impulse responses and are not absolutely summable. Thus, the ideal filters with the ideal “brick wall” frequency responses cannot be realized with finite dimensional LTI filter.

To develop stable and realizable transfer functions, the ideal frequency response specifications are relaxed by including a transition band between the passband and the stopband. This permits the magnitude response to decay slowly from its maximum value in the passband to the zero value in the stopband. Moreover, the magnitude response is allowed to vary by a small amount both in the passband and the stopband. Typical magnitude response specifications of a lowpass filter are showed in Figure 6.2.

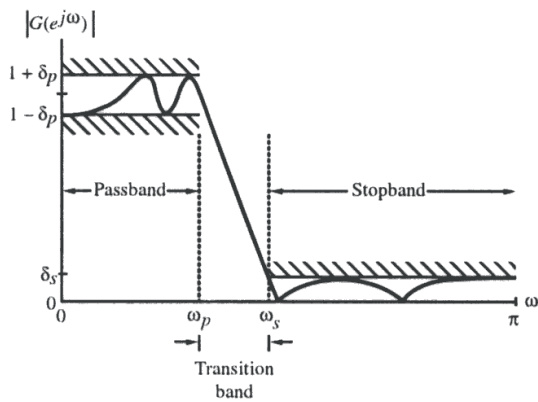


**Figure 6.2:** Typical magnitude response specifications of a lowpass filter.

### 6.2.2 Bounded Real transfer functions

A causal stable real-coefficient transfer function  $H(z)$  is defined as a bounded real (BR) transfer function if:

$$|H(e^{j\omega})| \leq 1 \quad \forall \omega \quad (6.9)$$

Let  $x[n]$  and  $y[n]$  denote, respectively, the input and output of a digital filter characterized by a BR transfer function  $H(z)$  with  $X(e^{j\omega})$  and  $Y(e^{j\omega})$  denoting their DTFTs. Then, the condition in Eq. 6.9 implies that:

$$|Y(e^{j\omega})|^2 \leq |X(e^{k\omega})|^2 \quad (6.10)$$

Integrating Eq. 6.10 from  $-\pi$  to  $\pi$  and applying Parseval's relation, we get:

$$\sum_{n=-\infty}^{\infty} y[n]^2 \leq \sum_{n=-\infty}^{\infty} x[n]^2 \quad (6.11)$$

Thus, for all finite-energy inputs, the output energy is less than or equal to the input energy implying that a digital filter characterized by a BR transfer function can be viewed as a passive structure. If  $|H(e^{j\omega})| = 1$ , then the output energy is equal to the input energy, and such a digital filter is therefore a lossless system.

A causal stable real-coefficient transfer function  $H(z)$  with  $|H(e^{j\omega})| = 1$  is thus called a lossless bounded real (LBR) transfer function. The BR and LBR transfer functions are the keys to the realization of digital filters with low coefficient sensitivity.

#### Example 49: Bounded Real transfer functions

Consider the causal stable IIR transfer function:

$$H(z) = \frac{k}{1 - \alpha z^{-1}}, \quad 0 < |\alpha| < 1 \quad (6.12)$$

where  $k$  is a real constant. Its square-magnitude function is given by:

$$|H(e^{j\omega})|^2 = [H(z)H(z^{-1})]_{z=e^{j\omega}} = \frac{k^2}{(1 + \alpha^2) - 2\alpha \cos \omega} \quad (6.13)$$

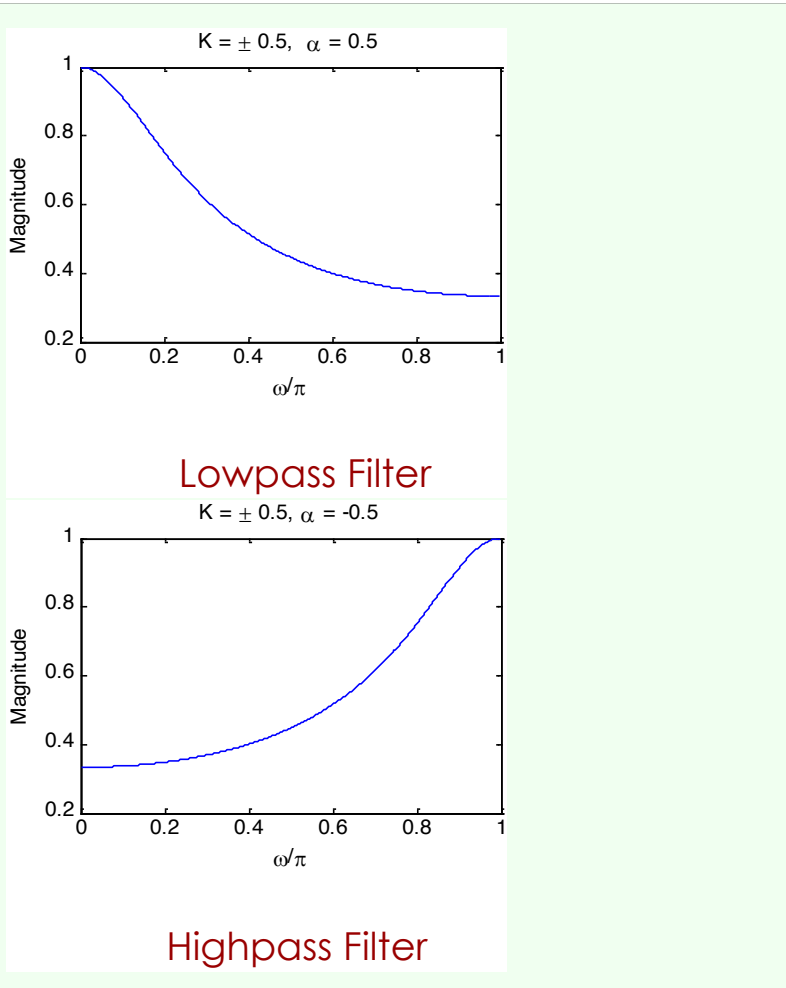
The maximum value of  $|H(e^{j\omega})|^2$  is obtained when  $2\alpha \cos \omega$  in the denominator is a maximum and the minimum value is obtained when  $2\alpha \cos \omega$  is a minimum. For  $\alpha > 0$ , the maximum value of  $2\alpha \cos \omega$  is equal to  $2\alpha$  at  $\omega = 0$ , and the minimum value is  $-2\alpha$  at  $\omega = \pi$ .

Thus, for  $\alpha > 0$ , the maximum value of  $|H(e^{j\omega})|^2$  is equal to  $\frac{k^2}{(1-\alpha)^2}$  at  $\omega = 0$  and the minimum value is equal to  $\frac{k^2}{(1+\alpha)^2}$  at  $\omega = \pi$ .

On the other hand, for  $\alpha < 0$ , the maximum value of  $2\alpha \cos \omega$  is equal to  $-2\alpha$  at  $\omega = \pi$  and the minimum value is equal to  $2\alpha$  at  $\omega = 0$ . Here, the maximum value of  $|H(e^{j\omega})|^2$  is equal to  $\frac{k^2}{(1-\alpha)^2}$  at  $\omega = \pi$ , and the minimum value is equal to  $\frac{k^2}{(1+\alpha)^2}$  at  $\omega = 0$ . Hence, the maximum value can be made equal to 1 by choosing  $k = \pm(1 - \alpha)$ , in which case the minimum value becomes  $\frac{(1-\alpha)^2}{(1+\alpha)^2}$ . Hence:

$$H(z) = \frac{k}{1 - \alpha z^{-1}}, \quad 0 < |\alpha| < 1 \quad (6.14)$$

is a BR function for  $k = \pm(1 - \alpha)$ . Plots of the magnitude function for  $\alpha = \pm 0.5$  with values of  $k$  chosen to make  $H(z)$  a BR function are showed below.



### 6.2.3 Allpass transfer function

**Definition 12: Allpass transfer function**

An IIR transfer function  $A(z)$  with unity magnitude response for all frequencies, i.e.:

$$|A(e^{j\omega})|^2 = 1 \quad \forall \omega \quad (6.15)$$

is called an allpass transfer function.

An  $M^{\text{th}}$  order causal real-coefficient allpass transfer function is of the form:

$$A_M(z) = \pm \frac{d_M + d_{M-1}z^{-1} + \dots + d_1z^{-M+1} + z^{-M}}{1 + d_1z^{-1} + \dots + d_{M-1}z^{-M+1} + d_Mz^{-M}} \quad (6.16)$$

If we denote the denominator polynomials of  $A_M(z)$  as  $D_M(z)$ :

$$D_M(z) = 1 + d_1z^{-1} + \dots + d_{M-1}z^{-M+1} + d_Mz^{-M} \quad (6.17)$$

then it follows that  $A_M(z)$  can be written as:

$$A_M(z) = \pm \frac{z^{-M} D_M(z^{-1})}{D_M(z)} \quad (6.18)$$

Note that if  $z = re^{j\omega}$  is a pole of a real coefficient allpass transfer function, then it has a zero at  $z = \frac{1}{r}e^{-j\varphi}$ .

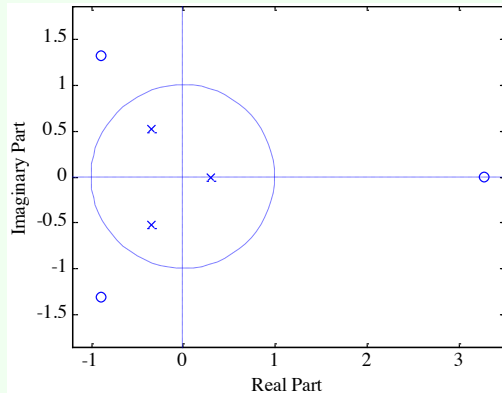
The numerator of a real-coefficient allpass transfer function is said to be the mirror-image polynomial of the denominator, and vice versa. We shall use the notation  $\tilde{D}_M(z)$  to denote the mirror-image polynomial of a degree- $M$  polynomial  $D_M(z)$ , i.e.:

$$\tilde{D}_M(z) = z^{-M} D_M(z^{-1}) \quad (6.19)$$

The expression in Eq. 6.18 implies that the poles and zeros of a real-coefficient allpass function exhibit mirror-image symmetry in the  $z$ -plane.

#### Example 50: Allpass transfer function

$$A_3(z) \frac{-0.2 + 0.81z^{-1} + 0.4z^{-2} + z^{-3}}{1 + 0.4z^{-1} + 0.18z^{-2} - 0.2z^{-3}} \quad (6.20)$$



To show that  $|A_M(e^{j\omega})|^2 = 1$ , we observe that:

$$A_M(z^{-1}) = \pm \frac{z^M D_M(z)}{D_M(z^{-1})} \quad (6.21)$$

Therefore:

$$A_M(z) A_M(z^{-1}) = \frac{z^{-M} D_M(z^{-1})}{D_M(z)} \frac{z^M D_M(z)}{D_M(z^{-1})} \quad (6.22)$$

Hence:

$$|A_M(e^{j\omega})|^2 = [A_M(z) A_M(z^{-1})]_{z=e^{j\omega}} = 1 \quad (6.23)$$

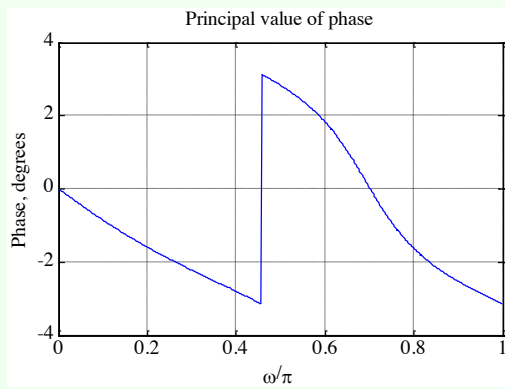
Now, the poles of a causal stable transfer function must lie inside the unit circle in the  $z$ -plane. Hence, all zeros of a causal stable allpass transfer function must lie outside the unit circle in a mirror-image symmetry with its poles situated inside the unit circle.

#### Example 51: Allpass transfer function

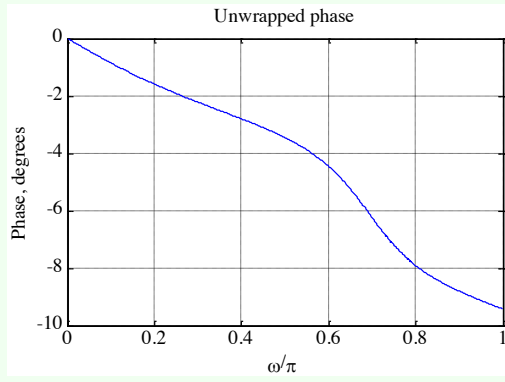
Consider the 3<sup>rd</sup> order allpass function:

$$A_3(z) = \frac{-0.2 + 0.18z^{-1} + 0.4z^{-2} + z^{-3}}{1 + 0.4z^{-1} + 0.18z^{-2} - 0.2z^{-3}} \quad (6.24)$$

The principal value of phase is showed in the plot below. Note the discontinuity by the amount of  $2\pi$  in the phase  $\theta(\omega)$ .



If we unwrap the phase by removing the discontinuity, we arrive at the unwrapped phase function  $\theta_c(\omega)$  indicated in the plot below. Note that the unwrapped phase function is a continuous function of  $\omega$ .



We list now the properties of allpass transfer function:

- a causal stable real-coefficient allpass transfer function is a lossless bounded real (LBR) function or, equivalently, a causal stable allpass filter is a lossless structure;
- the magnitude function of a stable allpass function  $A(z)$  satisfies:

$$|A(z)| \begin{cases} < 1 & |z| > 1 \\ = 1 & |z| = 1 \\ > 1 & |z| < 1 \end{cases} \quad (6.25)$$

- let  $\tau(\omega)$  denote the group delay function of an allpass filter  $A(z)$ :

$$\tau(\omega) = -\frac{d}{d\omega}[\theta_c(\omega)] \quad (6.26)$$

The unwrapped phase function  $\theta_c(\omega)$  of a stable allpass function is a monotonically decreasing function of  $\omega$  so that  $\tau(\omega)$  is everywhere positive in the range  $0 < \omega < \pi$ . The group delay of an  $M^{\text{th}}$  order stable real-coefficient allpass transfer function satisfies:

$$\int_0^\pi \tau(\omega) d\omega = M\pi \quad (6.27)$$

A simple but often used application of an allpass filter is as a delay equalizer. Let  $G(z)$  be the transfer function of a digital filter designed to meet a prescribed magnitude

response. The non-linear phase response of  $G(z)$  can be corrected by cascading it with an allpass filter  $A(z)$  so that the overall cascade has a constant group delay in the band of interest. Since  $|A_M(e^{j\omega})| = 1$ , we have:

$$|G(e^{j\omega})A(e^{j\omega})| = |G(e^{j\omega})| \quad (6.28)$$

The overall group delay is given by the sum of the group delays of  $G(z)$  and  $A(z)$ .

### 6.2.4 Phase characteristics

A second classification of a transfer function is with respect to its phase characteristics. In many applications, it is necessary that the digital filter designed does not distort the phase of the input signal components for frequencies in the passband. One way to avoid any phase distortion is to make the frequency response of the filter real and nonnegative, i.e., to design the filter with a zero-phase characteristic. However, it is not possible to design a causal digital filter with a zero phase.

For non-real-time processing of real-valued input signals of finite length, zero-phase filtering can be very simply implemented by relaxing the causality requirement. One zero-phase filtering scheme is sketched in Figure 6.3. It is easy to verify the ladder in the frequency domain.

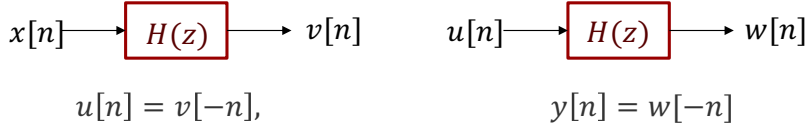


**Figure 6.3:** A possible zero-phase filtering scheme.

Let  $X(e^{j\omega})$ ,  $V(e^{j\omega})$ ,  $U(e^{j\omega})$ ,  $W(e^{j\omega})$  and  $Y(e^{j\omega})$  denote the DTFTs of  $x[n]$ ,  $v[n]$ ,  $u[n]$ ,  $w[n]$  and  $y[n]$ , respectively. Making use of the symmetry relations, we arrive at the relations between various DTFTs:

$$V(e^{j\omega}) = H(e^{j\omega})X(e^{j\omega}) \quad (6.29)$$

$$W(e^{j\omega}) = H(e^{j\omega})U(e^{j\omega}) \quad (6.30)$$

$$U(e^{j\omega}) = V^*(e^{j\omega}) \quad (6.31)$$

$$Y(e^{j\omega}) = W^*(e^{j\omega}) \quad (6.32)$$

Combining the above equations we get:

$$\begin{aligned} Y(e^{j\omega}) &= W^*(e^{j\omega}) \\ &= H^*(e^{j\omega})U^*(e^{j\omega}) \\ &= H^*(e^{j\omega})V(e^{j\omega}) \\ &= H^*(e^{j\omega})H(e^{j\omega})X(e^{j\omega}) \\ &= |H(e^{j\omega})|^2 X(e^{j\omega}) \end{aligned} \quad (6.33)$$

The most general type of a filter with a linear phase has a frequency response given by:

$$H(e^{j\omega}) = e^{-j\omega D} \quad (6.34)$$

which has a linear phase from  $\omega = 0$  to  $\omega = 2\pi$ . Note also that:

$$|H(e^{j\omega})| = 1 \quad (6.35)$$

and:

$$\tau(\omega) = -\frac{d}{d\omega}[\theta_c(\omega)] = D \quad (6.36)$$

The output  $y[n]$  of this filter to an input  $x[n] = Ae^{j\omega n}$  is then given by:

$$y[n] = Ae^{-j\omega D}e^{j\omega n} = Ae^{j\omega(n-D)} \quad (6.37)$$

If  $x_a(t)$  and  $y_a(t)$  represent the continuous-time signals whose sampled versions, sampled at  $t = nT$ , are  $x[n]$  and  $y[n]$  given above, then the delay between  $x_a(t)$  and  $y_a(t)$  is precisely the group delay of amount  $D$ . If  $D$  is an integer, then  $y[n]$  is identical to  $x[n]$ , but delayed by  $D$  samples. If  $D$  is not an integer,  $y[n]$ , being delayed by a fractional part, is not identical to  $x[n]$ . In the latter case, the waveform of the underlying continuous-time output is identical to the waveform of the underlying continuous-time input and delayed  $D$  units of time.

If it is desired to pass input signal components in a certain frequency range undistorted in both magnitude and phase, then the transfer function should exhibit a unity magnitude response and a linear-phase response in the band of interest. In Figure 6.4 the frequency response of a lowpass filter with a linear-phase characteristic in the passband is showed. Since the signal components in the stopband are blocked, the phase response in the stopband can be of any shape.

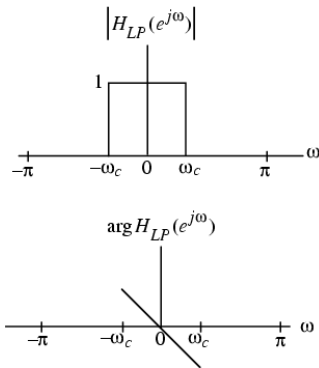


**Figure 6.4:** Frequency response of a lowpass filter with a linear-phase characteristic in the passband.

### Example 52: Linear-phase transfer function

We determine now the impulse response of an ideal lowpass filter with a linear phase response:

$$H_{LP}(e^{j\omega}) = \begin{cases} e^{-j\omega n_0} & 0 < |\omega| < \omega_c \\ 0 & \omega_c \leq |\omega| \leq \pi \end{cases} \quad (6.38)$$

Applying the frequency-shifting property of the DTFT to the impulse response of an ideal zero-phase lowpass filter we arrive at:

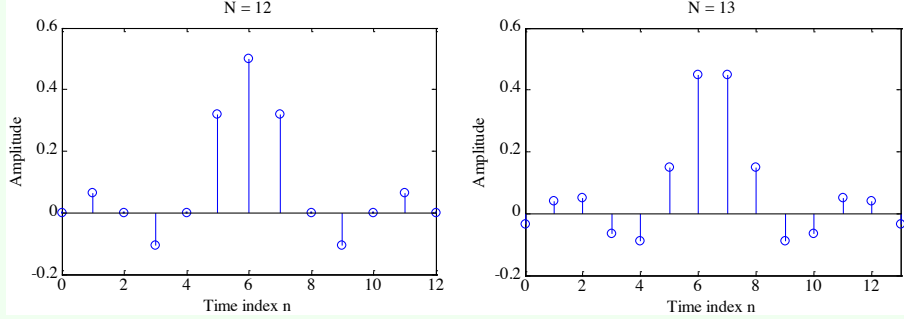
$$h_{LP}[n] = \frac{\sin(\omega(n - n_0))}{\pi(n - n_0)} \quad -\infty < n < \infty \quad (6.39)$$

As before, the above filter is noncausal and of doubly infinite length, and hence, unrealizable. By truncating the impulse response to a finite number of terms, a realizable FIR approximation to the ideal lowpass filter can be developed. The truncated approximation may or may not exhibit linear phase, depending on the value of  $n_0$  chosen.

If we choose  $n_0 = \frac{N}{2}$  with  $N$  a positive integer, the truncated and shifted approximation:

$$\hat{h}_{LP}[n] = \frac{\sin\left(\omega_c\left(n - \frac{N}{2}\right)\right)}{\pi\left(n - \frac{N}{2}\right)} \quad 0 \leq n \leq N \quad (6.40)$$

will be a length  $N + 1$  causal linear-phase FIR filter. In the plot below the filter coefficients are showed. They are obtained using the function sinc for two different values of  $N$ .



Because of the symmetry of the impulse response coefficients as indicated in the two plots, the frequency response of the truncated approximation can be expressed as:

$$\hat{H}_{LP}(e^{j\omega}) = \sum_{n=0}^N \hat{h}_{LP}[n] e^{-j\omega n} = e^{-j\omega \frac{N}{2}} \tilde{H}_{LP}(\omega) \quad (6.41)$$

where  $\tilde{H}_{LP}(\omega)$ , called the zero-phase response or amplitude response, is a real function of  $\omega$ .

**Lecture 19.**  
Thursday 3<sup>rd</sup>  
December, 2020.

### 6.2.5 Frequency response from transfer function

If the ROC of the transfer function  $H(z)$  includes the unit circle, then the frequency response  $H(e^{j\omega})$  of the LTI digital filter can be obtained simply as follows:

$$H(e^{j\omega}) = [H(z)]_{z=e^{j\omega}} \quad (6.42)$$

For a real coefficient transfer function  $H(z)$  it can be showed that:

$$|H(e^{j\omega})|^2 = H(e^{j\omega})H^*(e^{j\omega}) = H(e^{j\omega})H(e^{-j\omega}) = [H(z)H(z^{-1})]_{z=e^{j\omega}} \quad (6.43)$$

For a stable rational transfer function in the form:

$$H(z) = \frac{p_0}{d_0} z^{(N-M)} \frac{\prod_{k=1}^M (z - \xi_k)}{\prod_{k=1}^N (z - \lambda_k)} \quad (6.44)$$

the factored form of the frequency response is given by:

$$H(e^{j\omega}) = \frac{p_0}{d_0} e^{j\omega(N-M)} \frac{\prod_{k=1}^M (e^{j\omega} - \xi_k)}{\prod_{k=1}^N (e^{j\omega} - \lambda_k)} \quad (6.45)$$

It is convenient to visualize the contributions of the zero ( $z - \xi_k$ ) and the pole factor ( $z - \lambda_k$ ) from the factored form of the frequency response. The magnitude function is given by:

$$|H(e^{j\omega})| = \left| \frac{p_0}{d_0} \right| \frac{\prod_{k=1}^M |e^{j\omega} - \xi_k|}{\prod_{k=1}^N |e^{j\omega} - \lambda_k|} \quad (6.46)$$

The phase response for a rational transfer function is of the form:

$$\arg H(e^{j\omega}) = \arg \left( \frac{p_0}{d_0} \right) + \omega(N-M) + \sum_{k=1}^M \arg(e^{j\omega} - \xi_k) - \sum_{k=1}^N \arg(e^{j\omega} - \lambda_k) \quad (6.47)$$

The magnitude-squared function of a real-coefficient transfer function can be computed using:

$$|H(e^{j\omega})|^2 = \left| \frac{p_0}{d_0} \right|^2 \frac{\prod_{k=1}^M (e^{j\omega} - \xi_k)(e^{j\omega} - \xi_k^*)}{\prod_{k=1}^N (e^{j\omega} - \lambda_k)(e^{j\omega} - \lambda_k^*)} \quad (6.48)$$

### 6.2.6 Geometric interpretation of frequency response

The factored form of the frequency response in Eq. 6.45 is convenient to develop a geometric interpretation of the frequency response computation from the pole-zero plot as  $\omega$  varies from 0 to  $2\pi$  on the unit circle. The geometric interpretation can be used to obtain a sketch of the response as a function of the frequency. A typical factor in the factored form of the frequency response is given by  $(e^{j\omega} - \rho e^{j\varphi})$ , where  $\rho e^{j\varphi}$  is a zero if it is zero factor or is a pole if it is a pole factor. As showed in Figure 6.5, in the z-plane the factor  $(e^{j\omega} - \rho e^{j\varphi})$  represents a vector starting at the point  $z = \rho e^{j\varphi}$  and ending on the unit circle at  $z = e^{j\omega}$ .

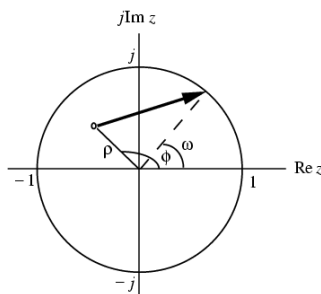


**Figure 6.5:** Factor  $(e^{j\omega} - \rho e^{j\varphi})$  in the z-plane.

As  $\omega$  is varied from 0 to  $2\pi$ , the tip of the vector moves counterclockwise from the point  $z = 1$ , tracing the unit circle, and back to the point  $z = 1$ .

As indicated by the modulus of  $H(e^{j\omega})$ , in Eq. 6.46, the magnitude response  $|H(e^{j\omega})|$  at a specific value of  $\omega$  is given by the product of the magnitudes of all zero vectors divided by the product of the magnitudes of all pole vectors. Likewise, from Eq. 6.47, we observe that the phase response at a specific value of  $\omega$  is obtained by adding the phase of the term  $\frac{p_0}{d_0}$  and the linear-phase term  $\omega(N - M)$  to the sum of the angles of the zero vectors minus the angles of the pole vectors. Thus, an approximate plot of the magnitude and phase responses of the transfer function of an LTI digital filter can be developed by examining the pole and zero locations.

Now, a zero (pole) vector has the smallest magnitude when  $\omega = \varphi$ . To highly attenuate signal components in a specified frequency range, we need to place zeros very close to or on the unit circle in this range. Likewise, to highly emphasize signal components in a specified frequency range, we need to place poles very close to or on the unit circle in this range.

## 6.3 Simple digital filters

Later in the course we shall review various methods of designing frequency-selective filters satisfying prescribed specifications. We now describe several low-order FIR and IIR digital filters with reasonable selective frequency responses that often are satisfactory in a number of applications. FIR digital filters considered here have integer-valued impulse response coefficients. These filters are employed in a number of practical applications, primarily because of their simplicity, which makes them amenable to inexpensive hardware implementations.

### 6.3.1 Lowpass FIR digital filters

The simplest lowpass FIR digital filter is the 2-point moving-average filter given by:

$$H_0(z) = \frac{1}{2}(1 + z^{-1}) = \frac{z + 1}{2z} \quad (6.49)$$

The above transfer function has a zero at  $z = -1$  and a pole at  $z = 0$ . Note that here the pole vector has a unity magnitude for all values of  $\omega$ . On the other hand, as  $\omega$  increases from 0 to  $\pi$ , the magnitude of the zero vector decreases from a value of 2, the diameter of the unit circle, to 0. Hence, the magnitude response  $|H_0(e^{j\omega})|$  is a monotonically decreasing function of  $\omega$  from  $\omega = 0$  to  $\omega = \pi$ . The maximum value of the magnitude function is 1 at  $\omega = 0$ , and the minimum value is 0 at  $\omega = \pi$ , i.e.:

$$|H_0(e^{j0})| = 1 \quad (6.50)$$

$$|H_0(e^{j\pi})| = 0 \quad (6.51)$$

The frequency response of the above filter is given by:

$$H_0(e^{j\omega}) = e^{-j\frac{\omega}{2}} \cos\left(\frac{\omega}{2}\right) \quad (6.52)$$

The magnitude response  $|H_0(e^{j\omega})| = \cos\left(\frac{\omega}{2}\right)$  can be seen to be a monotonically decreasing function of  $\omega$ , as showed in Figure 6.6.

The frequency  $\omega = \omega_c$  at which:

$$|H_0(e^{j\omega_c})| = \frac{1}{\sqrt{2}} H_0(e^{j0}) \quad (6.53)$$

is of practical interest since here the gain  $G(\omega_c)$  in dB is given by:

$$G(\omega_c) = 20 \log_{10} |H(e^{j\omega_c})| = 20 \log_{10} |H(e^{j0})| - 20 \log_{10} \sqrt{2} \approx -3 \text{ dB} \quad (6.54)$$

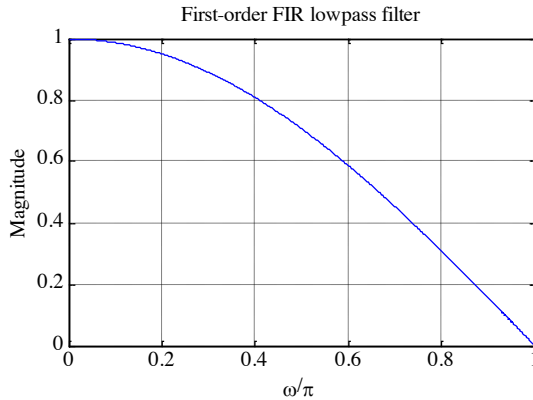


**Figure 6.6:** Magnitude response of the FIR lowpass filter.

since the dc gain  $G(0) = 20 \log_{10} |H(e^{j0})| = 0$ .

Thus, the gain  $G(\omega)$  at  $\omega = \omega_c$  is approximately 3 dB less than the gain at  $\omega = 0$ . As a result,  $\omega_c$  is called the 3-dB cutoff frequency. To determine the value of  $\omega_c$ , we set:

$$|H_0(e^{j\omega_c})|^2 = \cos^2\left(\frac{\omega_c}{2}\right) = \frac{1}{2} \quad (6.55)$$

which yields  $\omega_c = \frac{\pi}{2}$ .

The 3-dB cutoff frequency  $\omega_c$  can be considered as the passband edge frequency. As a result, for the filter  $H_0(z)$  the passband width is approximately  $\frac{\pi}{2}$ . The stopband is from  $\frac{\pi}{2}$  to  $\pi$ . Note that  $H_0(z)$  has a zero at  $z = -1$  or  $\omega = \pi$ , which is in the stopband of the filter.

A cascade of the simple FIR filter:

$$H_0(z) = \frac{1}{2}(1 + z^{-1}) \quad (6.56)$$

results in an improved lowpass frequency response as showed in Figure 6.7 for a cascade of 3 sections.

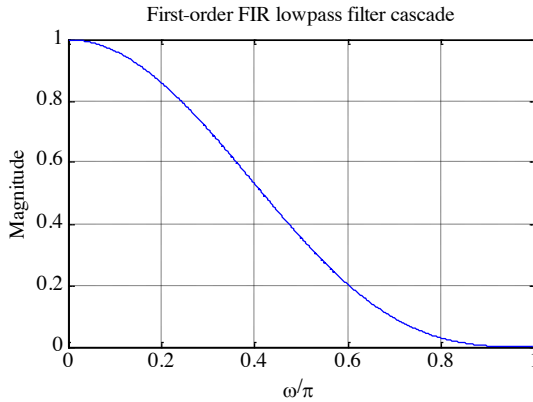


**Figure 6.7:** Magnitude response of the FIR lowpass filter cascade.

The 3-dB cutoff frequency of a cascade of  $M$  sections is given by:

$$\omega_c = 2 \arccos\left(2^{-\frac{1}{2M}}\right) \quad (6.57)$$

For  $M = 3$ , the above yields  $\omega_c = 0.302\pi$ . Thus, the cascade of first-order sections yields a sharper magnitude response but at the expense of a decrease in the width of the passband.

A better approximation to the ideal lowpass filter is given by a higher-order moving-average filter. Signals with rapid fluctuations in sample values are generally associated with high-frequency components. These high-frequency components are essentially removed by a moving-average filter resulting in a smoother output waveform.

### 6.3.2 Highpass FIR digital filters

The simplest highpass FIR filter is obtained from the simplest lowpass FIR filter by replacing  $z$  with  $-z$ . This results in:

$$H_1(z) = \frac{1}{2}(1 - z^{-1}) \quad (6.58)$$

The corresponding frequency response is given by:

$$H_1(e^{j\omega}) = j e^{-j\frac{\omega}{2}} \sin\left(\frac{\omega}{2}\right) \quad (6.59)$$

whose magnitude response is showed in Figure 6.8.

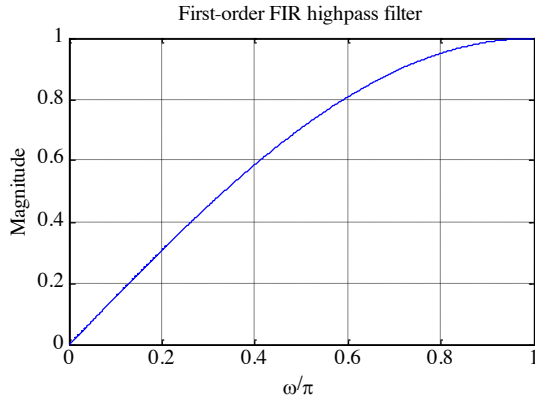


**Figure 6.8:** Magnitude response of the FIR highpass filter.

The monotonically increasing behavior of the magnitude function can again be demonstrated by examining the pole-zero pattern of the transfer function  $H_1(z)$ . The highpass transfer function  $H_1(z)$  has a zero at  $z = 1$  or  $\omega = 0$ , which is in the stopband of the filter.

Improved highpass magnitude response can be obtained by cascading several sections of the first-order highpass filter. Alternately, a higher-order highpass filter of the form:

$$H_1(z) = \frac{1}{M} \sum_{n=0}^{M-1} (-1)^n z^{-n} \quad (6.60)$$

is obtained by replacing  $z$  with  $-z$  in the transfer function of a moving average filter. An application of the FIR highpass filters is in moving-target-indicator (MTI) radars. In these radars, interfering signals, called clutters, are generated from fixed objects in the path of the radar beam. The clutter, generated mainly from ground echoes and weather returns, has frequency components near zero frequency (dc). The clutter can be removed by filtering the radar return signal through a two-pulse canceler, which is the first-order FIR highpass filter. For a more effective removal it may be necessary to use a three-pulse canceler obtained by cascading two two-pulse cancelers:

$$H_1(z) = \frac{1}{2}(1 - z^{-1}) \quad (6.61)$$

### 6.3.3 Lowpass IIR digital filters

We have already shown that the first-order causal IIR transfer function:

$$H(z) = \frac{k}{1 - \alpha z^{-1}} \quad 0 < \alpha < 1 \quad (6.62)$$

has a lowpass magnitude response for  $\alpha > 0$ . An improved lowpass magnitude response is obtained by adding a factor  $(1 + z^{-1})$  to the numerator of the transfer function:

$$H(z) = \frac{k(1 + z^{-1})}{1 - \alpha z^{-1}} \quad 0 < \alpha < 1 \quad (6.63)$$

This forces the magnitude response to have a zero at  $\omega = \pi$  in the stopband of the filter. On the other hand, the first-order causal IIR transfer function:

$$H(z) = \frac{k}{1 - \alpha z^{-1}} \quad -1 < \alpha < 0 \quad (6.64)$$

has a highpass magnitude response for  $\alpha < 0$ . However, the modified transfer function obtained with the addition of a factor  $(1 + z^{-1})$  to the numerator:

$$H(z) = \frac{k(1 + z^{-1})}{1 - \alpha z^{-1}} \quad -1 < \alpha < 0 \quad (6.65)$$

exhibits a lowpass magnitude response. The modified first-order lowpass transfer function for both positive and negative values of  $\alpha$  is then given by:

$$H_{LP}(z) = \frac{k(1 + z^{-1})}{1 - \alpha z^{-1}} \quad 0 < |\alpha| < 1 \quad (6.66)$$

As  $\omega$  increases from 0 to  $\pi$ , the magnitude of the zero vector decreases from a value of 2 to 0. The maximum values of the magnitude function is  $\frac{2k}{(1-\alpha)}$  at  $\omega = 0$  and the minimum value is 0 at  $\omega = \pi$ , i.e.:

$$|H_{LP}(e^{j0})| = \frac{2k}{(1 - \alpha)} \quad (6.67)$$

$$|H_{LP}(e^{j\pi})| = 0 \quad (6.68)$$

Therefore,  $|H_{LP}(e^{j\omega})|$  is a monotonically decreasing function of  $\omega$  from  $\omega = 0$  to  $\omega = \pi$ .

For most applications, it is usual to have a dc gain of 0 dB, that is to have the maximum magnitude  $|H(e^{j0})| = 1$ . To this end, we choose  $k = \frac{1-\alpha}{2}$ , resulting in the first-order IIR lowpass transfer function:

$$H_{LP}(z) = \frac{1 - \alpha}{2} \frac{(1 + z^{-1})}{1 - \alpha z^{-1}} \quad 0 < |\alpha| < 1 \quad (6.69)$$

The above transfer function has a zero at i.e., at  $\omega = \pi$ , which is in the stopband. It has also a real pole at  $z = \alpha$ .

As  $\omega$  increases from 0 to  $\pi$ , the magnitude of the zero vector decreases from a value of 2 to 0, whereas, for a positive value of  $\alpha$ , the magnitude of the pole vector increases from a value of  $1 - \alpha$  to  $1 + \alpha$ . The maximum value of the magnitude function is 1 at  $\omega = 0$ , and the minimum value is 0 at  $\omega = \pi$ , i.e.  $|H_{LP}(e^{j0})| = 1$ ,  $|H_{LP}(e^{j\pi})| = 0$ . Therefore,  $H_{LP}(e^{j\omega})$  is a monotonically decreasing function of  $\omega$  from  $\omega = 0$  to  $\omega = \pi$  as indicated in Figure 6.9.

The squared magnitude function is given by:

$$|H_{LP}(e^{j\omega})|^2 = \frac{(1 - \alpha)^2(1 + \cos \omega)}{2(1 + \alpha^2 - 2\alpha \cos \omega)} \quad (6.70)$$

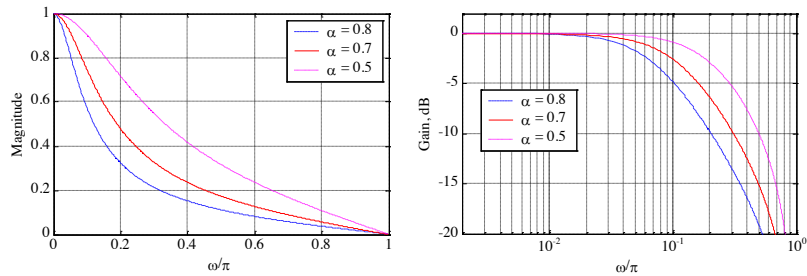


**Figure 6.9:** Magnitude (left) and gain (right) responses of the IIR lowpass filter.

The derivative of  $|H_{LP}(e^{j\omega})|^2$  with respect to  $\omega$  is given by:

$$\frac{d|H_{LP}(e^{j\omega})|^2}{d\omega} = \frac{-(1-\alpha)^2(1+\alpha^2+2\alpha)\sin\omega}{2(1+\alpha^2-2\alpha\cos\omega)^2} \quad (6.71)$$

The derivative in Eq. 6.71 is less or equal than zero in the range  $0 \leq \omega \leq \pi$ , verifying again the monotonically decreasing behaviour of the magnitude function. To determine the 3-dB cutoff frequency we set:

$$|H_{LP}(e^{j\omega})|^2 = \frac{1}{2} \quad (6.72)$$

in the expression for the square magnitude function, resulting in:

$$\frac{(1-\alpha)^2(1+\cos\omega_c)}{2(1+\alpha^2-2\alpha\cos\omega_c)} = \frac{1}{2} \quad (6.73)$$

which, when solved, yields:

$$\cos\omega_c = \frac{2\alpha}{1+\alpha^2} \quad (6.74)$$

The above quadratic equation can be solved for a yielding two solutions. The solution resulting in a stable transfer function  $H_{LP}(z)$  is given by:

$$\alpha = \frac{1-\sin\omega_c}{\cos\omega_c} \quad (6.75)$$

It follows from:

$$|H_{LP}(e^{j\omega})|^2 = \frac{(1-\alpha)^2(1+\cos\omega_c)}{2(1+\alpha^2-2\alpha\cos\omega_c)} \quad (6.76)$$

that  $H_{LP}(z)$  is a BR function for  $|\alpha| < 1$ .

### 6.3.4 Highpass IIR digital filters

A first-order causal highpass IIR digital filter has a transfer function given by:

$$H_{HP}(z) = \frac{1+\alpha}{2} \frac{1-z^{-1}}{1-\alpha z^{-1}} \quad (6.77)$$

where  $|\alpha| < 1$  in order to have stability. The transfer function in Eq. 6.77 has a zero at  $z = 1$ , i.e. at  $\omega = 0$ , which is in the stopband.

Its 3-dB cutoff frequency  $\omega_c$  is given by:

$$\alpha = \frac{1-\sin\omega_c}{\cos\omega_c} \quad (6.78)$$

which is the same as that of  $H_{LP}(z)$ . Magnitude and gain responses of  $H_{HP}(z)$  are showed in Figure 6.10.  $H_{HP}(z)$  is a BR function for  $|\alpha| < 1$ .

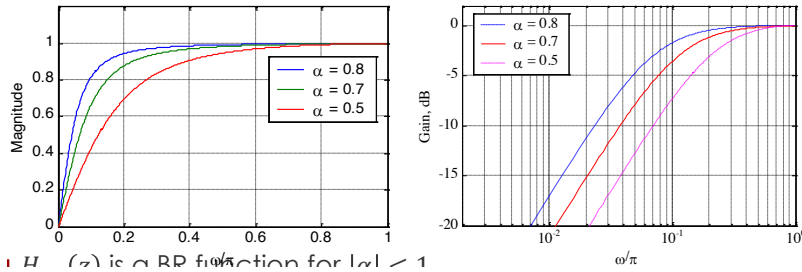


**Figure 6.10:** Magnitude (left) and gain (right) responses of the IIR highpass filter.

### Example 53: Design of a filter

We design a first-order highpass digital filter with a 3-dB cutoff frequency of  $0.8\pi$ .

Now, we consider that:

$$\begin{aligned}\sin(\omega_c) &= \sin(0.8\pi) = 0.587785 \\ \cos(\omega_c) &= \cos(0.8\pi) = -0.80902\end{aligned}$$

Therefore:

$$\alpha = \frac{1 - \sin \omega_c}{\cos \omega_c} = -0.5095245 \quad (6.79)$$

Therefore:

$$H_{HP}(z) = \frac{1 + \alpha}{2} \frac{1 - z^{-1}}{1 - \alpha z^{-1}} = 0.245238 \left( \frac{1 - z^{-1}}{1 + 0.5095245 z^{-1}} \right) \quad (6.80)$$

### 6.3.5 Bandpass IIR digital filters

A 2<sup>nd</sup>-order bandpass digital transfer function is given by:

$$H_{BP}(z) = \frac{1 - \alpha}{2} \left( \frac{1 - z^{-2}}{1 - \beta(1 + \alpha)z^{-1} + \alpha z^{-2}} \right) \quad (6.81)$$

Its squared magnitude function is:

$$|H_{BP}(e^{j\omega})|^2 = \frac{(1 - \alpha)^2(1 - \cos(2\omega))}{2[1 + \beta^2(1 + \alpha)^2 + \alpha^2 - 2\beta(1 + \alpha)^2 \cos \omega + 2\alpha \cos(2\alpha)]} \quad (6.82)$$

$|H_{BP}(e^{j\omega})|^2$  goes to zero at  $\omega = 0$  and  $\omega = \pi$ . It assumes a maximum value of 1 at  $\omega = \omega_0$ , called the center frequency of the bandpass filter, where:

$$\omega_0 = \cos^{-1}(\beta) \quad (6.83)$$

The frequencies  $\omega_{c1}$  and  $\omega_{c2}$  where  $|H_{BP}(e^{j\omega})|^2$  becomes  $\frac{1}{2}$  are called the 3-dB cutoff frequencies. The difference between the two cutoff frequencies, assuming  $\omega_{c2} > \omega_{c1}$  is called the 3-dB bandwidth and is given by:

$$B_w = \omega_{c2} - \omega_{c1} = \cos^{-1} \left( \frac{2\alpha}{1 + \alpha^2} \right) \quad (6.84)$$

The transfer function  $H_{BP}(e^{j\omega})$  is a BR function if  $|\alpha| < 1$  and  $|\beta| < 1$ . Some plots of  $|H_{BP}(e^{j\omega})|$  are showed in Figure 6.11.

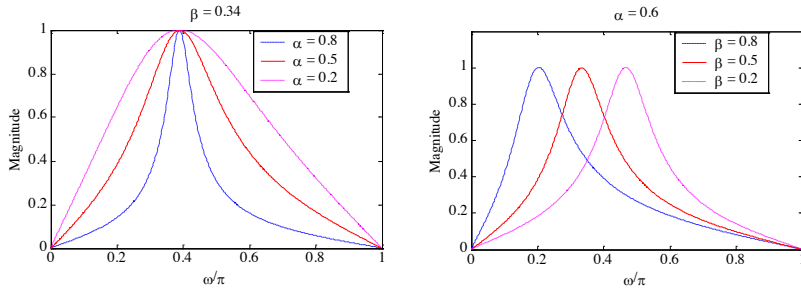


**Figure 6.11:** Magnitude responses of the IIR bandpass filter.

#### Example 54: Design of a filter

We design a 2<sup>nd</sup>-order bandpass digital filter with center frequency at  $0.4\pi$  and a 3-dB bandwidth of  $0.1\pi$ . We have:

$$\beta = \cos(\omega_0) = \cos(0.4\pi) = 0.309017 \quad (6.85)$$

and:

$$\frac{2\alpha}{1 + \alpha^2} = \cos(B_w) = \cos(0.1\pi) = 0.9510565 \quad (6.86)$$

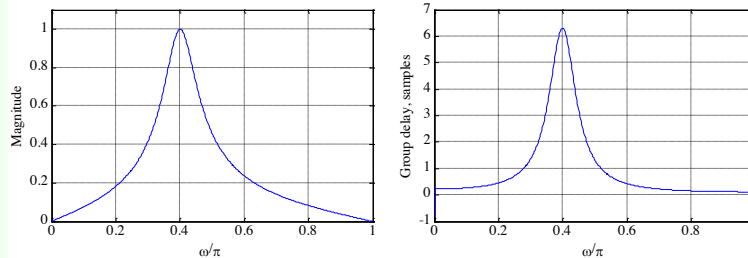
The solution of Eq. 6.86 yields  $\alpha = 1.376382$  and  $\alpha = 0.72654253$ . The corresponding transfer functions are:

$$H'_{BP}(z) = -0.18819 \frac{1 - z^{-2}}{1 - 0.7343424z^{-1} + 1.37638z^{-2}} \quad (6.87)$$

$$H''_{BP}(z) = 0.13673 \frac{1 - z^{-2}}{1 - 0.533531z^{-1} + 0.72654253z^{-2}} \quad (6.88)$$

The poles of  $H'_{BP}(z)$  are at  $z = 0.3671712 \pm j1.11425636$  and they have a magnitude greater than 1. Thus, the poles of  $H'_{BP}(z)$  are outside the unit circle making the transfer function unstable. On the other hand, the poles of  $H''_{BP}(z)$  are at  $z = 0.2667655 \pm j0.8095546$  and they have a magnitude of 0.8523746. Hence,  $H''_{BP}(z)$  is BIBO stable.

In the plot below, the plots of the magnitude function and the group delay of  $H''_{BP}(z)$  are showed.



#### 6.3.6 Bandstop IIR digital filters

A 2<sup>nd</sup>-order bandstop digital filter has a transfer function given by:

$$H_{BS}(z) = \frac{1 + \alpha}{2} \left( \frac{1 - 2\beta z^{-1} + z^{-2}}{1 - \beta(1 + \alpha)z^{-1} + \alpha z^{-2}} \right) \quad (6.89)$$

The transfer function  $H_{BS}(z)$  is a BR function if  $|\alpha| < 1$  and  $|\beta| < 1$ . Its magnitude response is showed in Figure 6.12.

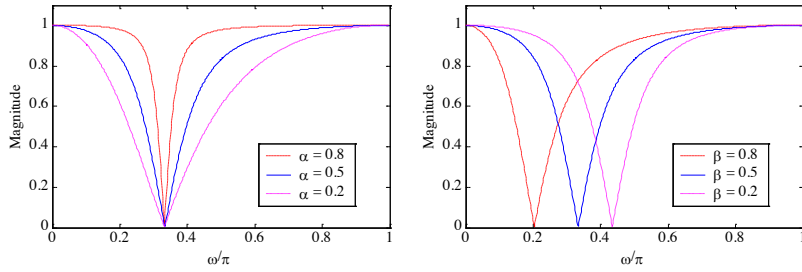


**Figure 6.12:** Magnitude responses of the IIR bandstop filter.

Here, the magnitude function takes the maximum value of 1 at  $\omega = 0$  and  $\omega = \pi$ . It goes to 0 at  $\omega = \omega_0$ , where  $\omega_0$ , called the notch frequency, is given by:

$$\omega_0 = \cos^{-1}(\beta) \quad (6.90)$$

The digital transfer function  $H_{BS}(z)$  is more commonly called a notch filter.

The frequencies  $\omega_{c1}$  and  $\omega_{c2}$  where  $|H_{BP}(e^{j\omega})|^2$  becomes  $\frac{1}{2}$  are called the 3-dB cutoff frequencies. The difference between them, assuming  $\omega_{c2} > \omega_{c1}$ , is called the 3-dB notch bandwidth and it is given by:

$$B_w = \omega_{c2} - \omega_{c1} = \cos^{-1} \left( \frac{2\alpha}{1 + \alpha^2} \right) \quad (6.91)$$

### 6.3.7 Higher-Order IIR digital filters

By cascading the simple digital filters discussed so far, we can implement digital filters with sharper magnitude responses. For example, let us consider a cascade of  $k$  first-order lowpass sections characterized by the transfer function:

$$H_{LP}(z) = \frac{1 - \alpha}{2} \frac{1 + z^{-1}}{1 - \alpha z^{-1}} \quad (6.92)$$

The overall structure has a transfer function given by:

$$G_{LP}(z) = \left( \frac{1 - \alpha}{2} \cdot \frac{1 + z^{-1}}{1 - \alpha z^{-1}} \right)^k \quad (6.93)$$

The corresponding squared-magnitude function is given by:

$$|G_{LP}(e^{j\omega})|^2 = \left[ \frac{(1 - \alpha)^2(1 + \cos \omega)}{2(1 + \alpha^2 - 2\alpha \cos \omega)} \right]^k \quad (6.94)$$

To determine the relation between its 3-dB cutoff frequency  $\omega_c$  and the parameter  $\alpha$ , we set:

$$\left[ \frac{(1 - \alpha)^2(1 + \cos \omega_c)}{2(1 + \alpha^2 - 2\alpha \cos \omega_c)} \right]^k = \frac{1}{2} \quad (6.95)$$

which when solved for  $\alpha$ , yields for a stable  $G_{LP}(z)$ :

$$\alpha = \frac{1 + (1 - C) \cos \omega_c - \sin \omega_c \sqrt{2C - C^2}}{1 - C + \cos \omega_c} \quad (6.96)$$

where:

$$C = 2^{\frac{k-1}{k}} \quad (6.97)$$

It should be noted that, for  $k = 1$ , the expression given in Eq. 6.96 reduces to:

$$\alpha = \frac{1 - \sin \omega_c}{\cos \omega_c} \quad (6.98)$$

**Example 55: Design of a filter**

We design a lowpass filter with a 3-dB cutoff frequency at  $\omega_c = 0.4\pi$  using a single first-order section and a cascade of 4 first-order sections, and we compare their gain responses.

For the single first-order lowpass filter we have:

$$\alpha = \frac{1 + \sin \omega_c}{\cos \omega_c} = \frac{1 + \sin(0.4\pi)}{\cos(0.4\pi)} \quad (6.99)$$

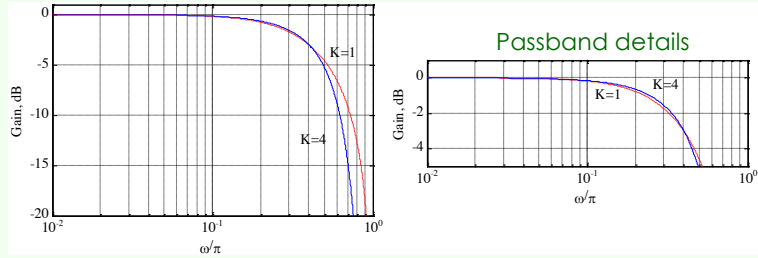
For the cascade of 4 first-order sections, we substitute  $k = 4$  and get:

$$C = 2^{\frac{k-1}{k}} = 2^{\frac{4-1}{4}} = 1.6818 \quad (6.100)$$

Next, we compute:

$$\begin{aligned} \alpha &= \frac{1 + (1 - C) \cos \omega_c - \sin \omega_c \sqrt{2C - C^2}}{1 - C + \cos \omega_c} \\ &= \frac{1 + (1 - 1.6818) \cos(0.4\pi) - \sin(0.4\pi) \sqrt{2(1.6818) - (1.6818)^2}}{1 - 1.6818 + \cos(0.4\pi)} \\ &= -0.251 \end{aligned} \quad (6.101)$$

The gain responses of the two filters are showed in the plots below. As can be seen, cascading has resulted in a sharper roll-off in the gain response



**Lecture 20.**  
Thursday 10<sup>th</sup>  
December, 2020.

## 6.4 Linear-phase FIR transfer functions

It is impossible to design an IIR transfer function with an exact linear-phase. However, it is always possible to design a FIR transfer function with an exact linear-phase response. We now develop the forms of the linear-phase FIR transfer function  $H(z)$  with real impulse response  $h[n]$ . Let:

$$H(z) = \sum_{n=0}^N h[n]z^{-n} \quad (6.102)$$

If  $H(z)$  is to have a linear-phase, its frequency response must be of the form:

$$H(e^{j\omega}) = e^{j(c\omega + \beta)} \tilde{H}(\omega) \quad (6.103)$$

where  $c$  and  $\beta$  are constants, and  $\tilde{H}(\omega)$ , called the amplitude response, also called the zero-phase response, is a real function of  $\omega$ . For a real impulse response, the magnitude response  $|H(e^{j\omega})|$  is an even function of  $\omega$ , i.e.:

$$|H(e^{j\omega})| = |H(e^{-j\omega})| \quad (6.104)$$

Since  $|H(e^{j\omega})| = \left| \check{H}(\omega) \right|$ , the amplitude response is then either an even function or an odd function of  $\omega$ , i.e.:

$$\check{H}(-\omega) = \pm \check{H}(\omega) \quad (6.105)$$

The frequency response satisfies the relation:

$$H(e^{j\omega}) = H^*(e^{-j\omega}) \quad (6.106)$$

or, equivalently, the relation:

$$e^{j(c\omega+\beta)} \check{H}(\omega) = e^{-j(c(-\omega)+\beta)} \check{H}(\omega) \quad (6.107)$$

If  $\check{H}(\omega)$  is an even function, then the above relation leads to:

$$e^{j\beta} = e^{-j\beta} \quad (6.108)$$

implying that either  $\beta = 0$  or  $\beta = \pi$ . From:

$$H(e^{j\omega}) = e^{j(c\omega+\beta)} \check{H}(\omega) \quad (6.109)$$

we have:

$$\check{H}(\omega) = e^{-j(c\omega+\beta)} H(e^{j\omega}) \quad (6.110)$$

Substituting the value of  $\beta$  in Eq. 6.110, we get:

$$\check{H}(\omega) = \pm e^{-jc\omega} H(e^{j\omega}) = \pm \sum_{n=0}^N h[n] e^{-j\omega(c+n)} \quad (6.111)$$

Replacing  $\omega$  with  $-\omega$  in Eq. 6.111, we get:

$$\check{H}(-\omega) = \pm \sum_{\ell=0}^N h[\ell] e^{j\omega(c+\ell)} \quad (6.112)$$

Making a change of variable  $\ell = N - n$ , we rewrite Eq. 6.112 as:

$$\check{H}(-\omega) = \pm \sum_{n=0}^N h[N-n] e^{j\omega(c+N-n)} \quad (6.113)$$

Now, as  $\check{H}(\omega) = \check{H}(-\omega)$ , we have:

$$h[n] e^{-j\omega(c+n)} = h[N-n] e^{j\omega(c+N-n)} \quad (6.114)$$

Eq. 6.114 leads to the condition:

$$h[n] = h[N-n] \quad 0 \leq n \leq N \quad (6.115)$$

with  $c = -\frac{N}{2}$ . Thus, the FIR filter with an even amplitude response will have a linear phase if it has a symmetric impulse response. If  $\check{H}(\omega)$  is an odd function of  $\omega$ , then from:

$$e^{j(c\omega+\beta)} \check{H}(\omega) = e^{-j(-c\omega+\beta)} \check{H}(-\omega) \quad (6.116)$$

we get  $e^{j\beta} = -e^{-j\beta}$  as  $\check{H}(-\omega) = -\check{H}(\omega)$ . Eq. 6.116 is satisfied if  $\beta = \pm\frac{\pi}{2}$ . Then  $H(e^{j\omega}) = e^{j(c\omega+\beta)}$  reduces to:

$$H(e^{j\omega}) = j e^{j c \omega} \check{H}(\omega) \quad (6.117)$$

Eq. 6.117 can be rewritten as:

$$\check{H}(\omega) = -j e^{-j c \omega} H(e^{j\omega}) = -j \sum_{m=0}^N h[m] e^{-j\omega(m+c)} \quad (6.118)$$

Again, as  $\check{H}(\omega) = \check{H}(-\omega)$ , from Eq. 6.118 we get:

$$\check{H}(-\omega) = j \sum_{\ell=0}^N h[\ell] e^{j\omega(\ell+c)} \quad (6.119)$$

Making a change of variable  $\ell = N - n$ , we rewrite Eq. 6.119 as:

$$\check{H}(-\omega) = j \sum_{\ell=0}^N h[\ell] e^{j\omega(\ell+c)} \quad (6.120)$$

Equating the RHS of Eq. 6.120 with the RHS of Eq. 6.118, we arrive at the condition for linear phase as:

$$h[n] = h[N-n] \quad 0 \leq n \leq N \quad (6.121)$$

with  $c = -\frac{N}{2}$ . Therefore, a FIR filter with an odd amplitude response will have linear-phase response if it has an antisymmetric impulse response.

Since the length of the impulse response can be either even or odd, we can define four types of linear-phase FIR transfer functions. In particular, for an antisymmetric FIR filter of odd length, namely  $N$  even,  $h[\frac{N}{2}] = 0$ . We examine in the following discussion each of the four cases, sketched in Figure 6.13.

#### 6.4.1 Symmetric impulse response with odd length

In this case, the degree  $N$  is even. In the following discussion we assume also  $N = 8$  for simplicity. Therefore, the transfer function  $H(z)$  is given by:

$$H(z) = h[0] + h[1]z^{-1} + h[2]z^{-2} + h[3]z^{-3} + h[4]z^{-4} + h[5]z^{-5} + h[6]z^{-6} + h[7]z^{-7} + h[8]z^{-8} \quad (6.122)$$

Because of symmetry, we have:

$$h[0] = h[8] \quad (6.123)$$

$$h[1] = h[7] \quad (6.124)$$

$$h[2] = h[6] \quad (6.125)$$

$$h[3] = h[5] \quad (6.126)$$

Thus, we can write:

$$\begin{aligned} H(z) &= h[0](1 + z^{-8}) + h[1](z^{-1} + z^{-7}) + h[2](z^{-2} + z^{-6}) + h[3](z^{-3} + z^{-5}) + h[4]z^{-4} \\ &= z^{-4} \{ h[0](z^4 + z^{-4}) + h[1](z^3 + z^{-3}) + h[2](z^2 + z^{-2}) + h[3](z + z^{-1}) + h[4] \} \end{aligned} \quad (6.127)$$

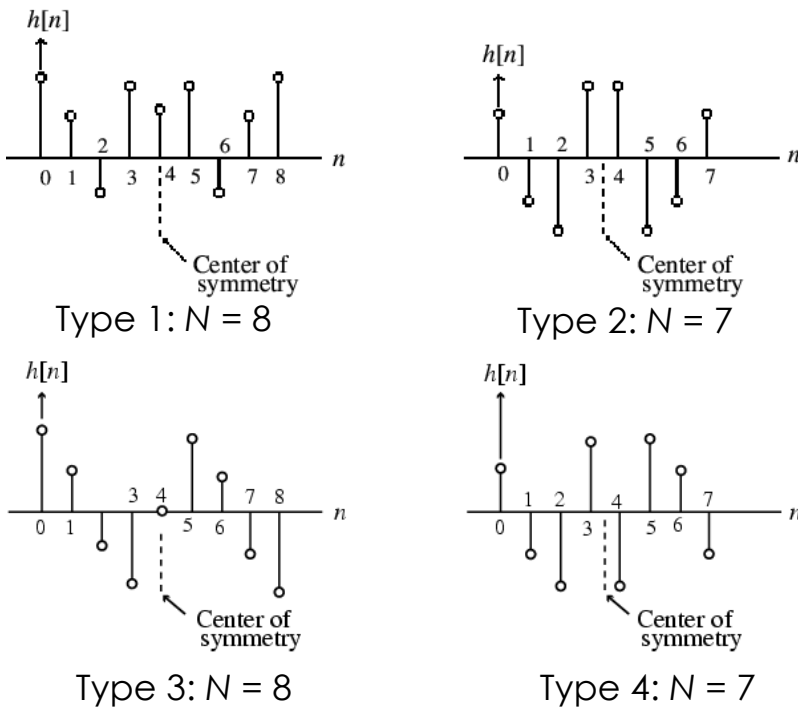


**Figure 6.13:** The four types of linear-phase FIR transfer functions.

The corresponding frequency response is then given by:

$$H(e^{j\omega}) = e^{-j4\omega} \{2h[0]\cos(4\omega) + 2h[1]\cos(3\omega) + 2h[2]\cos(2\omega) + 2h[3]\cos(\omega) + h[4]\} \quad (6.128)$$

The quantity inside the braces is a real function of  $\omega$  and can assume positive or negative values in the range  $0 \leq |\omega| \leq \pi$ . The phase function is given by:

$$\theta(\omega) = -4\omega + \beta \quad (6.129)$$

where  $\beta$  is either 0 or  $\pi$ , and hence, it is a linear function of  $\omega$ . The group delay is given by:

$$\tau(\omega) = -\frac{d\theta(\omega)}{d\omega} = 4 \quad (6.130)$$

indicating a constant group delay of 4 samples.

In the general case for Type 1 FIR filters, the frequency response is of the form:

$$H(e^{j\omega}) = e^{-jN\frac{\omega}{2}} \check{H}(\omega) \quad (6.131)$$

where the amplitude response  $\check{H}(\omega)$ , also called the zero-phase response, is of the form:

$$\check{H}(\omega) = h\left[\frac{N}{2}\right] + 2 \sum_{n=1}^{\frac{N}{2}} h\left[\frac{N}{2} - n\right] \cos(\omega n) \quad (6.132)$$

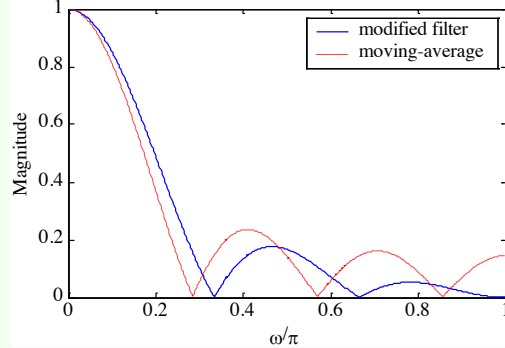
**Example 56: Symmetric impulse response with odd length**

We consider:

$$H_0(z) = \frac{1}{6} \left[ \frac{1}{2} + z^{-1} + z^{-3} + z^{-4} + z^{-5} + \frac{1}{2} z^{-6} \right] \quad (6.133)$$

which is seen to be a slightly modified version of a length-7 moving-average FIR filter.

This transfer function has a symmetric impulse response and therefore a linear phase response. A plot of the magnitude response of  $H_0(z)$  along with that of the 7-point moving-average filter is showed below.



Note the improved magnitude response obtained by simply changing the first and the last impulse response coefficients of a moving-average (MA) filter. It can be showed that we can express:

$$H_0(z) = \frac{1}{2}(1+z^{-1}) \cdot \frac{1}{6}(1+z^{-1}+z^{-2}+z^{-3}+z^{-4}+z^{-5}) \quad (6.134)$$

which is seen to be a cascade of a 2-point MA filter with a 6-point MA filter. Thus,  $H_0(z)$  has a double zero at  $z = -1$ , i.e.  $\omega = \pi$ .

#### 6.4.2 Symmetric impulse response with even length

In this case, the degree  $N$  is odd and we assume  $N = 7$  for simplicity for the following discussion. Therefore, the transfer function is of the form:

$$H(z) = h[0] + h[1]z^{-1} + h[2]z^{-2} + h[3]z^{-3} + h[4]z^{-4} + h[5]z^{-5} + h[6]z^{-6} + h[7]z^{-7} \quad (6.135)$$

Making use of the symmetry of the impulse response coefficients, the transfer function can be rewritten as:

$$\begin{aligned} H(z) &= h[0](1+z^{-7}) + h[1](z^{-1}+z^{-6}) + h[2](z^{-2}+z^{-5}) + h[3](z^{-3}+z^{-4}) \\ &= z^{-\frac{7}{2}} \left\{ h[0](z^{\frac{7}{2}}+z^{-\frac{7}{2}}) + h[1](z^{\frac{5}{2}}+z^{-\frac{5}{2}}) + h[2](z^{\frac{3}{2}}+z^{-\frac{3}{2}}) + h[3](z^{\frac{1}{2}}+z^{-\frac{1}{2}}) \right\} \end{aligned} \quad (6.136)$$

The corresponding frequency response is given by:

$$H(e^{j\omega}) = e^{-j\frac{7\omega}{2}} \left\{ 2h[0] \cos\left(\frac{7\omega}{2}\right) + 2h[1] \cos\left(\frac{5\omega}{2}\right) + 2h[2] \cos\left(\frac{3\omega}{2}\right) + 2h[3] \cos\left(\frac{\omega}{2}\right) \right\} \quad (6.137)$$

As before, the quantity inside the braces is a real function of  $\omega$  and can assume positive or negative values in the range  $0 \leq |\omega| \leq \pi$ . Here, the phase function is given by:

$$\theta(\omega) = -\frac{7}{2}\omega + \beta \quad (6.138)$$

where  $\beta$  is either 0 or  $\pi$ . As a result, the phase is also a linear function of  $\omega$  and the corresponding group delay is:

$$\tau(\omega) = \frac{7}{2} \quad (6.139)$$

indicating a group delay of  $\frac{7}{2}$  samples.

The expression for the frequency response in the general case for Type 2 FIR filters is of the form:

$$H(e^{j\omega}) = e^{-jN\frac{\omega}{2}} \check{H}(\omega) \quad (6.140)$$

where the amplitude response is given by:

$$\check{H}(\omega) = 2 \sum_{n=1}^{\frac{N+1}{2}} h\left[\frac{N+1}{2} - n\right] \cos\left(\omega\left(n - \frac{1}{2}\right)\right) \quad (6.141)$$

### 6.4.3 Antisymmetric impulse response with odd length

In this case, the degree  $N$  is even and we assume  $N = 8$  for simplicity for the following discussion. Therefore, applying the symmetry condition we get:

$$H(z) = z^{-4} \{ h[0](z^4 - z^{-4}) + h[1](z^3 - z^{-3}) + h[2](z^2 - z^{-2}) + h[3](z - z^{-1}) \} \quad (6.142)$$

The corresponding frequency response is given by:

$$H(e^{j\omega}) = e^{-j4\omega} e^{j\frac{\pi}{2}} \{ 2h[0] \sin(4\omega) + 2h[1] \sin(3\omega) + 2h[2] \sin(2\omega) + 2h[3] \sin(\omega) \} \quad (6.143)$$

It also exhibits a linear phase response given by:

$$\theta(\omega) = -4\omega + \frac{\pi}{2} + \beta \quad (6.144)$$

where  $\beta$  is either 0 or  $\pi$ . The group delay here is:

$$\tau(\omega) = 4 \quad (6.145)$$

indicating a constant group delay of 4 samples.

The expression for the frequency response in the general case for Type 3 FIR filters is of the form:

$$H(e^{j\omega}) = e^{-jN\frac{\omega}{2}} \check{H}(\omega) \quad (6.146)$$

where the amplitude response is given by:

$$\check{H}(\omega) = 2 \sum_{n=1}^{\frac{N}{2}} h\left[\frac{N}{2} - n\right] \sin(\omega n) \quad (6.147)$$

#### 6.4.4 Antisymmetric impulse response with even length

In this case, the degree  $N$  is even and we assume  $N = 7$  for simplicity for the following discussion. Therefore, applying the symmetry condition we get:

$$H(z) = z^{\frac{7}{2}} \left\{ h[0](z^{\frac{7}{2}} - z^{-\frac{7}{2}}) + h[1](z^{\frac{5}{2}} - z^{-\frac{5}{2}}) + h[2](z^{\frac{3}{2}} - z^{-\frac{3}{2}}) + h[3](z^{\frac{1}{2}} - z^{-\frac{1}{2}}) \right\} \quad (6.148)$$

The corresponding frequency response is given by:

$$H(e^{j\omega}) = e^{-j\frac{7\omega}{2}} e^{j\frac{\pi}{2}} \left\{ 2h[0] \sin\left(\frac{7\omega}{2}\right) + 2h[1] \sin\left(\frac{5\omega}{2}\right) + 2h[2] \sin\left(\frac{3\omega}{2}\right) + 2h[3] \sin\left(\frac{\omega}{2}\right) \right\} \quad (6.149)$$

It again exhibits a linear phase response given by:

$$\theta(\omega) = -\frac{7}{2}\omega + \frac{\pi}{2} + \beta \quad (6.150)$$

where  $\beta$  is either 0 or  $\pi$ . The group delay is constant and is given by:

$$\tau(\omega) = \frac{7}{2} \quad (6.151)$$

The expression for the frequency response in the general case for Type 4 FIR filters is of the form:

$$H(e^{j\omega}) = e^{-jN\frac{\omega}{2}} \check{H}(\omega) \quad (6.152)$$

where the amplitude response is given by:

$$\check{H}(\omega) = 2 \sum_{n=1}^{\frac{N+1}{2}} h\left[\frac{N+1}{2} - n\right] \sin\left(\omega\left(n - \frac{1}{2}\right)\right) \quad (6.153)$$

#### 6.4.5 General form of frequency response

In each of the four types of linear-phase FIR filters, the frequency response is of the form:

$$H(e^{j\omega}) = e^{-jN\frac{\omega}{2}} e^{j\beta} \check{H}(\omega) \quad (6.154)$$

The amplitude response  $\check{H}(\omega)$  for each type can become negative over certain frequency ranges, typically in the stopband.

##### Example 57: General form of frequency response

We consider the causal Type 1 FIR transfer function:

$$H_1(z) = -1 + 2z^{-1} - 3z^{-2} + 6z^{-3} - 3z^{-4} + 2z^{-5} - z^{-6} \quad (6.155)$$

Its amplitude and phase responses are given by:

$$\check{H}_1(\omega) = 6 - 6 \cos(\omega) + 4 \cos(2\omega) - 2 \cos(3\omega) \quad (6.156)$$

$$\theta_1(\omega) = -3\omega \quad (6.157)$$

Next, we consider the causal Type 1 FIR transfer function:

$$H_2(z) = 1 - 2z^{-1} + 3z^{-2} - 6z^{-3} + 3z^{-4} - 2z^{-5} + z^{-6} \quad (6.158)$$

Its amplitude and phase responses are given by:

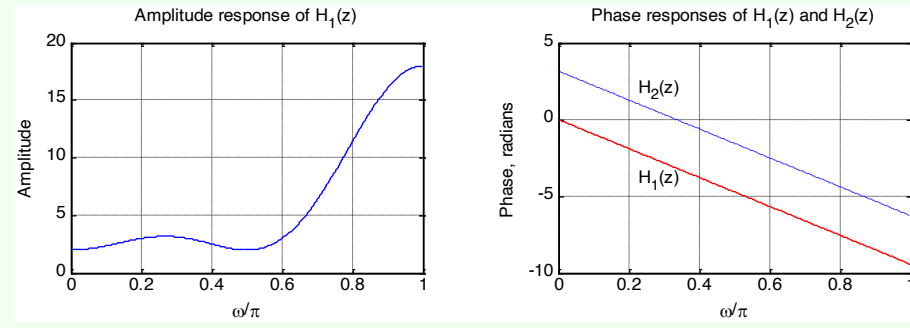
$$\check{H}_2(\omega) = -\check{H}_1(\omega) \quad (6.159)$$

$$\theta_2(\omega) = -3\omega + \pi \quad (6.160)$$

Note that:

$$|H_1(e^{j\omega})| = |H_2(e^{j\omega})| \quad (6.161)$$

Hence,  $H_1(z)$  and  $H_2(z)$  have identical magnitude responses but phase responses differing by  $\pi$ , as showed in the figure below.



### Example 58: General form of frequency response

We consider the causal Type 1 FIR transfer function:

$$H_3(z) = 1 - 2z^{-1} + 3z^{-2} - 3z^{-4} + 2z^{-5} - z^{-6} \quad (6.162)$$

Its amplitude and phase responses are given by:

$$\check{H}_3(\omega) = -6 \sin(\omega) + 4 \sin(2\omega) + 2 \sin(3\omega) \quad (6.163)$$

$$\theta_3(\omega) = -3\omega + \frac{\pi}{2} \quad (6.164)$$

Next, we consider the causal Type 1 FIR transfer function:

$$H_4(z) = -1 + 2z^{-1} - 3z^{-2} + 3z^{-4} - 2z^{-5} + z^{-6} \quad (6.165)$$

Its amplitude and phase responses are given by:

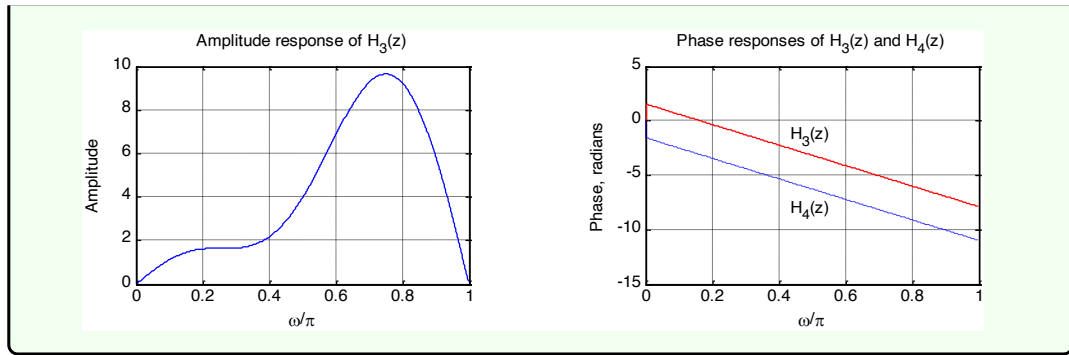
$$\check{H}_4(\omega) = -\check{H}_3(\omega) \quad (6.166)$$

$$\theta_4(\omega) = -3\omega - \frac{\pi}{2} \quad (6.167)$$

Note that:

$$|H_3(e^{j\omega})| = |H_4(e^{j\omega})| \quad (6.168)$$

Hence,  $H_3(z)$  and  $H_4(z)$  have identical magnitude responses but phase responses differing by  $\pi$ , as showed in the figure below.



Now, in general, the magnitude and phase responses of the linear-phase FIR are given by:

$$|H(e^{j\omega})| = |\check{H}(\omega)| \quad (6.169)$$

$$\theta(\omega) = \begin{cases} -\frac{N\omega}{2} + \beta & \check{H}(\omega) \geq 0 \\ -\frac{N\omega}{2} + \beta - \pi & \check{H}(\omega) < 0 \end{cases} \quad (6.170)$$

The group delay in each case is:

$$\tau(\omega) = \frac{N}{2} \quad (6.171)$$

Note that, even though the group delay is constant, since in general  $|H(e^{j\omega})|$  is not a constant, the output waveform is not a replica of the input waveform.

A FIR filter with a frequency response that is a real function of  $\omega$  is often called a zero-phase filter. Such a filter must have a noncausal impulse response: a zero-phase filter needs to have a purely real-valued frequency response, and, consequently, it must have an impulse response that is even with respect to the time index  $n = 0$ , i.e., it is non-causal.

#### 6.4.6 Zero locations

Let us consider first a FIR filter with a symmetric impulse response:

$$h[n] = h[N - n] \quad (6.172)$$

Its transfer function can be written as:

$$H(z) = \sum_{n=0}^N h[n]z^{-n} = \sum_{n=0}^N h[N - n]z^{-n} \quad (6.173)$$

By making a change of variable  $m = N - n$ , we can write:

$$H(z) = \sum_{n=0}^N h[N - n]z^{-n} = \sum_{m=0}^N h[m]z^{-N+m} = z^{-N} \underbrace{\sum_{m=0}^N h[m]z^m}_{H(z^{-1})} \quad (6.174)$$

Hence, for a FIR filter with a symmetric impulse response of length  $N + 1$  we have:

$$H(z) = z^{-N}H(z^{-1}) \quad (6.175)$$

A real-coefficient polynomial  $H(z)$  satisfying the above condition is called a mirror-image polynomial (MIP).

Now, let us consider first an FIR filter with an antisymmetric impulse response:

$$h[n] = -h[N-n] \quad (6.176)$$

Its transfer function can be written as:

$$H(z) = \sum_{n=0}^N h[n]z^{-n} = -\sum_{n=0}^N h[N-n]z^{-n} \quad (6.177)$$

By making a change of variable  $m = N - n$ , we can write:

$$H(z) = -\sum_{n=0}^N h[N-n]z^{-n} = -\sum_{m=0}^N h[m]z^{-N+m} = -z^{-N}H(z^{-1}) \quad (6.178)$$

Hence, the transfer function  $H(z)$  of an FIR filter with an antisymmetric impulse response satisfies the condition:

$$H(z) = z^{-N}H(z^{-1}) \quad (6.179)$$

A real-coefficient polynomial  $H(z)$  satisfying the above condition is called antimirror-image polynomial (AIP).

Now, it follows from the relation  $H(z) = \pm z^{-N}H(z^{-1})$  that if  $z = \xi_0$  is a zero of  $H(z)$ , so is  $z = \frac{1}{\xi_0}$ . Moreover, for an FIR filter with a real impulse response, the zeros of  $H(z)$  occur in complex conjugate pairs. Hence, a zero at  $z = \xi_0$  is associated with a zero at  $z = \xi_0^*$ . Thus, a complex zero that is not on the unit circle is associated with a set of 4 zeros given by:

$$z = re^{\pm j\varphi}, \quad \frac{1}{r}e^{\pm j\varphi} \quad (6.180)$$

A zero on the unit circle appear as a pair:

$$z = e^{\pm j\varphi} \quad (6.181)$$

as its reciprocal is also its complex conjugate. Since a zero at  $z = \pm 1$  is its own reciprocal, it can appear only singly.

Now, a Type 2 FIR filter satisfies:

$$H(z) = z^{-N}H(z^{-1}) \quad (6.182)$$

with degree  $N$  odd. Hence,  $H(-1) = (-1)^{-N}H(-1) = -H(-1)$ , implying  $H(-1) = 0$ , i.e.,  $H(z)$  must have a zero at  $z = -1$ .

Likewise, a Type 3 or 4 FIR filter satisfies:

$$H(z) = -z^{-N}H(z^{-1}) \quad (6.183)$$

Thus:

$$H(1) = (-1)^{-N}H(1) = -H(1) \quad (6.184)$$

implying that  $H(z)$  must have a zero at  $z = 1$ . On the other hand, only the Type 3 FIR filter is restricted to have a zero at  $z = -1$  since here the degree  $N$  is even and hence:

$$H(-1) = -(-1)^{-N}H(-1) = -H(-1) \quad (6.185)$$

Typical zero locations are showed in Figure 6.14.

So, to summarize:

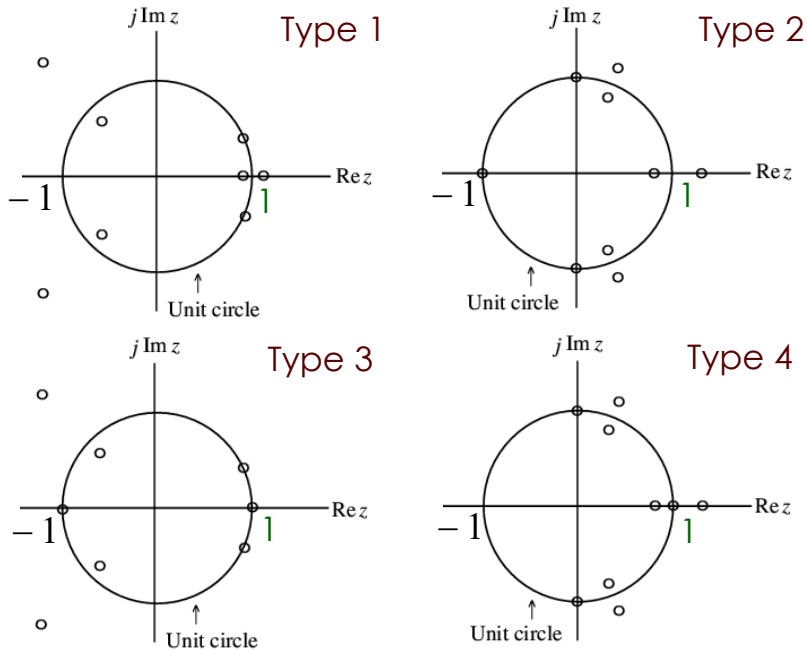


**Figure 6.14:** Typical zero locations.

- Type 1 FIR filter: either an even number or no zeros at  $z = 1$  and  $z = -1$ ;
- Type 2 FIR filter: either an even number or no zeros at  $z = 1$  and an odd number of zeros at  $z = -1$ ;
- Type 3 FIR filter: an odd number of zeros at  $z = 1$  and  $z = -1$ ;
- Type 4 FIR filter: an odd number of zeros at  $z = 1$  and either an even number or no zeros at  $z = -1$ .

The presence of zeros at  $z = \pm 1$  leads to the following limitations on the use of these linear-phase transfer functions for designing frequency-selective filters:

- a Type 2 FIR filter cannot be used to design a highpass filter since it always has a zero;
- a Type 3 FIR filter has zeros at both  $z = 1$  and  $z = -1$ , and hence cannot be used to design either a lowpass or a highpass or a bandstop filter;
- a Type 4 FIR filter is not appropriate to design lowpass and bandstop filters due to the presence of a zero at  $z = 1$ ;
- a Type 1 FIR filter has no such restrictions and can be used to design almost any type of filter.

# Bibliography

- [1] *Signal Processing for Communications*, P. Prandoni and M. Vetterli, [https://www.sp4comm.org/docs/sp4comm\\_corrected.pdf](https://www.sp4comm.org/docs/sp4comm_corrected.pdf)
- [2] *Digital Signal Processing*, A. V. Oppenheim and R. W. Schafer, Prentice Hall
- [3] *Digital Signal Processing: Digital Signal Processing: A Computer-Based Approach*, S. K. Mitra